



US 20230077899A1

(19) **United States**

(12) **Patent Application Publication**

**Mardinly et al.**

(10) **Pub. No.: US 2023/0077899 A1**

(43) **Pub. Date: Mar. 16, 2023**

(54) **CELL-BASED BRAIN-MACHINE  
INTERFACE**

(71) Applicant: **Neuralink Corp.**, Fremont, CA (US)

(72) Inventors: **Alan R. Mardinly**, Oakland, CA (US); **Madison D. Taylor**, Hillsborough, CA (US); **Alexandra Borog**, Fremont, CA (US); **Kevin S. Smith**, Fremont, CA (US); **Viktor Kharazia**, Berkeley, CA (US); **Thomas K. Roseberry**, Palo Alto, CA (US); **Jean-Charles Neel**, San Francisco, CA (US); **Emilienne M. Repak**, Oakland, CA (US); **Timothy J. Gardner**, Eugene, OR (US); **Max J. Hodak**, San Francisco, CA (US); **Sunny Y. Weber**, San Luis Obispo, CA (US)

(73) Assignee: **Neuralink Corp.**, Fremont, CA (US)

(21) Appl. No.: **17/545,843**

(22) Filed: **Dec. 8, 2021**

**Related U.S. Application Data**

(60) Provisional application No. 63/242,281, filed on Sep. 9, 2021.

**Publication Classification**

(51) **Int. Cl.**

*A61L 27/38* (2006.01)  
*A61N 1/05* (2006.01)  
*A61K 35/30* (2006.01)  
*A61P 25/28* (2006.01)

(52) **U.S. Cl.**

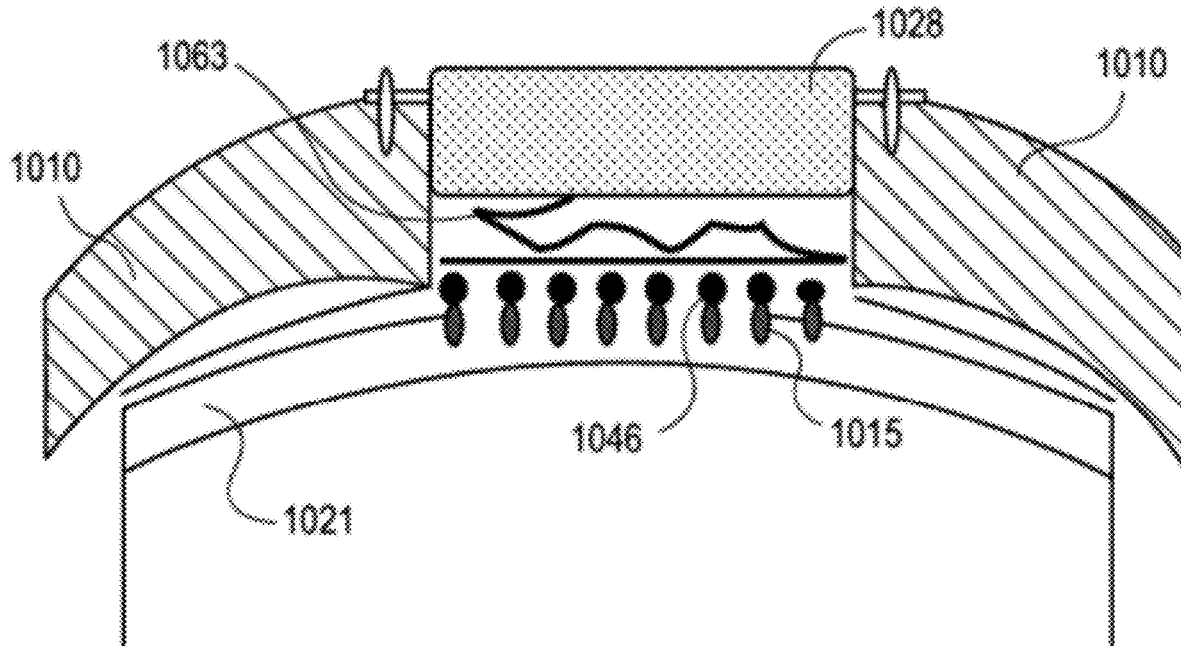
CPC ..... *A61L 27/383* (2013.01); *A61L 27/3895* (2013.01); *A61L 27/3834* (2013.01); *A61N 1/0531* (2013.01); *A61L 27/3878* (2013.01); *A61K 35/30* (2013.01); *A61P 25/28* (2018.01)

(57)

**ABSTRACT**

The disclosure provides a biological brain-computer interface comprising genetically modified cells engrafted onto an adult mammal (e.g., mouse) above cortical layer 1, forming an artificial cortical layer termed layer zero (L0). Following engraftment, L0 goes through a developmental process characterized by synchronous waves of activity that gradually recede to resemble spontaneous cortical activity. Axons and dendrites from L0 nondestructively infiltrated the host cortex and formed synaptic connections necessary for bidirectional communication with the brain.

**Implant 'tethered' cells: 100% juxtra recording yield**



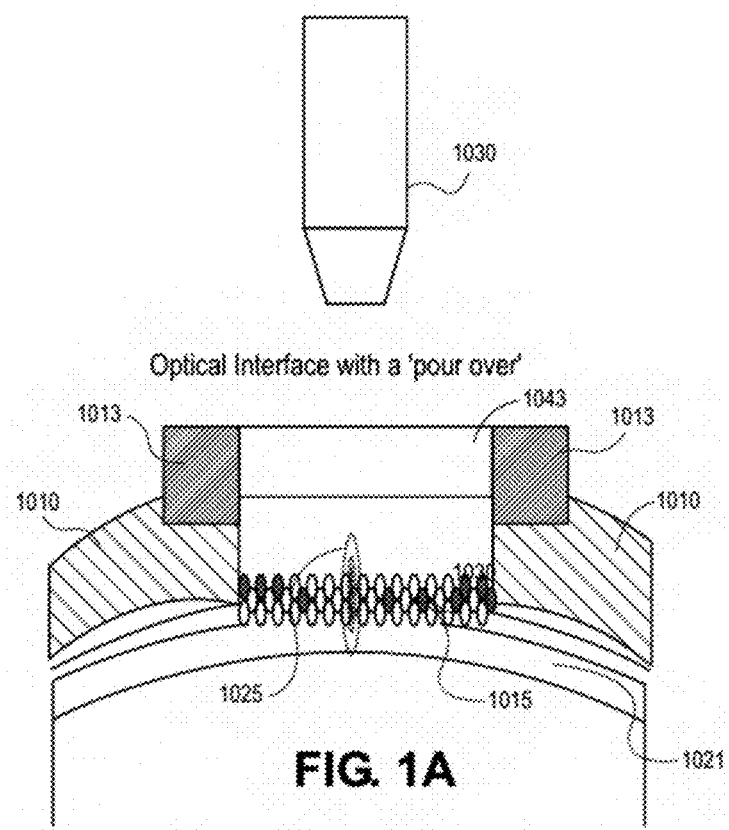


**FIG. 1A**

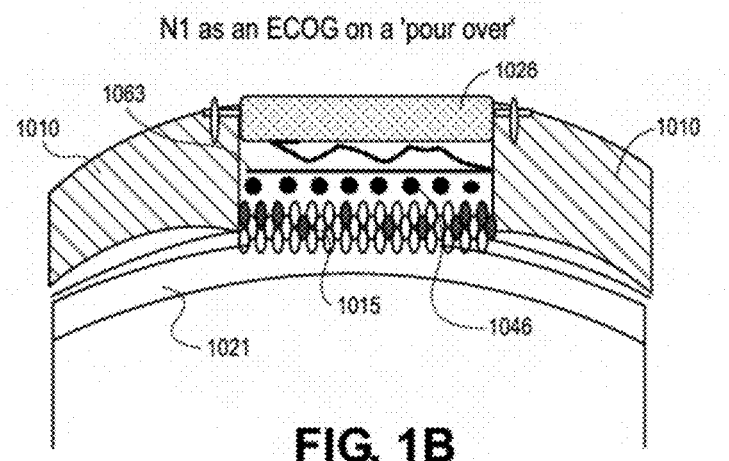


**FIG. 1B**

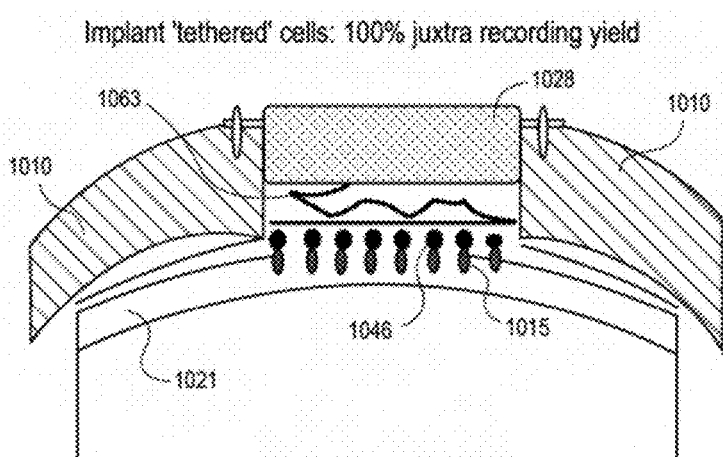


**FIG. 1C**

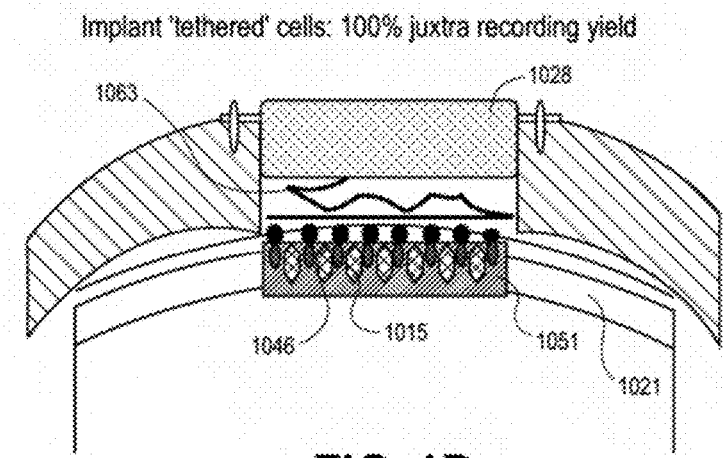


**FIG. 1D**

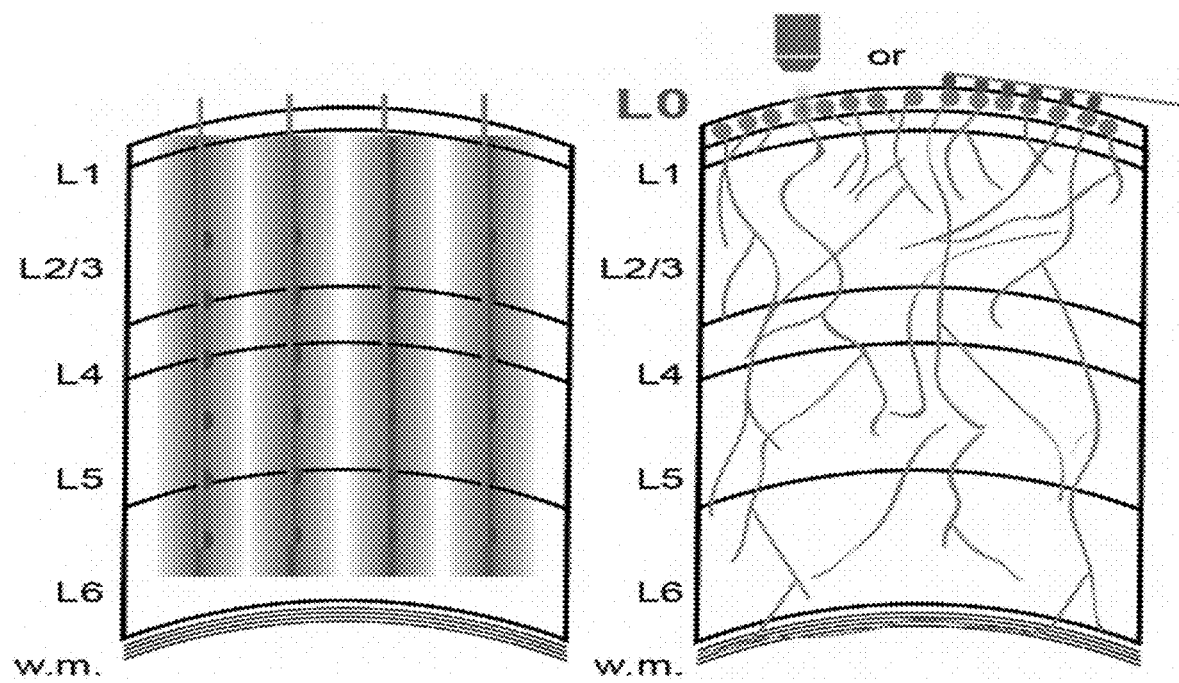


FIG. 1E

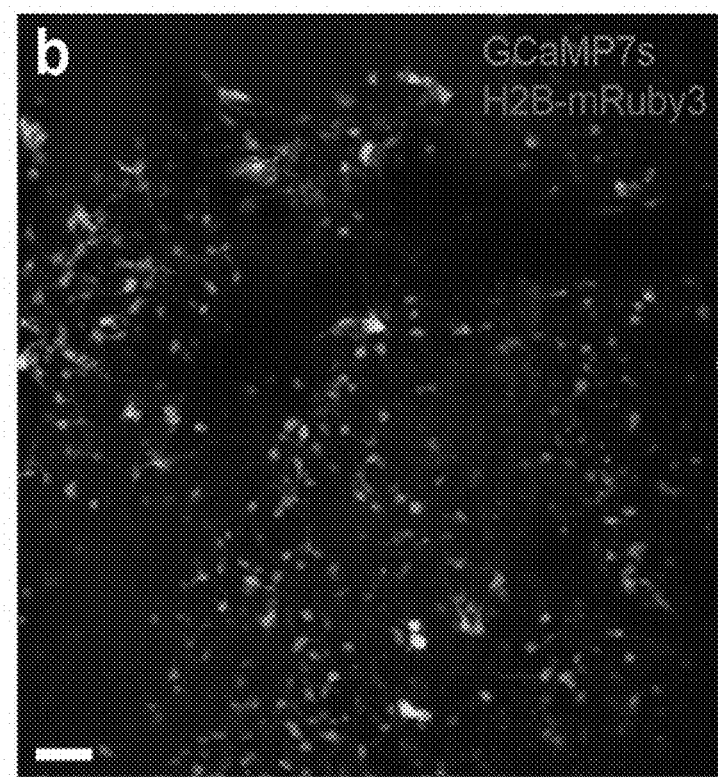


FIG. 1F

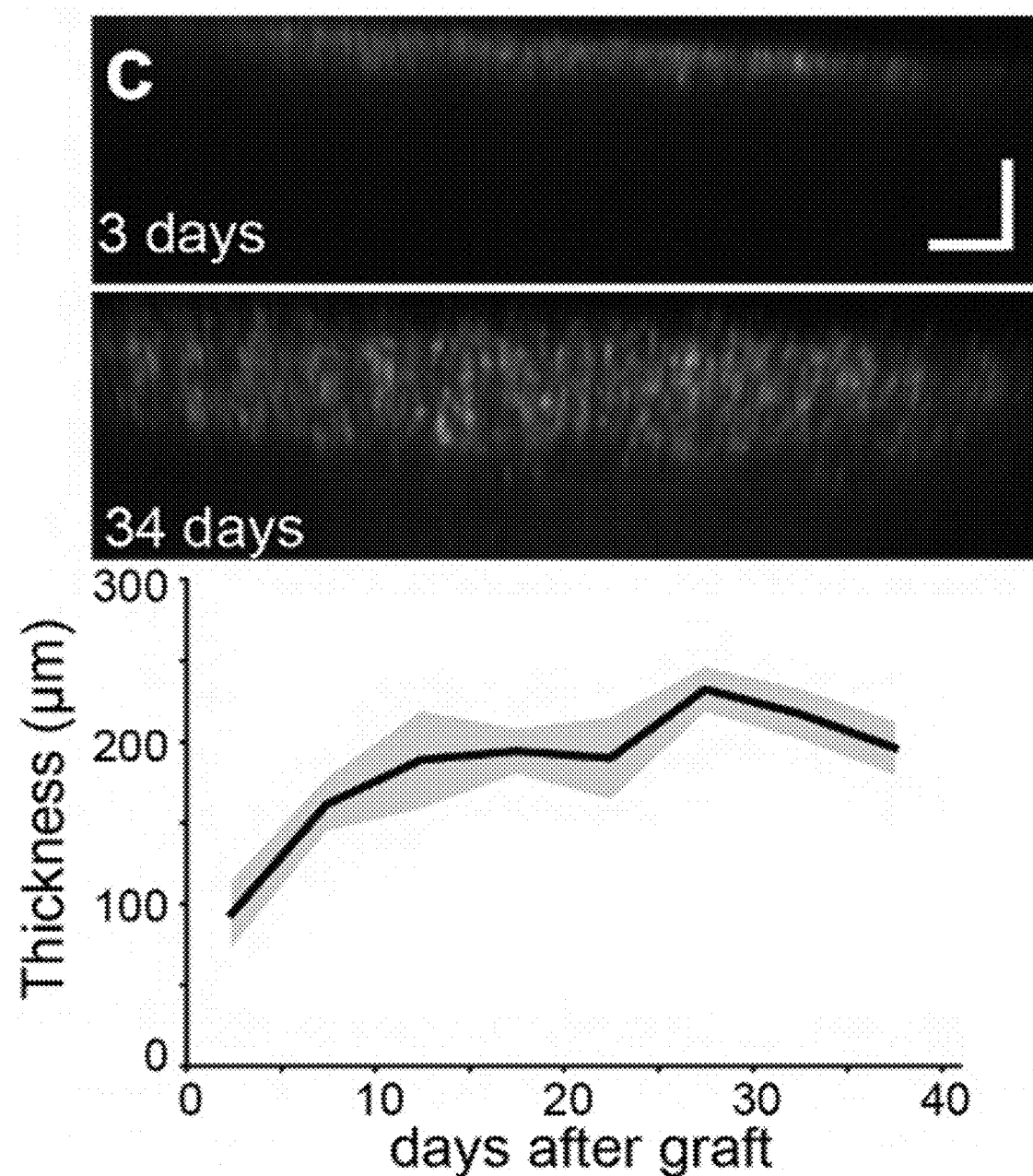


FIG. 1G

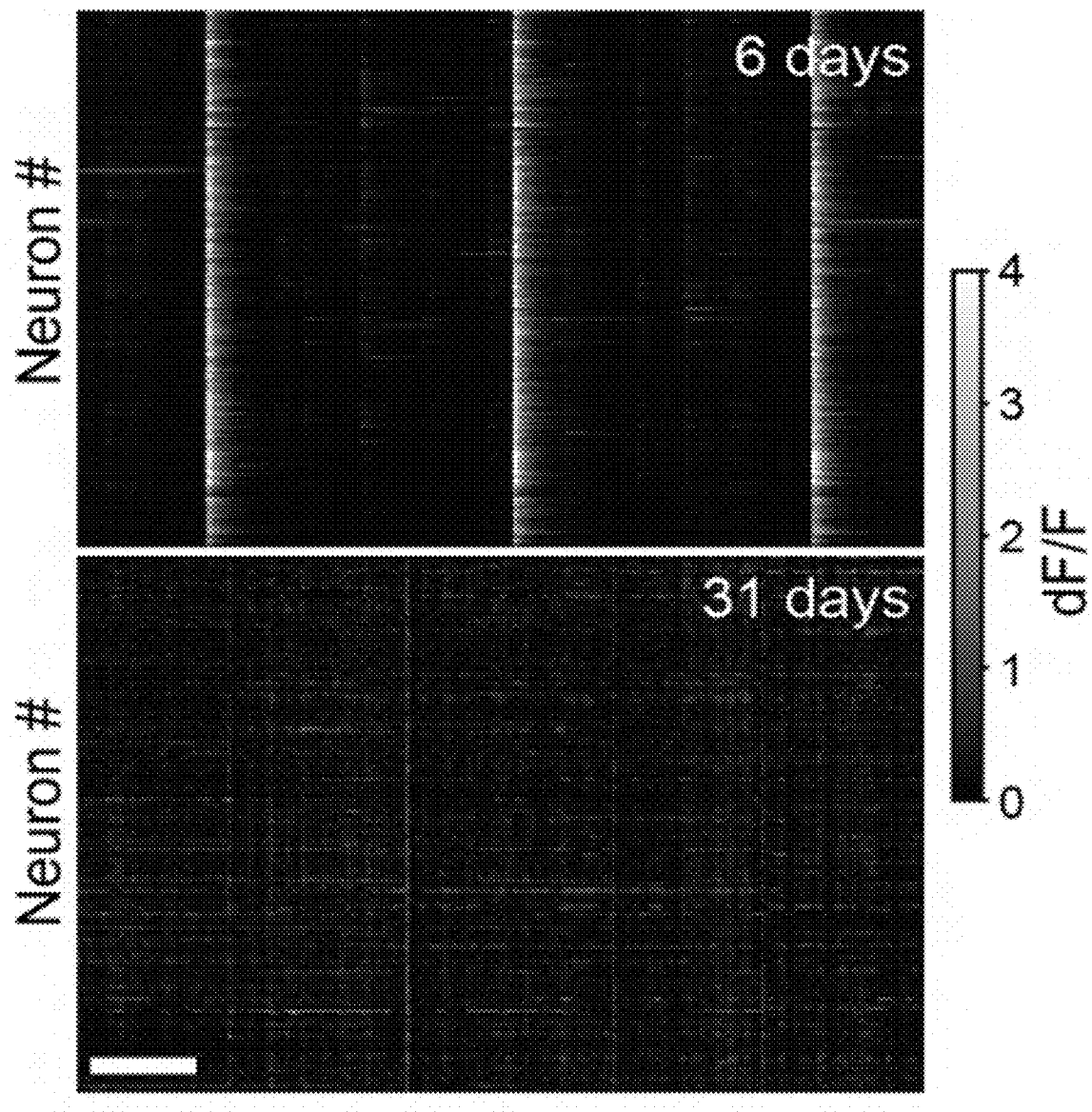


FIG. 1H

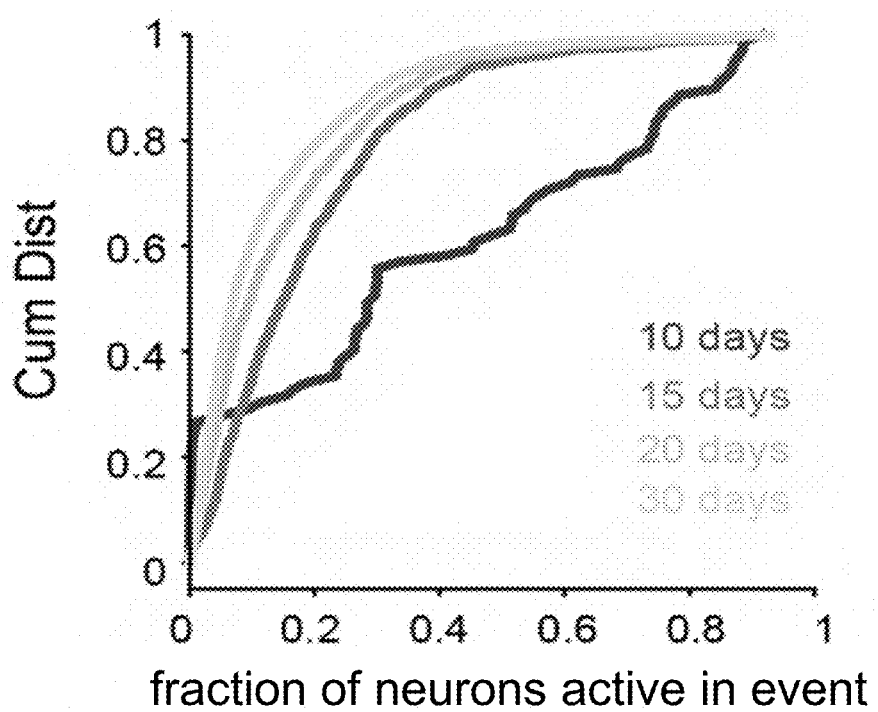


FIG. 1I

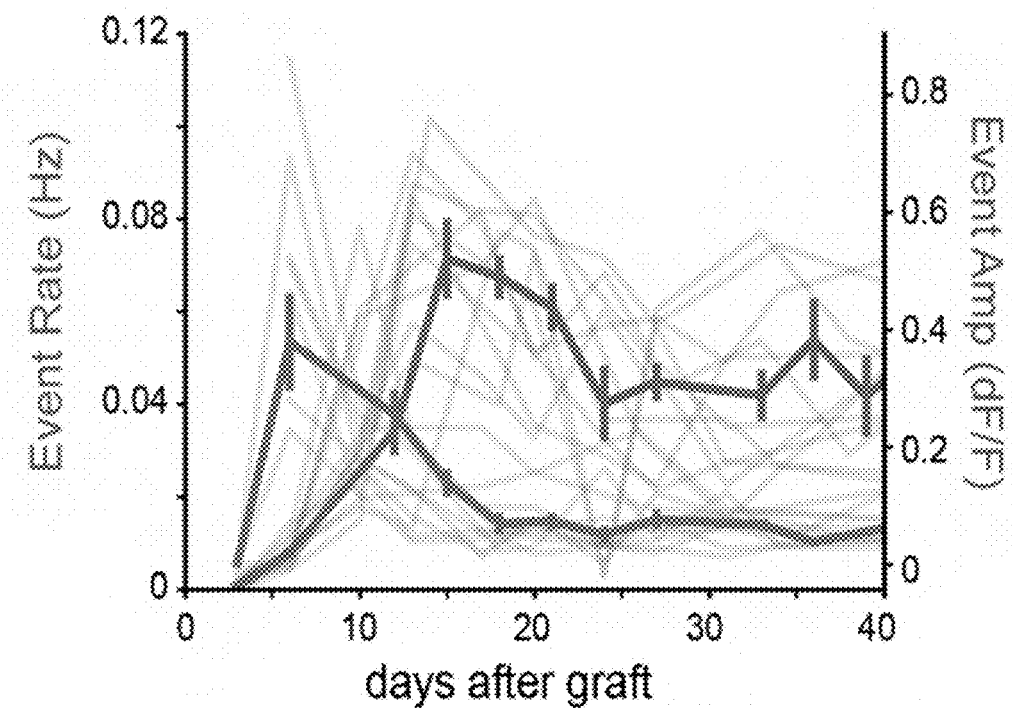


FIG. 1J

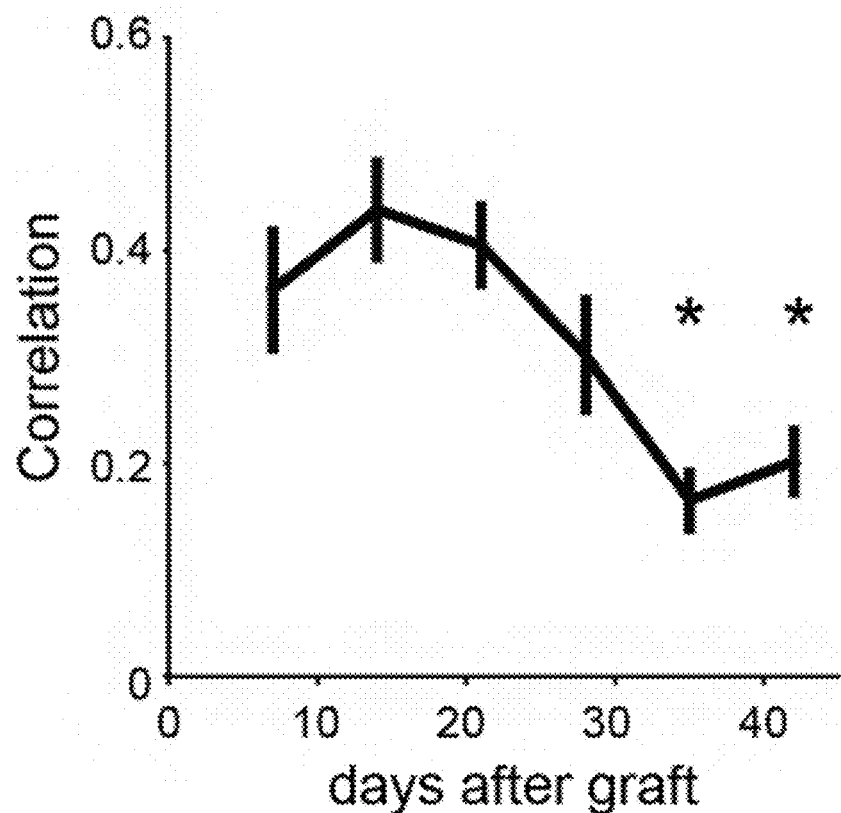


FIG. 1K

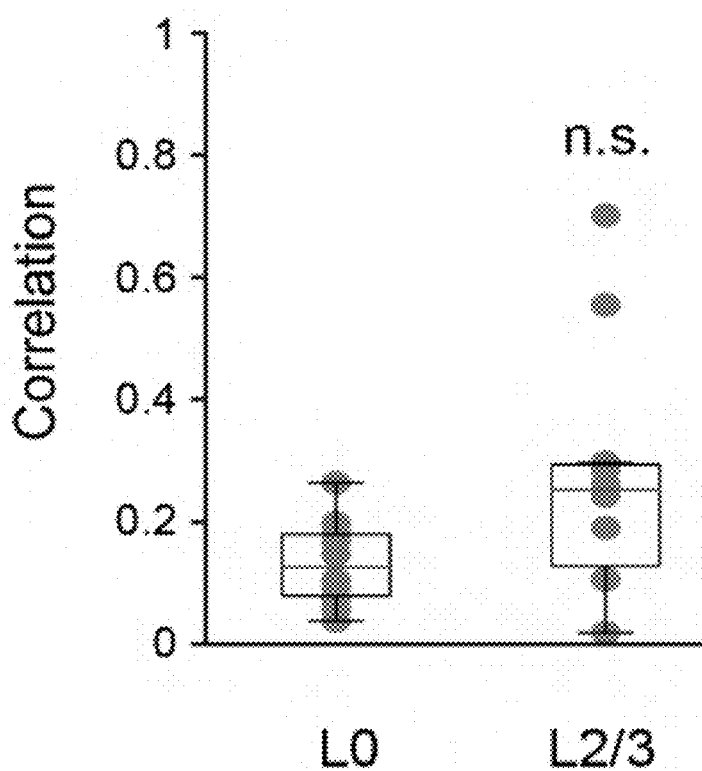


FIG. 1L

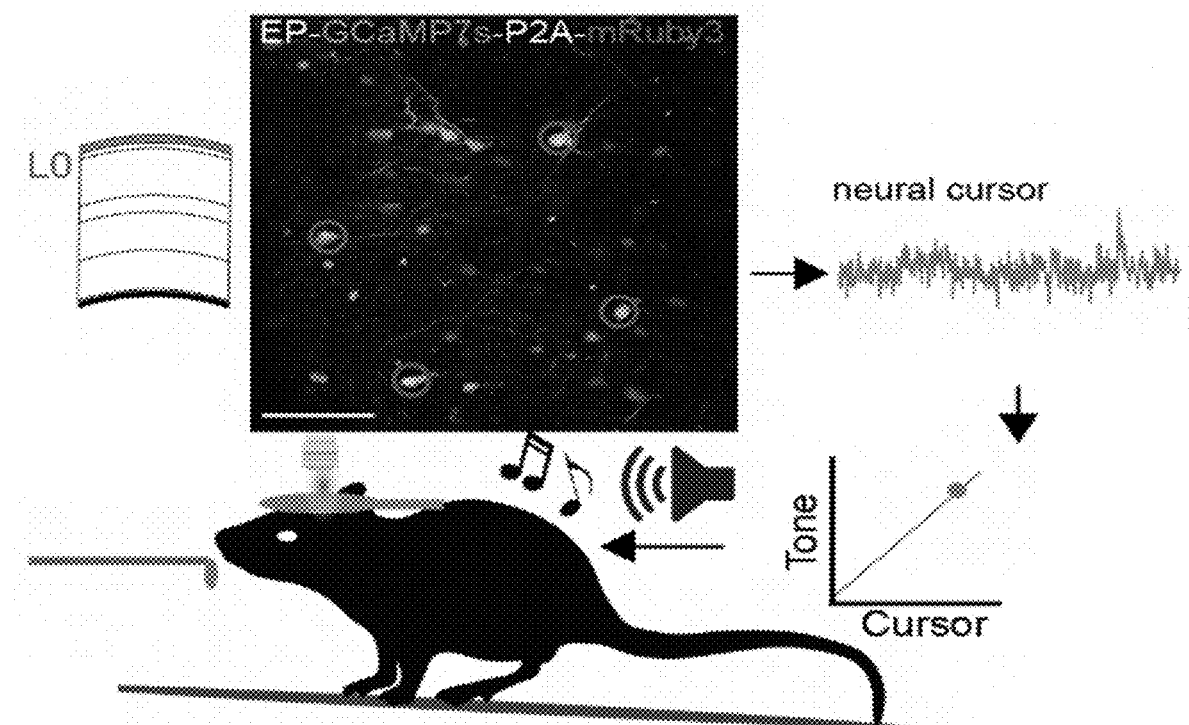


FIG. 2A

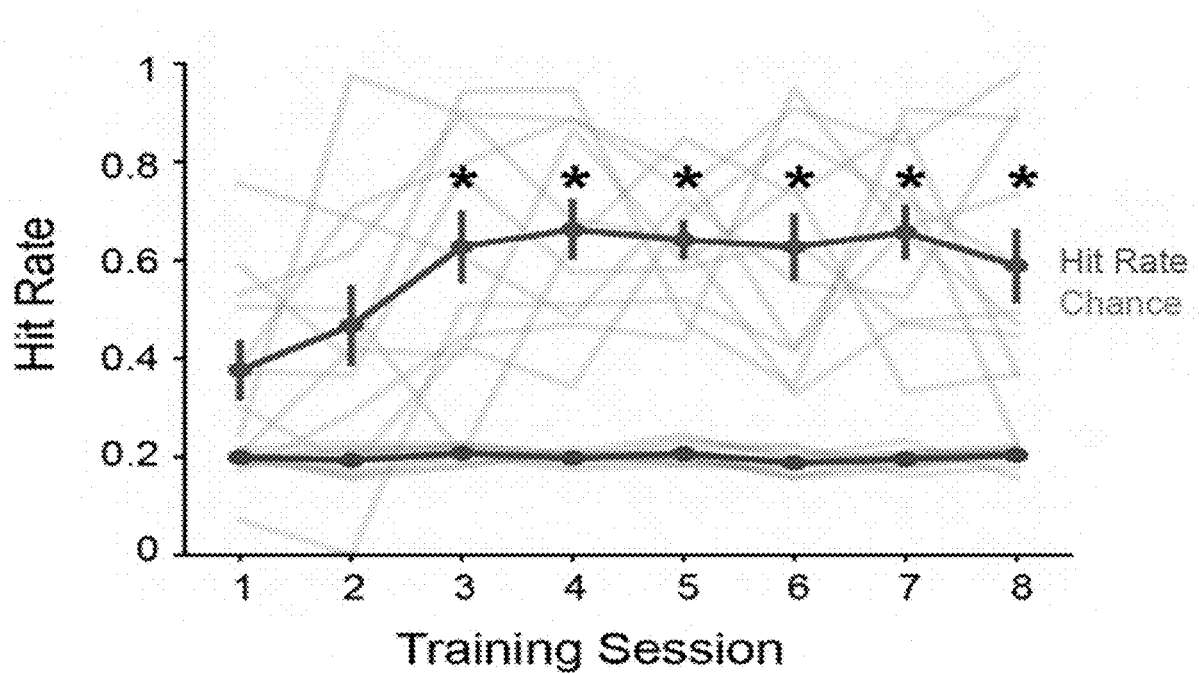


FIG. 2B

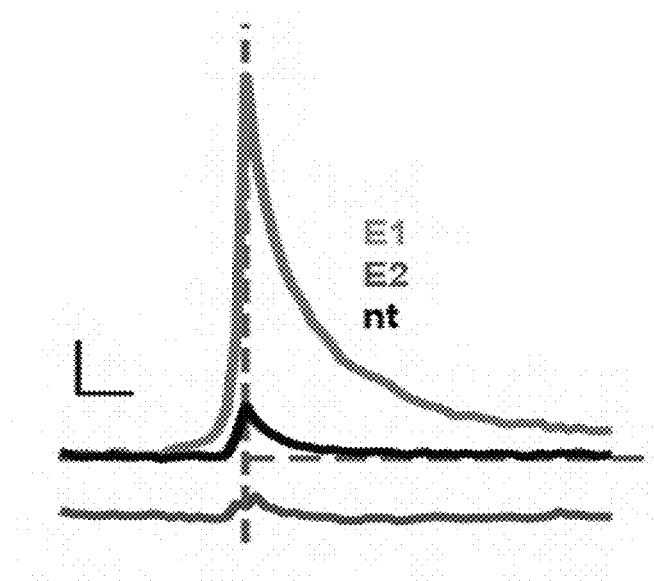


FIG. 2C

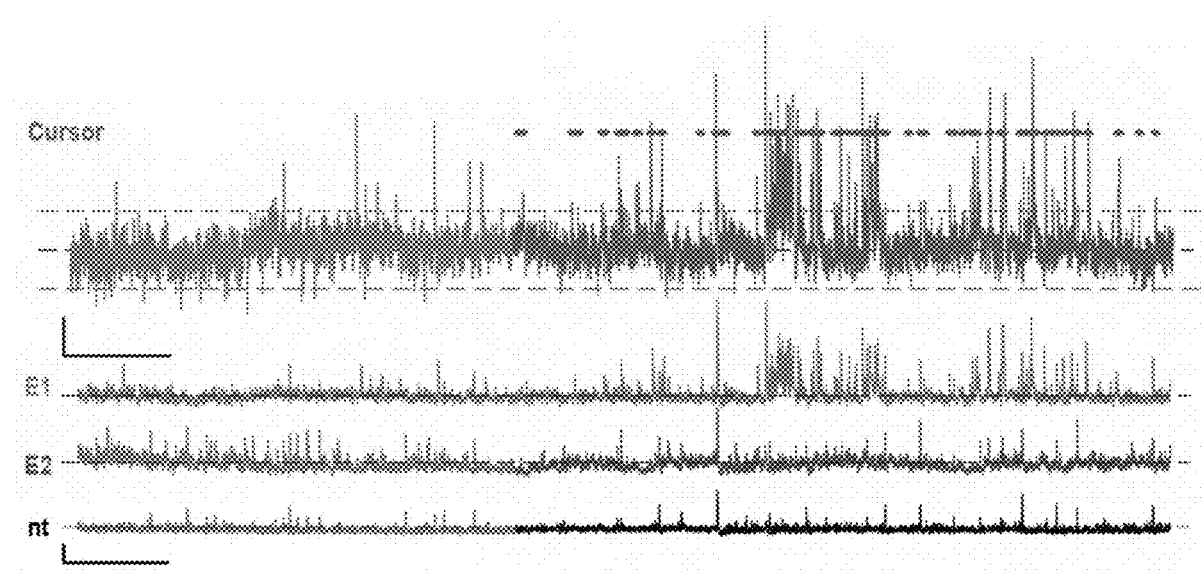


FIG. 2D

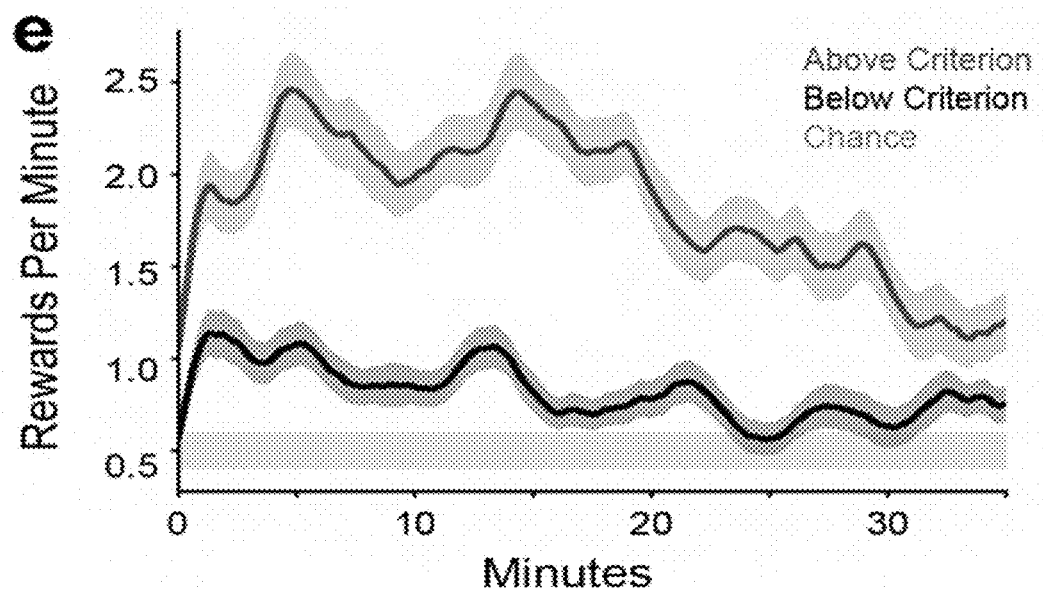


FIG. 2E

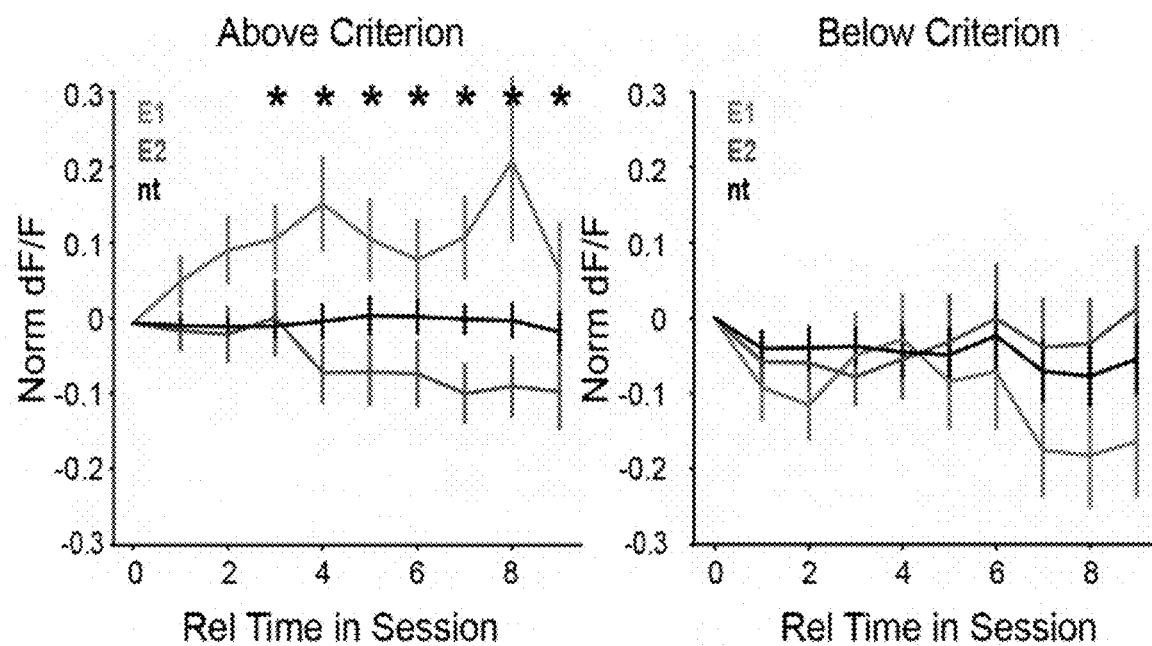


FIG. 2F

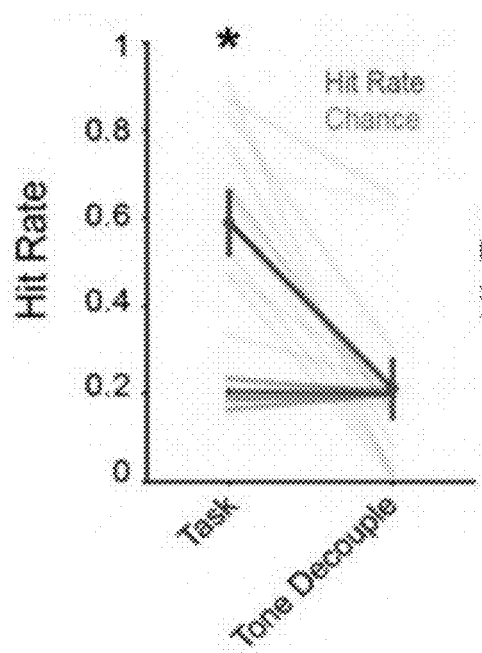


FIG. 2G

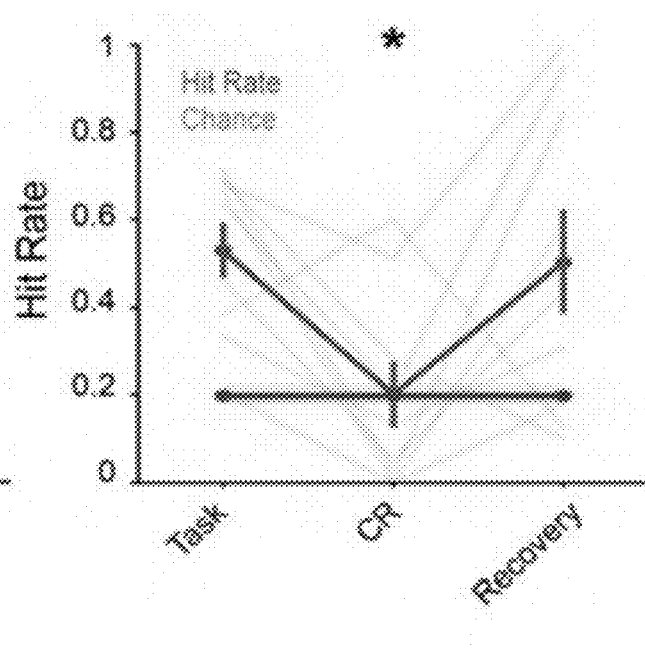


FIG. 2H

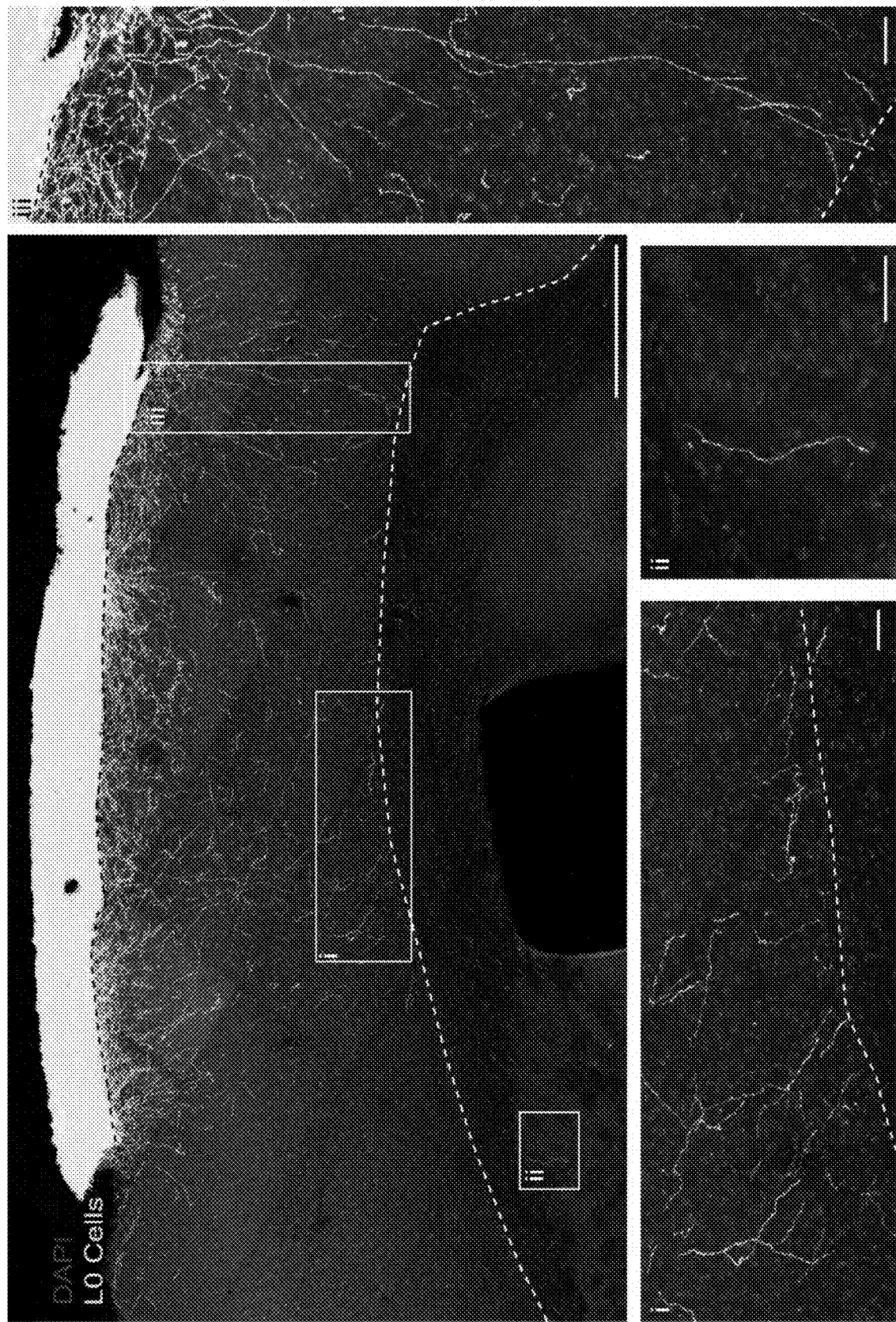


FIG. 3

FIG. 4A

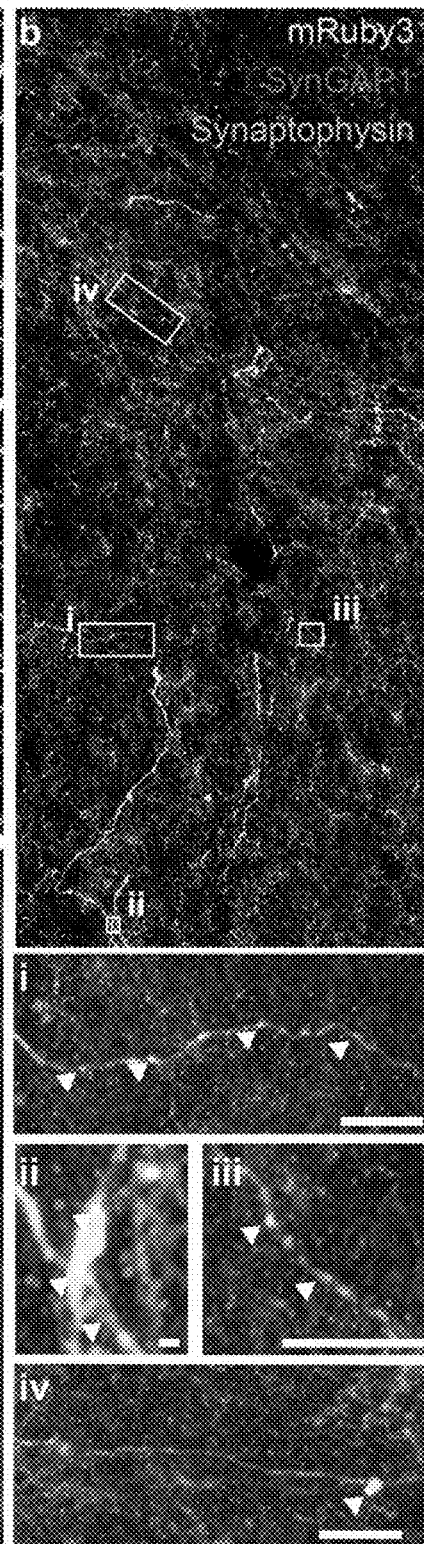
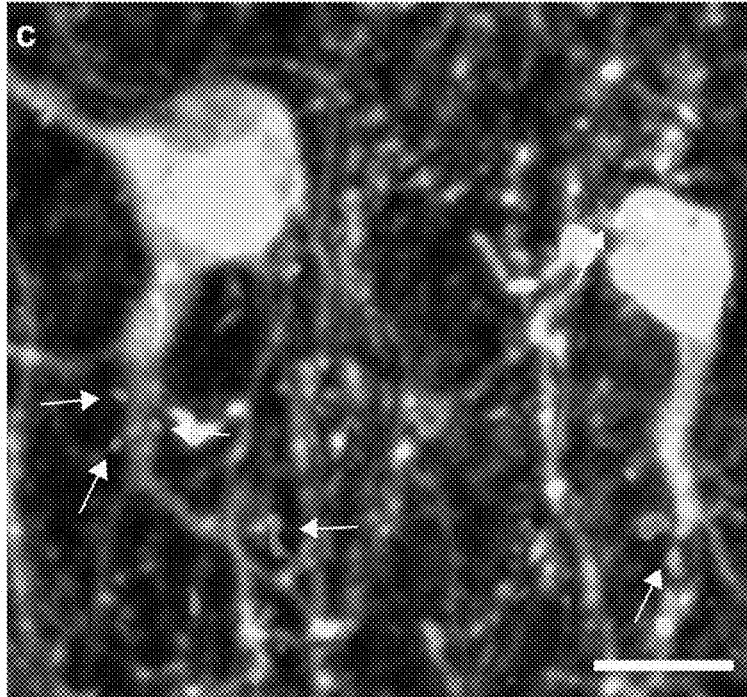
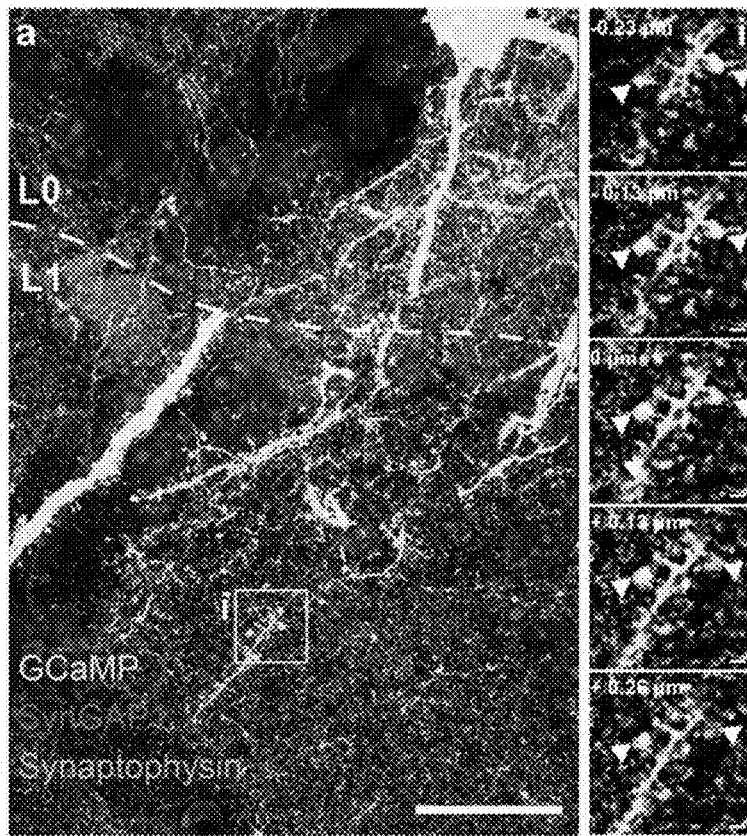


FIG. 4C

FIG. 4B

FIG. 5B

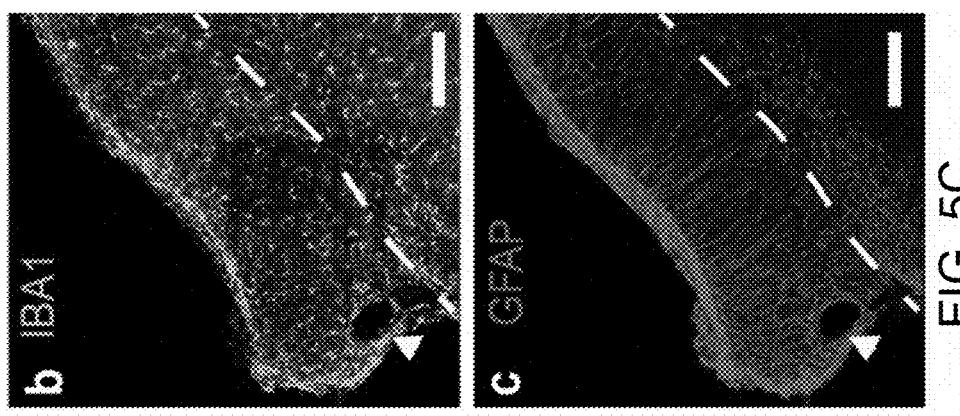


FIG. 5C

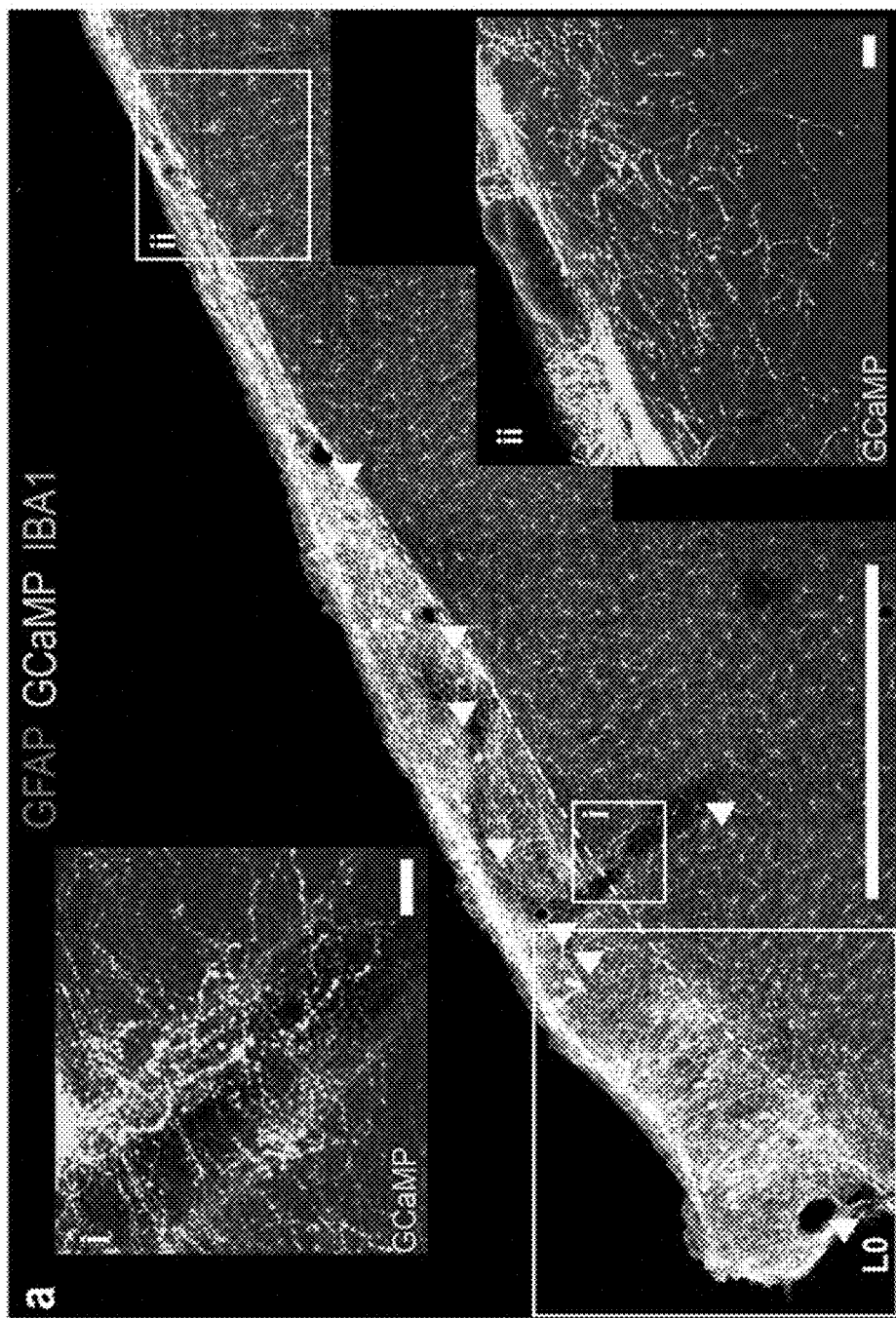


FIG. 5A

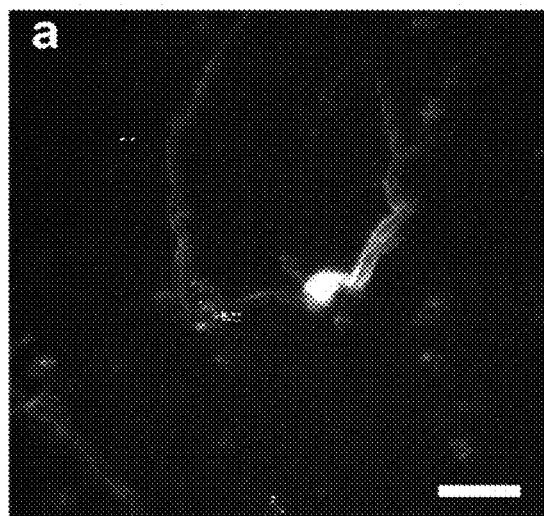


FIG. 6A

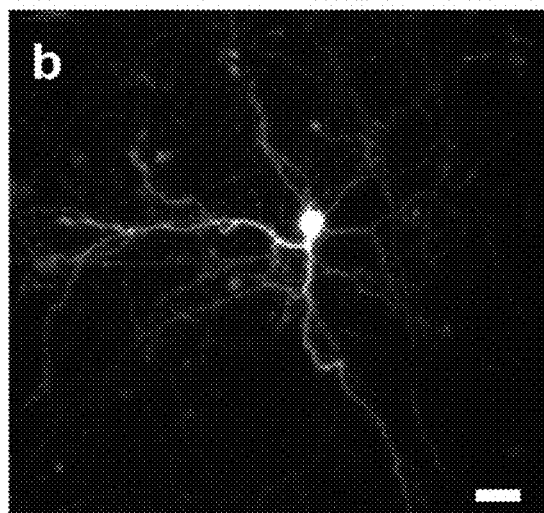


FIG. 6B

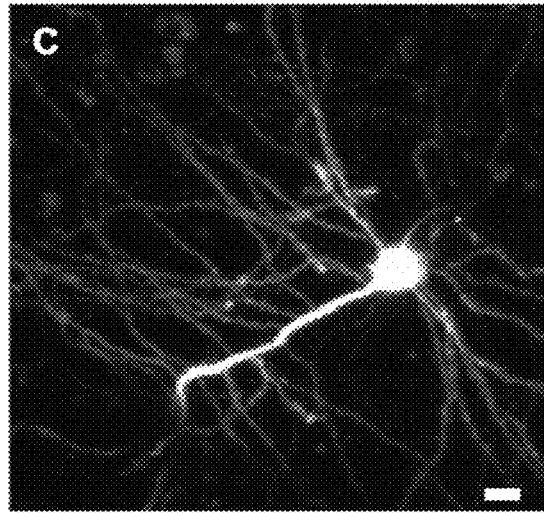


FIG. 6C

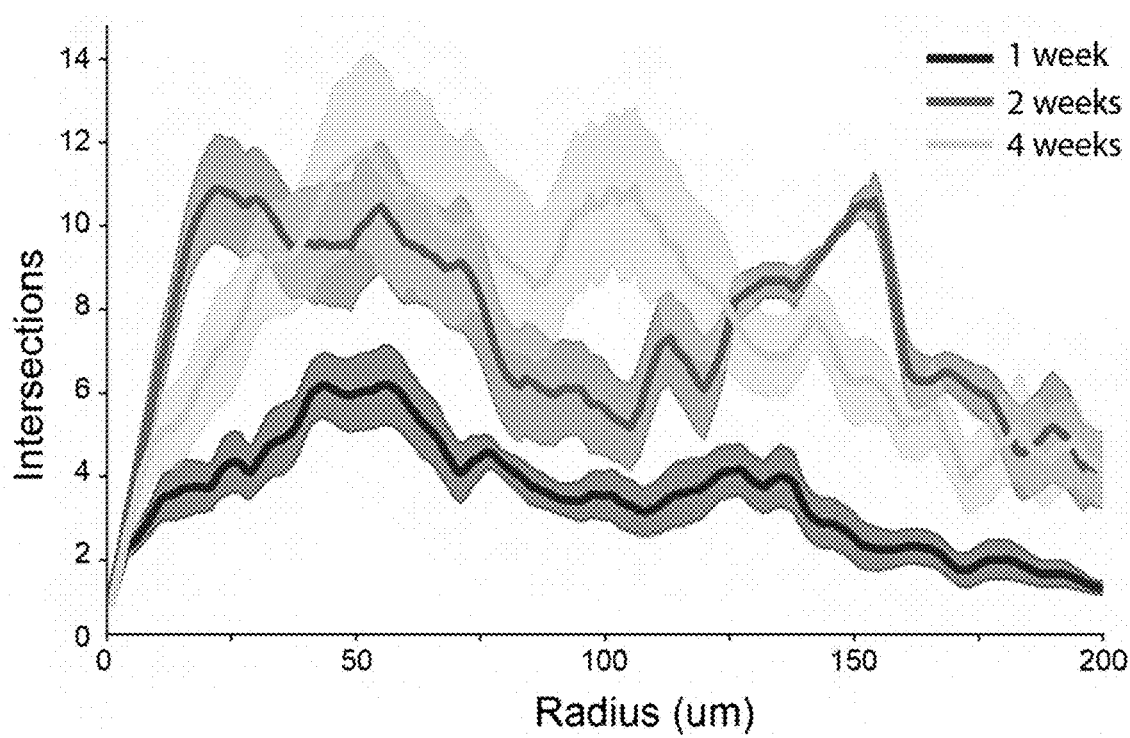


FIG. 6D

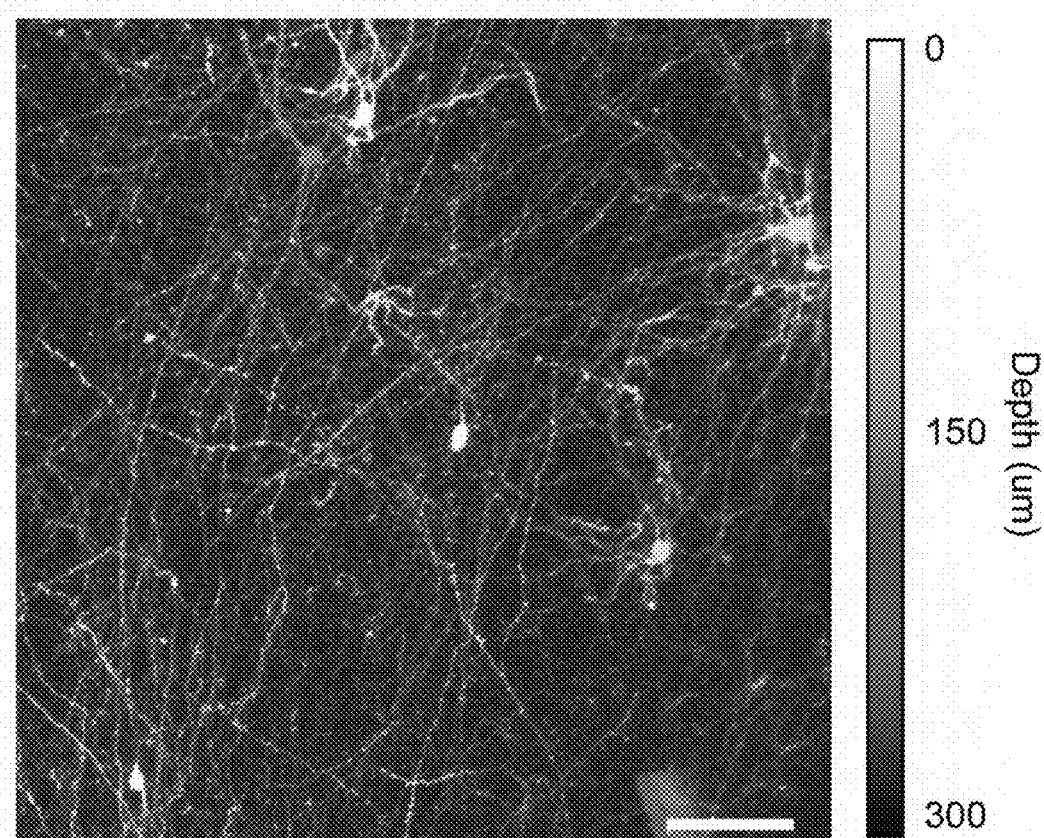


FIG. 6E

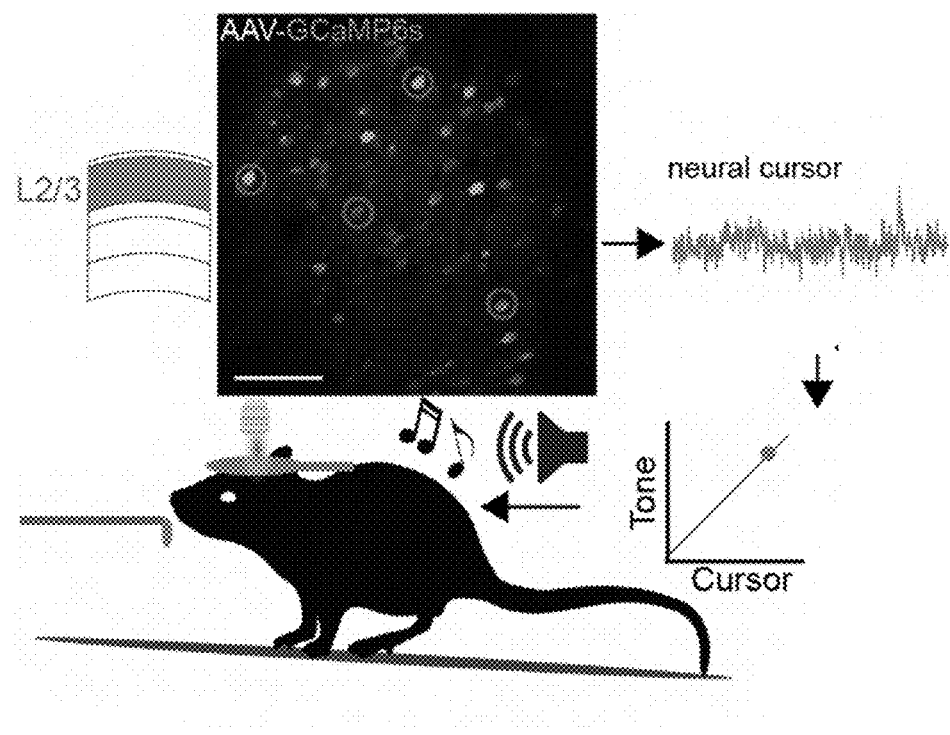


FIG. 7A

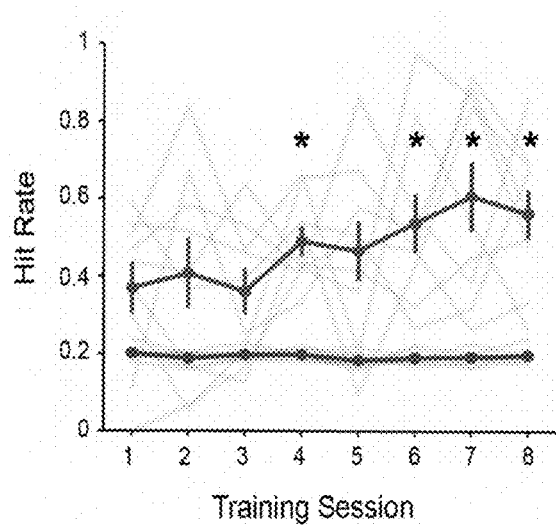


FIG. 7B

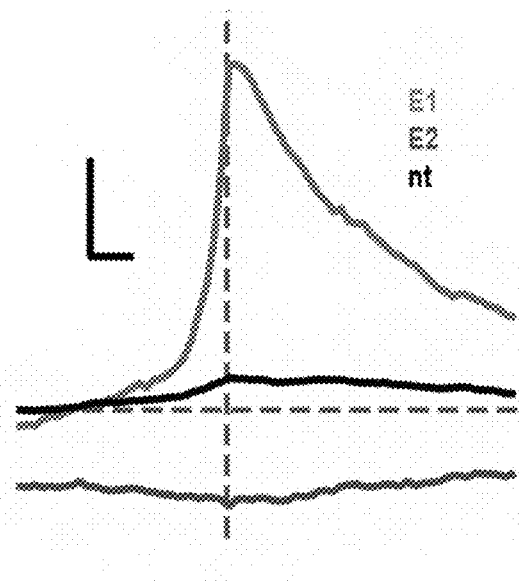


FIG. 7C

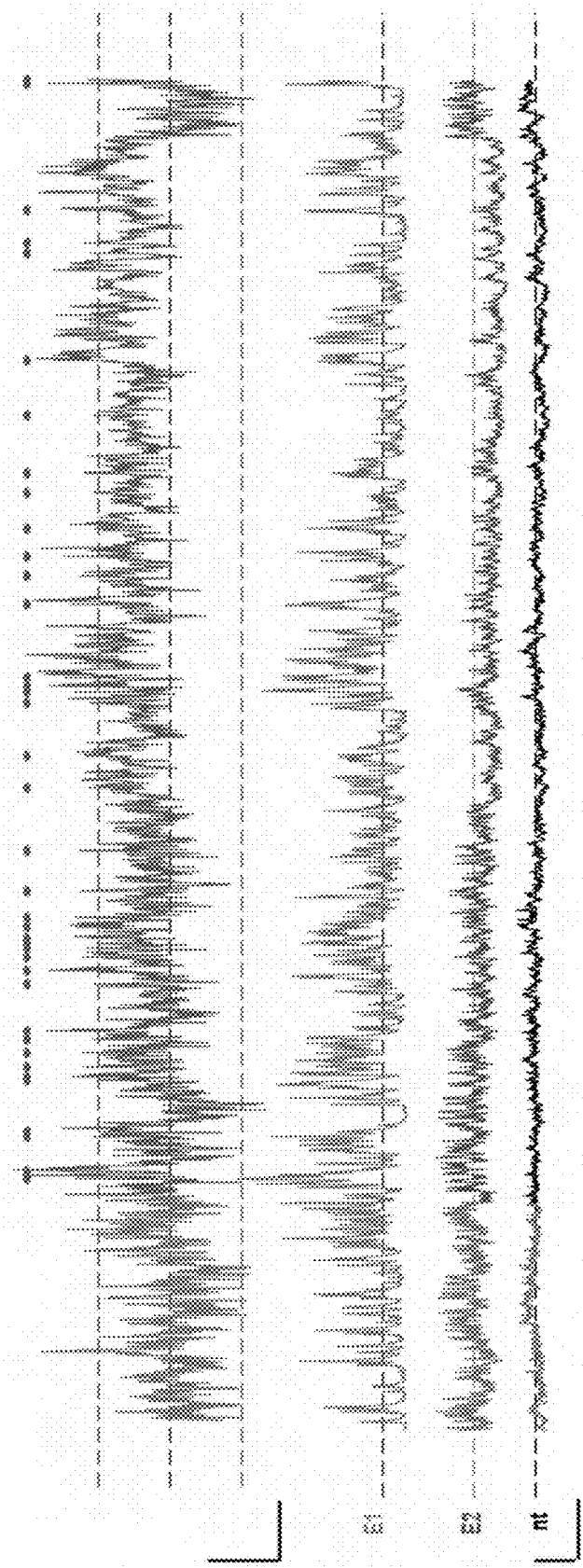


FIG. 7D

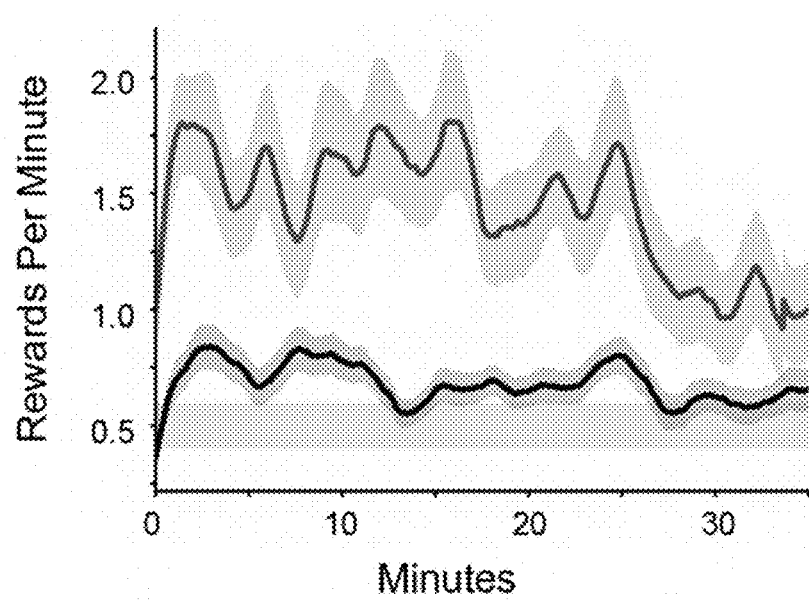


FIG. 7E

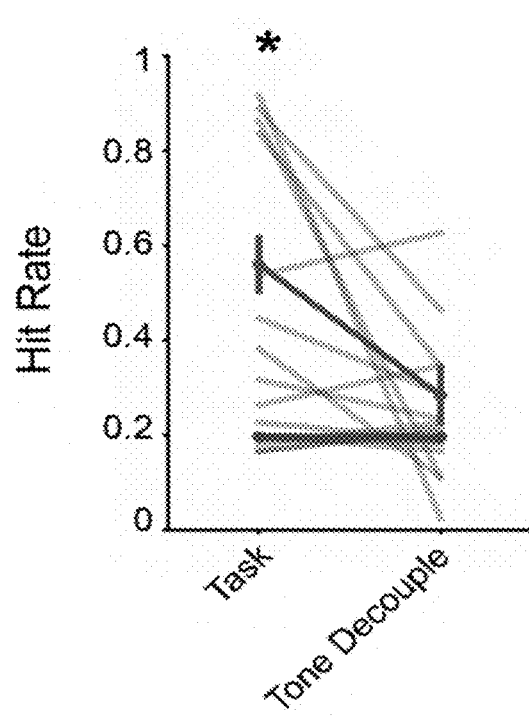


FIG. 7F

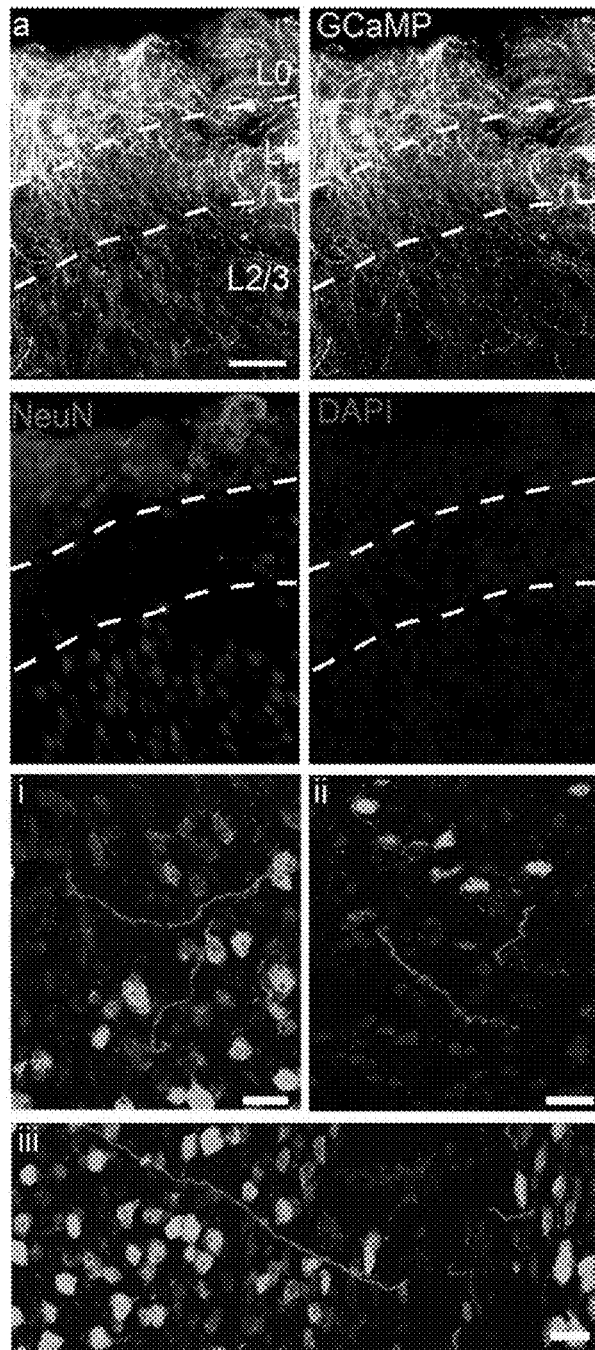


FIG. 8A

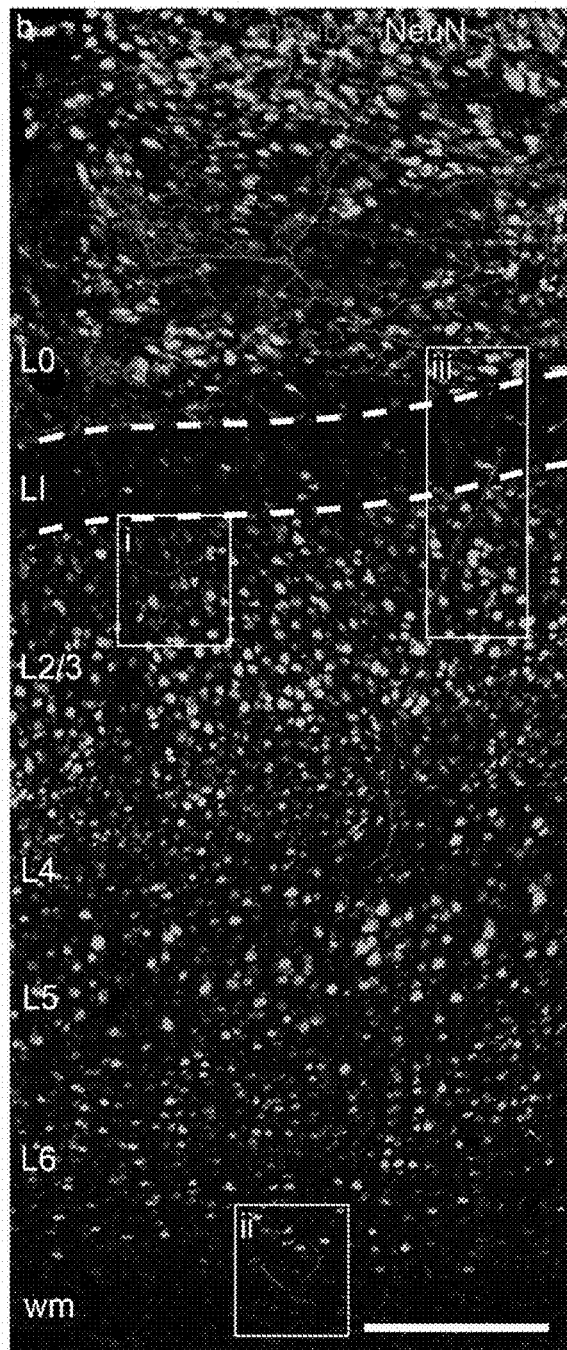


FIG. 8B

FIG. 9A

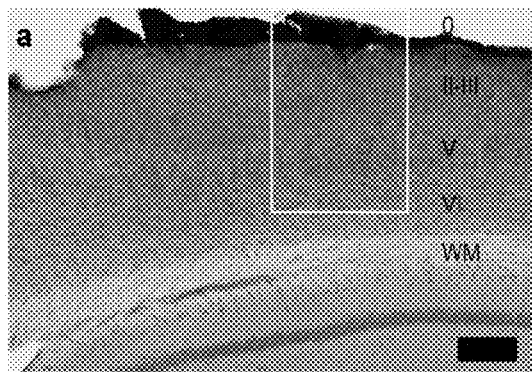


FIG. 9C

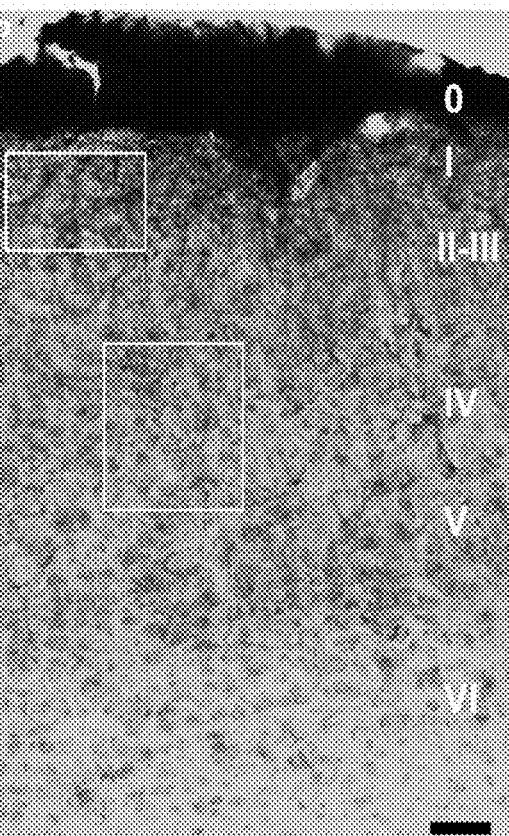
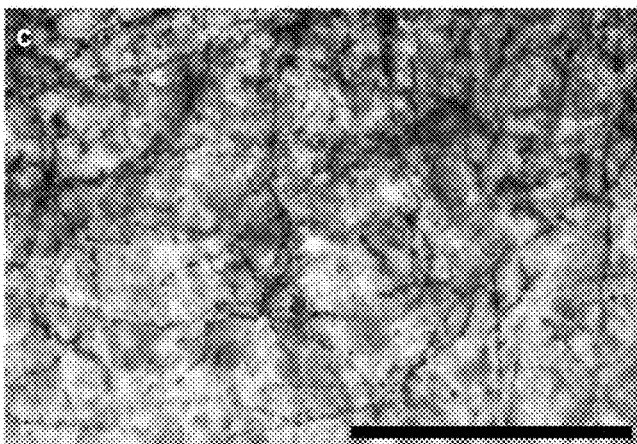


FIG. 9D

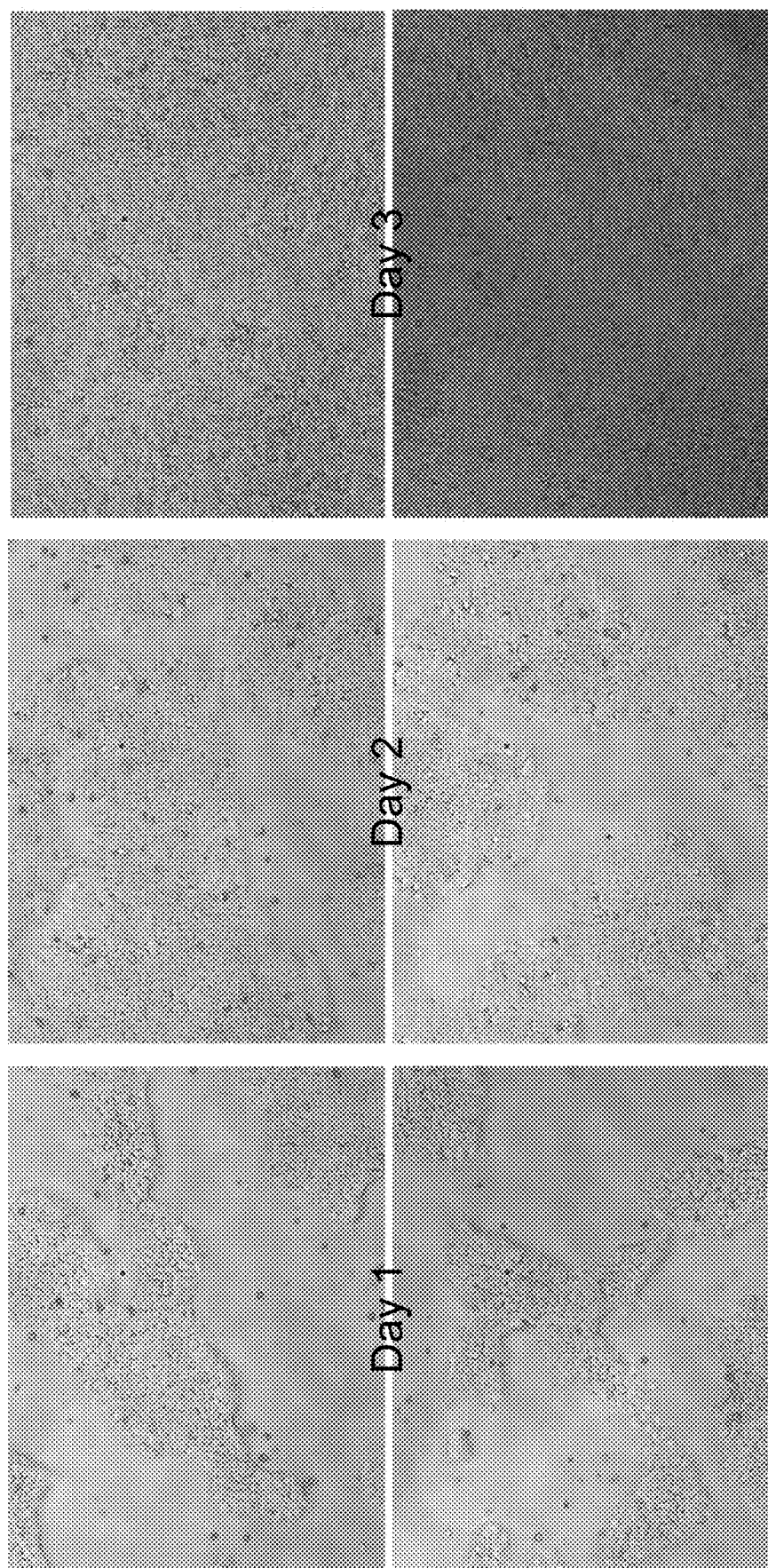


FIG. 10 A

FIG. 10 B

FIG. 10 C

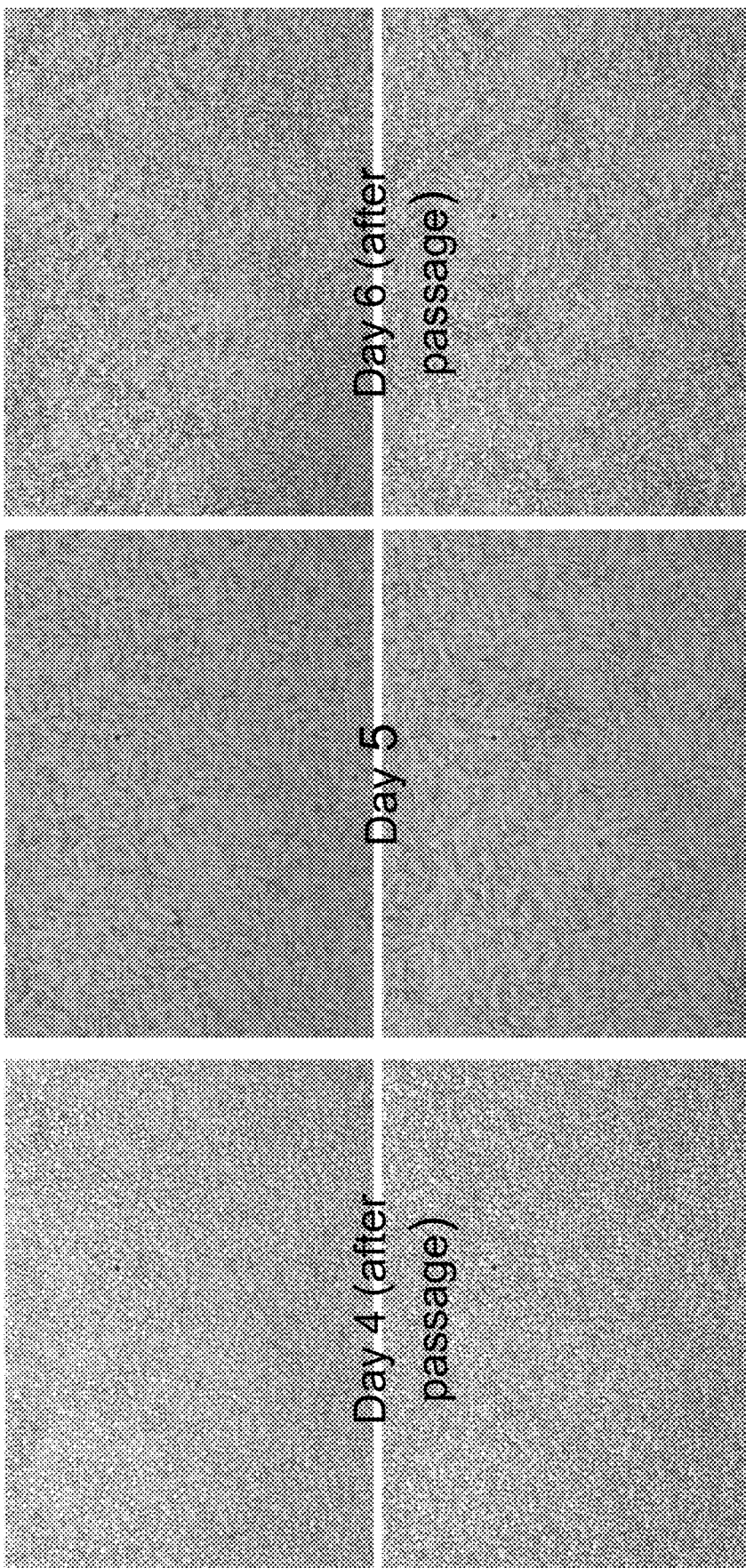


FIG. 10 D

FIG. 10 E

FIG. 10 F

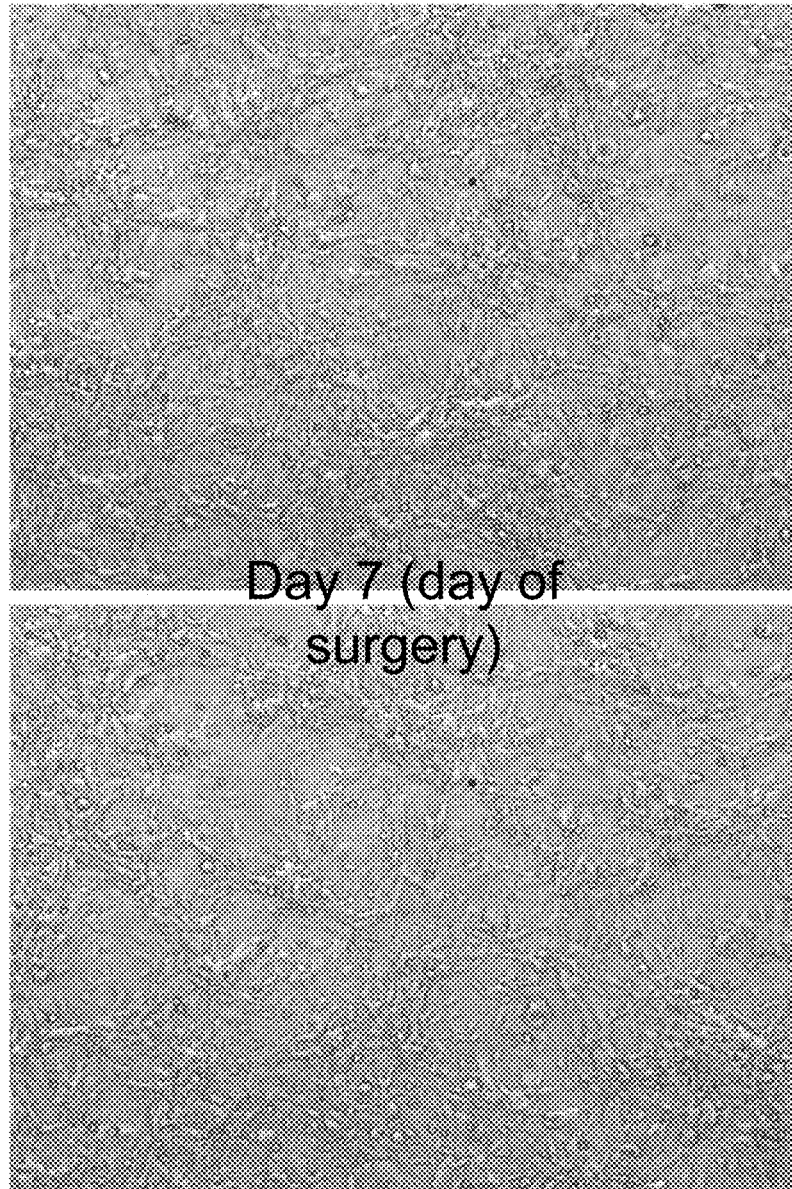


FIG. 10G



FIG. 11B

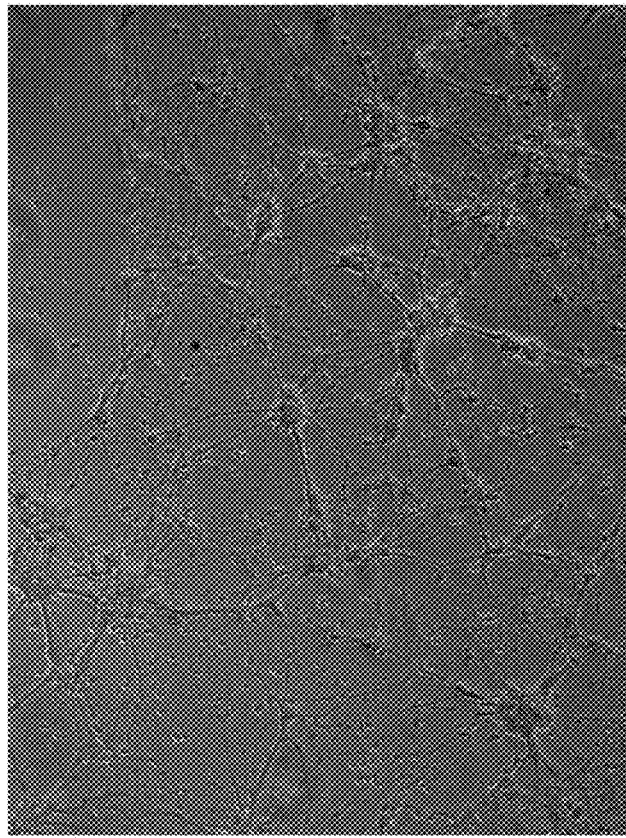


FIG. 11A

## CELL-BASED BRAIN-MACHINE INTERFACE

### CROSS-REFERENCE TO RELATED APPLICATIONS

[0001] The present application claims priority to U.S. Provisional Application No. 63/242,281, filed Sep. 9, 2021, the disclosure of which is hereby incorporated by reference in its entirety for all purposes.

### BACKGROUND

[0002] There are numerous challenges to scaling brain-machine interfaces (BMIs) to achieve bidirectional communication with the millions of neurons likely needed to seamlessly interface humans with technology. A stable, very high-bandwidth interface between human brains and computers would enable therapies for neurological disorders and reduce the bottleneck of information transfer between the biological and digital domains.

[0003] Non-invasive BMIs can extract useful information from bulk optical or electrical signals spatially distributed across the cranium, but these signals represent the summed and convolved activity of millions of neurons, making non-invasive devices poor candidates for high-bandwidth communication. Recording from the brain surface, as in electrocorticography (ECoG) recordings, improves signal quality and allows more impressive demonstrations of neural decoding. However, these recordings still mix signals from thousands of neurons and only rarely record action potentials due to the paucity of neurons in cortical layer 1 (L1). In contrast, penetrating intracortical BMIs communicate with the brain at the level with which it functions i.e., specific action potentials from specific neurons. This enables penetrating BMIs to achieve bit rates that enable useful neurally-controlled typing.

[0004] However, stably recording from a large number of channels via penetrating implants is challenging as each penetration of the brain displaces tissue, limiting the scale at which intracortical arrays can be deployed. For traditional stiff arrays, damage from probe penetrations disrupts microvasculature and activates neuroimmune cells, leading to biofouling, formation of a glial scar, and fibrotic encapsulation. Recently, a new generation of fine and flexible electrode arrays have been developed to mitigate the biological response to implantation. Decoupling the stiffness required for insertion from the array allows use of materials better matched to the physical properties of brain tissue. These implants have improved damage profiles that allow for stable recordings with increased channel count relative to previous chronically implanted electrode arrays. While flexible probes cause less cortical damage and disruption of the blood-brain barrier than stiff penetrating electrodes, tissue displacement is likely to become a prohibitive obstacle to scaling them to record from millions of neurons. Additionally, since electrical stimulation of the brain through implanted electrode arrays excites both axons and cell bodies, the activated neurons are spatially distributed and extremely sensitive to small changes in stimulation parameters. Together, these obstacles represent significant challenges to developing stable ultra-high-bandwidth bidirectional BMIs.

[0005] Biological approaches have been deployed in conjunction with conventional recording techniques in an

attempt to ameliorate these challenges. For instance, electrodes that coax neurons to grow into a glass pipette using neurotrophins showed promise for improving recording longevity. Coating neural probes with cell-surface proteins has reduced the foreign body response and shown promise for improving recording quality. Extending this line of investigation, neural probes seeded with neural progenitor cells were implanted in the hopes of providing trophic support to damaged cells and providing a biocompatible surface to reduce the glial foreign body response. Alternatively, using calcium imaging, BMIs can record from large numbers of neurons without invasive electrodes, an approach that has recently gained traction in large animal models. However, this carries the very significant drawback of requiring viral infection of a large neural population.

[0006] There is a need in the art for new brain-machine interfaces (BMI) that use living neuronal cells optionally coupled to electrodes that communicate to an external device. The current disclosure satisfies this need and offers other advantages as well.

### BRIEF SUMMARY

[0007] In one embodiment, the present disclosure provides a brain-computer interface (BCI) engrafted on a brain of a mammal, the BCI comprising:

[0008] a cortical graft layer comprising a plurality of neuronal cells transplanted on a brain's cerebral cortex, wherein the plurality of cells engraft on the brain and respond to an external stimulus with a detectable signal.

[0009] In another embodiment, the present disclosure provides a method for bi-directional communication between a brain-computer interface (BCI) engrafted on a brain of a mammal and a computer, the method comprising:

[0010] providing a cortical graft layer comprising a plurality of neuronal cells transplanted on a brain's cerebral cortex of the mammal; and

[0011] providing an external stimulus to the mammal wherein the plurality of cells engrafted on the brain respond to an external stimulus with a detectable neural signal.

[0012] In still another embodiment, the present disclosure provides a method of connecting a biological brain-machine interface with a subject, the method comprising:

[0013] depositing neuronal cells onto a cortical surface of a brain of a subject, the cells being selected to emit light or an electrical signal in response to a neural signal;

[0014] allowing the cells to form an additional cortical layer that grows and integrates into the brain; and

[0015] recording light or an electrical signal emitted from the cells in response to a neural signal in the brain.

[0016] In still yet another embodiment, the present disclosure provides a method of stimulating a brain with a biological brain-machine interface, the method comprising:

[0017] depositing neuronal cells onto a cortical surface of a brain of a subject, the cells being selected to convert light or an electrical signal to an electrical signal compatible with neurons in the brain;

[0018] allowing the cells to form an additional cortical layer that grows and integrates into the brain;

[0019] directing light at or an electrical signal to the cells in the additional cortical layer such that the cells convert the light or the electrical signal to a neural signal; and

[0020] measuring a response or a behavior of the subject correlated with the directed light or electrical signal.

[0021] These and other objects, aspects and embodiments will become more apparent when read with the detailed description and figures which follow.

#### BRIEF DESCRIPTION OF THE DRAWINGS

[0022] FIG. 1A-1D show various embodiments of a Brain Machine Interface (BMI) using an optical approach (FIG. 1A); an approach using a ECoG and pour-over cells (FIG. 1B); an approach using tethered cells (FIG. 1C); and an approach using embedded cells in a polymer (FIG. 1D).

[0023] FIG. 1E is a schematic illustrating damage to the cortex done by penetrating electrodes (left) and an alternative scheme to transplant an artificial cortical L0 that is easily accessible to recording devices and non-traumatically penetrates the brain (right).

[0024] FIG. 1F is an example 2P image of L0 3 days after engrafting. Cells are electroporated with pCAG-GCaMP7s-P2A-H2B-mRuby3. Scale bar is 100  $\mu$ m.

[0025] FIG. 1G is an example XZ projections of L0 3 (top) and 34 (middle) days after engraftment (red: H2B-mRuby3, green: GCaMP7s). Bottom, graph showing thickness of L0 versus days after engraftment (n=11 mice). X and Z scale bars are both 100  $\mu$ m. Data are the mean $\pm$ s.e.m. of all observations from n=11 mice in a five day sliding window.

[0026] FIG. 1H is a representative raster plots of spontaneous activity from L0 neurons 6 (top) or 31 (bottom) days after engraftment. Graphs show dF/F for neurons (y-axis) vs time (x-axis). Scale bar is 1 minute.

[0027] FIG. 1I is a cumulative distribution showing the fraction of neurons active in each population event. Shaded bars denote events from different time periods after analysis. Data represent events from n=11 mice.

[0028] FIG. 1J is a graph showing the L0 population event rate (Hz, green) versus event amplitude (purple, dF/F) over time. Thick lines indicate mean $\pm$ s.e.m. of all observations from n=11 mice in a five day sliding window.

[0029] FIG. 1K is a graph showing the mean pairwise correlation of L0 neurons over time. Data are the mean $\pm$ s.e.m. of n=11 mice (\* indicates p<0.05, Kruskal-Wallis with Dunn's post-hoc test).

[0030] FIG. 1L is a boxplot of the mean pairwise correlation of neurons in L0 (left—electroporated GCaMP7s, n=11 mice) or L2/3 (viral GCaMP6s, n=9 mice) before the first behavioral training session (p=0.053, two-sided t-test).

[0031] FIG. 2A is a schematic illustrating optical BMI task where calcium signals from L0 are transformed into a neural cursor corresponding to a tone which is played back to the animal. A water reward is administered when the cursor hits a threshold level. Image is the field of view used for the representative experiment in (d). Green in GCaMP7s and red is H2B-mRuby3. The magenta circles indicate E1 ensemble neurons and the green circles indicate E2 ensemble neurons. Scale bar is 100  $\mu$ m.

[0032] FIG. 2B is a behavior performance of L0 engrafted mice over 8 sessions (x-axis). Hit rate (green) versus chance (purple) is plotted for n=11 mice. Solid lines indicate

mean $\pm$ s.e.m., \* indicates p<0.05 (Wilcoxon signed-rank test with Bonferroni post-hoc correction).

[0033] FIG. 2C is a reward-triggered grand average of neurons in E1 (magenta), E2 (green), or non-target neurons (black). Scalebars are 0.2 dF/F and 200 ms. Dashed red lines indicate reward time (vertical) and 0 dF/F (horizontal).

[0034] FIG. 2D charts calcium signals from an example behavior session from neural cursor (top, blue), E1 (magenta), E2 (green), and non-target neurons (bottom, black). Baseline period is colored gray. For the neural cursor, dashed black line indicates mean value and dashed red lines indicate positive and negative reward thresholds. Red dots indicate when rewards were administered. For ensembles, dashed black line indicates dF/F=0. Scale bars are 5 mins and 100% dF/F.

[0035] FIG. 2E charts a running average of rewards per minutes for trials in which animals hit criterion (green) or failed to hit criterion (black). Rewards per minute at chance performance is highlighted in magenta. Data represent the mean $\pm$ s.e.m. of 40 sessions (above criterion) and 46 (below criterion) sessions from n=11 mice.

[0036] FIG. 2F is a graph showing dF/F normalized to trial start for trials where the animal performed above criterion (left) and where it did not (right) over relative time in the trial. Data represent the mean $\pm$ s.e.m. of 40 above criterion (left), and 46 sessions below criterion (right) from n=11 mice for E1 (magenta), E2 (green), and non-target neurons (black). \* indicates p<0.05 (two-way RM-ANOVA).

[0037] FIG. 2G is a graph showing hit rate (green) and chance (magenta) for training day 7 (left, 'Task') or a tone-decouple (right), where the auditory tone no longer contained information about the neural cursor. Thick lines indicate the mean $\pm$ s.e.m. of n=11 mice (\* indicates p<0.05, Wilcoxon signed-rank test).

[0038] FIG. 2H is a graph showing hit rate (green) and chance (magenta) for a contingency reversal experiment. Mice performed the task normally for 40 trials ('task'), then the reward contingency was reversed ('CR') such that the lowest, instead of highest possible cursor value triggered rewards. After 40 trials, the original task rules were restored ('recovery'). \* indicates p<0.05, Kruskal-Wallis Test with Dunn's post-hoc test.

[0039] FIG. 3 is a representative confocal image from cortical section of a mouse implanted with cortical L0 and electroporated with pCAG-ChR2-tdTomato (yellow) and stained with DAPI (blue). L0-L1 border is marked by the dashed black line, and the L6-white matter border is marked by the dashed white line. Image is overexposed in L0 to reveal neurites integrating into the cortex. Scale bar is 500  $\mu$ m, 50  $\mu$ m for insets. Insets i) axons deep in L6 entering white matter. ii) L0 axon present in striatum. iii) axon descending directly from L0 to white matter.

[0040] FIG. 4A is a representative confocal image from a cortical section of a mouse implanted with L0 neurons electroporated with GCaMP (yellow) and stained for pre- and post-synaptic markers (Synaptophysin: cyan, SynGAP1: magenta) showing spiny dendrites crossing from L0-L1 (Scale bar 20  $\mu$ m). Dashed line indicates the L0-L1 border. Inset i shows serial sections of a z-stack through a section of spiny dendrites showing colocalization of the dendrite with synGAP1 (white) and closely opposed by synaptophysin. Scale Bar on the inset is 1  $\mu$ m.

[0041] FIG. 4B is a representative confocal image from a cortical section of a mouse implanted with L0 sparsely

electroporated with mRuby3 (1:50 normal cell concentration) and stained with synaptic markers as in (a). Scale bar is 100  $\mu$ m. Insets i-iv: blow ups of examples of axons originating in L0 colocalizing with synaptophysin (white) and closely opposed to synGAP1 puncta. Scale bars in i, iii, iv are 10  $\mu$ m and 1  $\mu$ m in ii.

[0042] FIG. 4C is a representative confocal image from a cortical section of a mouse implanted with L0 neurons electroporated with GCaMP (yellow) stained with GAD65 (magenta) and DAPI (blue). Scale bar is 10  $\mu$ m.

[0043] FIG. 5A shows tiled high resolution confocal images of a coronal brain section from a representative engrafted mouse. Yellow: antibody-enhanced GCaMP, Cyan: Iba1, Magenta: GFAP. Arrowheads indicate blood vessels that appear to be infiltrating L0. Scale bar is 500  $\mu$ m. Insets i-ii) overexposed GCaMP to show robust L0 neurite infiltration into the cortex in the presence (i) or absence (ii) of blood vessel penetration. Scalebars are 20  $\mu$ m.

[0044] FIG. 5B shows the Iba1 channel from inset iii in (a) showing non-phagocytic microglia tiling L0. Scale bar is 100  $\mu$ m.

[0045] FIG. 5C shows the GFAP channel from inset iii in (a) showing vertically oriented astrocytes sealing L0 from the glass coverslip and supporting vascularization (arrowhead). Scale bar is 100  $\mu$ m.

[0046] FIGS. 6A-6C show maximal intensity projections of example neurons labeled with mRuby3 1 (Supp. 4a), 2 (Supp. 4b), or 4 (Supp. 4c) weeks after engraftment. Scale-bars in each image are 10  $\mu$ m.

[0047] FIG. 6D shows a Sholl analysis of traced dendritic arbors from engrafted neurons, 1, 2 or 4 weeks after engraftment. Data represent the mean and s.e.m. from n=8, 9, and 7 neurons (1, 2, 4 weeks) from N=2 mice.

[0048] FIG. 6E shows a depth-coded maximal intensity projection of a zoomed out field of view from an example mouse 4 weeks after engraftment. Scale bar is 100  $\mu$ m.

[0049] FIG. 7A is a schematic illustrating an optical BMI task where calcium signals from L2/3 are transformed into a neural cursor corresponding to a tone which is played back to the animal. A water reward is administered when the cursor hits a threshold level. Image is the field of view used for the representative experiment in (d). Green is AAV-GCaMP6s. The magenta circles indicate E1 ensemble neurons and the green circles indicate E2 ensemble neurons. Scale bar is 100  $\mu$ m.

[0050] FIG. 7B shows behavior performance of wt mice over 8 sessions (x-axis). Hit rate (green) versus chance (purple) is plotted for n=9 mice. Solid lines indicate mean $\pm$ s.e.m., \* indicates p<0.05 (Wilcoxon signed-rank test with Bonferroni post-hoc correction).

[0051] FIG. 7C shows a reward-triggered grand average of neurons in E1 (magenta), E2 (green), or non-target neurons (black). Scale bar are 0.2 dF/F and 200 ms. Dashed red lines indicate reward time (vertical) and 0 dF/F (horizontal).

[0052] FIG. 7D shows calcium signals from an example behavior session from neural cursor (top, blue), E1 (magenta), E2 (green), and non-target neurons (bottom, black). Baseline period is colored gray. For the neural cursor, dashed black line indicates mean value and dashed red lines indicate positive and negative reward thresholds. Red dots indicate when rewards were administered. For ensembles, dashed black line indicates dF/F=0. Scalebars are 5 mins and 100% dF/F.

[0053] FIG. 7E shows a running average of rewards per minutes for trials in which animals hit criterion (green) or failed to hit criterion (black). Rewards per minute at chance performance is highlighted in magenta. Data represent the mean $\pm$ s.e.m. of sessions from n=9 mice.

[0054] FIG. 7F is a graph showing hit rate (green) and chance (magenta) for training day 7 (left, 'Task') or a tone-decouple (right), where the auditory tone no longer contained information about the neural cursor. Thick lines indicate the mean $\pm$ s.e.m. of n=9 mice (\* indicates p<0.05, Wilcoxon signed-rank test).

[0055] FIG. 8A is a representative confocal image of a mouse implanted with L0 neurons electroporated with GCaMP (yellow) and stained with NeuN (magenta) and DAPI (blue). Scale bar is 100  $\mu$ m.

[0056] FIG. 8B is a representative confocal image of a mouse implanted with L0 neurons sparsely electroporated with mRuby3 (magenta, 1:50 typical labeling density) and stained with NeuN (yellow) and DAPI (blue). Scale bar is 100  $\mu$ m. Insets i-iii show example axons extending horizontally (i), descending vertically from L0 (ii) or entering white matter (iii). Scale bars are 10  $\mu$ m.

[0057] FIG. 9A shows a layer Zero brain section stained with DAB-enhanced anti-GFP against GCaMP-expressing engrafted neurons (black), cresyl violet (blue). Scale bar is 200  $\mu$ m

[0058] FIG. 9B shows an inset showing penetration of superficial cortical layers by L0 dendrites. Scale bar is 200  $\mu$ m.

[0059] FIG. 9C shows an inset showing higher magnification image of L0 dendrites in L2. Scale bar is 50  $\mu$ m

[0060] FIG. 9D shows an inset showing L0 axons in L4. Scale bar is 50  $\mu$ m.

[0061] FIG. 10A-10G show stem cell to human neuron differentiation from Day 1 to Day 7.

[0062] FIG. 11A-B show neuronal growth on an indium tin oxide (ITO) substrate in the presence of poly-D-lysine and laminin.

## DETAILED DESCRIPTION

[0063] In the present disclosure, an artificial cortical layer or graft (layer zero or "L0") has been generated by depositing GCaMP-expressing neurons onto the cortical surface where they are easily accessed by optical or electronic recording. GCaMP is a genetically encoded calcium indicator (GECI), which in certain instances, is a synthetic fusion of green fluorescent protein, calmodulin, and M13 (a peptide sequence from myosin light-chain kinase). The graft integrates with the brain to form an interface layer capable of transforming information from the brain to its surface, where it can then be read. Thereafter, L0 undergoes a developmental process over several weeks characterized by strong waves of activity that gradually decorrelate to resemble spontaneous cortical activity. After this developmental process, mammals (e.g., mice) were trained to use L0 to perform an optical brain machine interface task. The results indicate that the mammal (e.g. mice) can perform at levels similar to mice expressing viral GCaMP in layer 2 (L2). Histological analysis shows that L0 neurons extend dendrites into the superficial cortical layers and axons that extend throughout the cortical volume. Advantageously, this data provides a demonstration of a biological brain-computer interface capable of bidirectional communication in a mammal.

## Definitions

[0064] As used herein, the term “brain-machine interface” or “BMI” refers to a layer of neuronal cells engrafted onto and that integrates into a surface or layer of a mammalian brain. A BMI is capable of communicating a neural activation into a response recordable in an external device. Bidirectional brain-machine interfaces (BMIs) establish a two-way direct communication link between the mammalian brain and the external device. The term “brain-computer-interface (BCI) is used interchangeably with BMI herein.

[0065] As used herein, the term “cerebral cortex” is the outer most layer of neural tissue of the cerebrum of a brain in a mammal, such as a human.

[0066] As used herein, the term “tethered” refers to a cell, such as a neuronal cell that is attached or joined (e.g., chemically) to an electrode or pad.

[0067] As used herein, the term “cortical graft layer” refers to a layer of cells that is deposited or poured over a cerebral cortex of a mammal.

[0068] As used herein, the term “electrocorticography” refers to the process of recording electrical activity in a brain by placing electrodes in direct contact with the cerebral cortex or surface of the brain. An electrocorticogram (ECOG) is the tracing of a brain wave made by an electrocorticographic apparatus (an ECoG) used for detecting and recording brain waves made with the electrodes in direct contact with the brain.

[0069] As used herein, the term “external stimulus” refers to an outside change to the external environment that is detected by a mammalian subject. Changes to light, an electrical impulse, sound and temperature are examples of external stimuli. The external environment can be external to a neuron or external to the mammalian subject.

[0070] As used herein, the term “hydrogel” refers to a water-insoluble, optionally cross-linked, three-dimensional network of polymer chains with voids between polymer chains filled with or capable of being filled with water. A hydrogel package is a construct or structure made of one or more hydrogel polymer(s).

[0071] As used herein, the term “L1” or “layer 1” refers to the first layer of the cerebral cortex or the sheet of neural tissue that is outermost to the cerebrum.

[0072] As used herein, the term “L0” or “layer 0” refers to a layer of exogenous cells placed or poured over the cerebral cortex. The poured over cells can be a transfected cell with exogenous functionalities.

[0073] As used herein, the term “transfection” refers to the taking up of exogenous nucleic acid, e.g., an expression vector, by a host cell whether or not any coding sequences are, in fact, expressed. Numerous methods of transfection are known to an ordinarily skilled artisan, for example, by *Agrobacterium*-mediated transformation, protoplast transformation, lipid-mediated delivery, liposomes, electroporation, sonoporation, microinjection, particle bombardment and silicon carbide whisker-mediated transformation and combinations thereof.

[0074] As used herein, the term “neural network” refers to a plurality of interconnected neurons (i.e., at least two neurons) whose activation defines a recognizable linear pathway. The interface through which neurons interact with their neighbors usually consists of several axon terminals connected via synapses to dendrites on other neurons. If the sum of the input signals into one neuron surpasses a certain

threshold, the neuron sends an action potential (AP) at the axon hillock and transmits this electrical signal along the axon.

[0075] As used herein, the term “nervous system” refers to a complex network of nerve cells, or neurons, found centrally in the brain and spinal cord and peripherally in the various nerves of the body. Neurons have a cell body, dendrites and an axon.

[0076] As used herein, the term “nerve” refers to a group of neurons that serves a particular part of the body. Nerves can contain several hundred neurons to several hundred thousand neurons. Nerves often contain both afferent neurons (which carry signals back to the central nervous system) and the efferent neurons (which carry signals to the periphery). Electrical signals are conducted via neurons and nerves. Neurons release neurotransmitters at synapses with other nerves to allow continuation and modulation of the electrical signal. A “ganglion” refers to a group of neuronal cell bodies in one location

[0077] As used herein “subject” or “patient” or “individual” refers to any subject, patient, or individual, and the terms are used interchangeably herein. In this regard, the terms “subject,” “patient,” and “individual” includes mammals, and, in particular humans.

## EMBODIMENTS

[0078] The present disclosure provides a brain-machine interface (BMI) in the form of a layer of neuronal cells that can be grafted onto the outer layer of the cerebral cortex to provide-bidirectional communication between the brain and an external device. An artificial cortical L0 formed from transplanted neurons functions as a BMI or an interface between external recording devices and the brain. This L0 layer survives, develops, and integrates with the brain.

[0079] In certain aspects, L0 is utilized as an a BCI by requiring a mammal (e.g., a mouse) to volitionally modulate L0 activity to obtain rewards. These results indicate that L0 is integrated with the brain to a degree sufficient for the animal to control, or modulate, it's activity patterns. Histology supports these results by revealing that L0 extends spiny dendrites that possess synaptic markers into the superficial layers of the cortex.

[0080] By grafting neurons to form L0, recordings from the brain at single neuron resolution are obtained without genetic modification of the host organism and with no traumatic penetration of the brain's parenchyma. Instead, the brain is penetrated by naturally in-growing neurites, and bidirectional communication is achieved via chemical synapses, blurring the boundary between implant and host.

[0081] In certain aspects, an optical approach is used to complete a BMI task in a mammal. In some instances, neuronal activity is measured using genetically encoded calcium indicators and microscopy. Various fluorescent proteins enhance the detection of neural activity.

[0082] The present disclosure provides a brain-computer interface (BCI) engrafted on a brain of a mammal, the BCI comprising:

[0083] a cortical graft layer comprising a plurality of neuronal cells transplanted on a brain's cerebral cortex, wherein the plurality of cells engraft on the brain and respond to an external stimulus with a detectable signal.

[0084] In certain instances, fluorescently labeled cells derived from established lines such as neural cells or autolo-

gous stem cells, are deposited on top of a mammalian cortex, spinal cord, cranial nerve or a combination thereof and a clear window is fixed over the transplantation site. In one instance, the cells are deposited on top of a mammalian cortex.

[0085] In certain aspects, the plurality of neuronal cells are transfected, wherein the transfection can be ex vivo with a plasmid such as by electroporation. Alternatively, in certain aspects, transfection is via virus-mediated transfection.

[0086] In certain aspects, the plurality of neuronal cells are tissue cultured mammalian stem cells. Other suitable cells include, but are not limited to, a glial cell, an embryonic cell, a mesenchymal stem cell, a cell derived from an induced pluripotent stem cell, a sympathetic neuron, a parasympathetic neuron, a spinal motor neurons, a central nervous system neuron, a peripheral nervous system neuron, an enteric nervous system neurons, a motor neuron, a sensory neuron, a cholinergic neuron, a GABAergic neuron, a glutamatergic neuron, a dopaminergic neuron, a serotonergic neuron, an interneuron, an adrenergic neuron, a trigeminal ganglion, an astrocyte, an oligodendrocyte, a Schwann cell, a microglial cell, an ependymal cell, a radial glial cell, a satellite cell, an enteric glial cell, a pituicyte, an embryonic stem cell, an induced pluripotent stem cell, and combinations thereof. The cells can be autologous cells or allogenic cells.

[0087] The cells (e.g., neuronal cells) in the disclosure can be derived from one site and transplanted to another site within the same subject as an autograft. Furthermore, the cells (e.g., neuronal cells) in the disclosure can be derived from a genetically identical donor and transplanted as an isograft. Still further, the cells (e.g., neuronal cells) in the disclosure can be derived from a genetically non-identical member of the same species and transplanted as an allograft. Alternatively, cells (e.g., neuronal cells) can be derived from non-human origin and transplanted as a xenograft. With the development of powerful immunosuppressants, allografts and xenografts of non-human neural precursors, such as neural precursors of porcine origin or other mammals, can be grafted into human subjects. Cell engraftment typically involves the administration or injection of either whole cells or cell extracts that are xenogenic, allogenic (from another human donor), or autologous (wherein the cells are extracted from and transplanted back into the same patient or subject).

[0088] In certain aspects, the plurality of neuronal cells are tethered (e.g., chemically such as covalently) to an electrode. For example, in one approach, a ligand on the surface of an electrode is bound through a protein-protein interaction to specific areas of neuronal cells. The functionalized electrode surface is genetically engineered to express a neuroligin-1 protein that forms a nascent presynaptic bouton upon binding to neurexin-1 $\beta$  on the presynaptic membrane of neurons. (See, Jeon J, Yoon et al., S H, "Neuroligin-1-Modified Electrodes for Specific Coupling with a Presynaptic Neuronal Membrane" *ACS Appl Mater Interfaces*. May 2021, 13(18):21944-21953). Other polymers used for tethering are known to those skilled in the art.

[0089] In certain aspects, the neuronal response is detected optically. For example, the response can be detected using microscopy, such as by using calcium imaging microscopy. Calcium imaging takes advantage of calcium indicators, fluorescent molecules that respond to the binding of Ca<sup>2+</sup> ions by fluorescent properties. Two main classes of calcium indicators exist i.e., chemical indicators and genetically

encoded calcium indicators (GECI). This technique allows calcium signaling in a wide variety of cell types. In neurons, electrical activity is typically accompanied by an influx of Ca<sup>2+</sup> ions. When bound to Ca<sup>2+</sup>, GCaMP fluoresces green with a peak excitation wavelength of 480 nm and a peak emission wavelength of 510 nm. In this manner, intracellular Ca<sup>2+</sup> levels are measured using transfected or transgenic cells.

[0090] GCaMP is commonly used to measure increases in intracellular Ca<sup>2+</sup> in neurons as a proxy for neuronal activity in animal models. Action potentials induce neurotransmitter release at axon terminals by opening voltage-gated Ca<sup>2+</sup> channels, allowing for Ca<sup>2+</sup> influx. GCaMP can be used to identify and measure activity patterns in specific regions of a mammalian brain.

[0091] In certain aspects, the plasmid contains an exogenous nucleic acid sequence selected from the group consisting of pCAG-H2B-mRuby3-P2A-GCaMP7s, pCAG-ChRimson-tdTomato (SEQ ID NO: 3), pCAG-ChR2-tdTomato, and pCAG-mRuby3 (SEQ ID NO: 4) to facilitate imaging. In certain instances, the exogenous nucleic acid is a calcium indicator such as pCAG-H2B-mRuby3-P2A-GCaMP7s.

[0092] As shown in FIG. 1A, an imaging device 1030, for example, a multi-photon microscope or Miniscope is utilized to observe and image in vivo neural activity and complete a BMI task. A clear cranial window 1043 is fixed 1013 on the cranium 1010 over a transplantation site. The device 1030 is configured to excite 1025 and detect fluorescent changes and responses in the genetically modified cells 1015. The genetically modified cells 1015 are deposited on top of the cortex 1021 of a mammal. The combination of genetically encoded calcium (Ca<sup>2+</sup>) indicators (GECIs) and imaging techniques enables recording of neuronal population activity at high speed and single-cell resolution. A biological BCI residing on the cortical surface allows straightforward connection to recording devices, an ECoG, microarrays or thin-film arrays.

[0093] For example, using genetically encoded calcium indicators such as pCAG-GCaMP7s-P2A-H2B-mRuby3, it is possible to interrogate L0 and assess whether it survives, integrates, and exhibits spontaneous activity. After neurons electroporated with a GECI were transplanted as L0 in a small mammal, cell counting and visualization of neural activity was assessed. Two days post transplantation, strong H2B-mRuby3 signal was visible in a mammal (e.g., mouse), which appeared as a thin band of cells on the cortical surface. The results indicated that the thickness of L0 doubled over the first two weeks of engraftment before stabilizing and maintaining thickness.

[0094] In certain instances, fluorescent images can be obtained using a confocal microscope. Fluorophores are excited using laser lines (e.g., 405, 488, 561 and 639 nm), with corresponding emission bandpass filters (e.g., of 420-480 nm, 495-550 nm, 573-615 nm and 607-750 nm). Wide-field images are thereafter collected and processed.

[0095] In one aspect, 2 photon calcium imaging is utilized for neuronal imaging. The imaging laser source can be for example, a Mai Tai Ti:Sapphire laser (Spectra-Physics) mode locked at 920 nm for calcium imaging or at 1000 nm for structural imaging. Signals can be collected with a photomultiplier tube. The imaging system is computer controlled. Functional images can be acquired at 920 nm with ~50 mW average power. For developmental structural analy-

sis, volumes can be acquired at  $1250 \times 1250 \mu\text{m}$  field of view covering  $300 \mu\text{m}$  in Z with  $2 \mu\text{m}$  steps. For imaging of spontaneous L0 events, a single  $1250 \times 1250 \mu\text{m}$  field of view was imaged at 30 Hz. For online BMI, a single plane  $430 \times 430 \mu\text{m}$  was imaged at 30 Hz. For neuronal morphology, images can be acquired from a  $215 \times 215 \mu\text{m}$  FOV.

[0096] In certain instances, stimulus-evoked fluorescence transients are observed for individual implanted cells and thereafter recorded. The fluorescently modified cells can detect single action potentials and can be imaged over a period of time. Co-expression of a second fluorescent cellular marker aids in detection of the fluorescent expressing calcium cells. Excitation of the transplanted calcium expressing cells modulate (input) and/or record (output) brain activity as a neural interface.

[0097] The calcium imaging methods disclosed herein allow tracking of a single neuron's activity of a subject over long time-lapse sequences in response to stimuli.

[0098] The engrafted BMI enables functional imaging of a mammal to characterize changes in spontaneous activity of L0. For example, the first calcium signals observed are large, infrequent population events that occur about one week after engraftment. Two weeks after engraftment, population events are more frequent, with localized spatial clustering. By four weeks after engraftment, spontaneous activity in L0 qualitatively resembled typical cortical activity, with generally asynchronous calcium signals that exhibit no apparent spatial structure. The results indicate that L0 survives transplantation onto the cortical surface, extends neuronal arbors, and undergoes developmental changes in spontaneous activity patterns from synchronous waves to decorrelated activity that resembles endogenous cortical activity.

[0099] In certain aspects, the cortical graft layer extends axons and dendrites into the cerebral cortex, striatum or completely integrating into the subject's brain. In certain aspects, the cortical graft layer forms synaptic connections to enable bidirectional communication, wherein the subject sends a response to an external device, and the device sends a response to the subject or vice versa.

[0100] In certain aspects, the cortical graft layer (L0) is engrafted over a lobe of the cerebral cortex such as the frontal lobe, the parietal lobe, the temporal lobe, the occipital lobe or a combination thereof.

[0101] In certain aspects, the cortical graft layer of cells has a thickness of about 50 microns to about 1 mm such as about  $50 \mu\text{m}$ ,  $75 \mu\text{m}$ ,  $100 \mu\text{m}$ ,  $125 \mu\text{m}$ ,  $150 \mu\text{m}$ ,  $175 \mu\text{m}$ ,  $200 \mu\text{m}$ ,  $225 \mu\text{m}$ ,  $250 \mu\text{m}$ ,  $275 \mu\text{m}$ ,  $300 \mu\text{m}$ ,  $325 \mu\text{m}$ ,  $350 \mu\text{m}$ ,  $375 \mu\text{m}$ ,  $400 \mu\text{m}$ ,  $425 \mu\text{m}$ ,  $450 \mu\text{m}$ ,  $475 \mu\text{m}$ ,  $500 \mu\text{m}$ ,  $525 \mu\text{m}$ ,  $550 \mu\text{m}$ ,  $575 \mu\text{m}$ ,  $600 \mu\text{m}$ ,  $625 \mu\text{m}$ ,  $650 \mu\text{m}$ ,  $675 \mu\text{m}$ ,  $700 \mu\text{m}$ ,  $725 \mu\text{m}$ ,  $750 \mu\text{m}$ ,  $775 \mu\text{m}$ ,  $800 \mu\text{m}$ ,  $825 \mu\text{m}$ ,  $850 \mu\text{m}$ ,  $875 \mu\text{m}$ ,  $900 \mu\text{m}$ ,  $925 \mu\text{m}$ ,  $950 \mu\text{m}$  or about 1 mm. The L0 layer can be uneven with different thicknesses over the cortex.

[0102] In certain aspects, the BCI can be used to complete bidirectional communication. In one experiment, a neural cursor was defined as the difference between the mean activity of an ensemble of 'go' neurons (E1) and 'no-go' neurons (E2) in a BCI task for reward. Animals could not get rewards by simply increasing the mean activity of all neurons. In one aspect, this neural cursor is transformed into a stimulus (e.g., tone played back to the mammal) to provide information about the cursor value. The mammal must modulate the activity of the cursor to a threshold value within a timeframe (e.g., 30 seconds) to receive a reward;

this counts as a 'hit' trial, whereas failure to gain a reward within the timeframe is considered a 'miss' trial, and triggers a timeout.

[0103] After receiving a reward, the mammal must modulate the neural cursor back to the baseline value to initiate another trial, such that the animal is required to move the cursor up and back down, and cannot gain rewards by maintaining the cursor in a reward zone.

[0104] In these experiments, engrafted mice performed above chance by day three, and maintained performance for the duration of the experiment. The calcium waveforms showed that rewards were associated with a large peak in E1 activity and a chronic suppression of E2.

[0105] In sessions where animals performed above criterion, they were able to rapidly achieve rewards at a rate well above chance early in the session and maintained high reward rates before a decrease after around 25 minutes, perhaps due to encroaching satiety. These results demonstrate that mice can volitionally control the activity of L0 neurons to perform a simple BCI task.

[0106] In certain aspects, the external stimulus is outside the mammalian brain and is a member selected from the group consisting of a light signal, an audio signal, and an electrical signal. In certain aspects, the external stimulus, which triggers a response, is outside the cell, but within the mammalian brain.

[0107] In certain aspects, the light signal has a wavelength of about 300 nm to about 1.5 microns such as about 300 nm, 350 nm, 400 nm, 450 nm, 500 nm, 550 nm, 600 nm, 650 nm, 700 nm, 750 nm, 800 nm, 850 nm, 900 nm, 950 nm, 1000 nm, 1050 nm, 1100 nm, 1150 nm, 1200 nm, 1250 nm, 1300 nm, 1350 nm, 1400 nm, 1450 nm, and/or 1500 nm.

[0108] In certain aspects, the detectable signal represents neuronal activity.

[0109] In certain aspects, the detectable signal connects to an external device such as a recording device and a device having a CPU.

[0110] In certain aspects, the mammal is a human.

[0111] In certain aspects, the human has an impairment selected from the group of an impairment of a motor skill, a sight function, an auditory function, a taste function and an olfactory function.

[0112] In a second aspect, the disclosure provides a method for bi-directional communication between a brain-computer interface (BCI) engrafted on a brain of a mammal and a computer, the method comprising:

[0113] providing a cortical graft layer comprising a plurality of neuronal cells transplanted on the brain's cerebral cortex of the mammal; and

[0114] providing an external stimulus to the mammal wherein the plurality of cells engrafted on the brain respond to an external stimulus with a detectable neural signal.

[0115] In addition to an optical approach, an electrical approach can be used to complete a BMI task in a mammal. The electrical approach eliminates the need for fluorescently labeled cells and an optical cranial window on the skull (or spinal cord, or cranial nerve). Turning now to FIG. 1B, one approach uses an electrocorticographic (ECoG) array 1028 that is placed flat on the cortex 1021, spinal cord, cranial nerve, or combination thereof on top of the deposited or poured-over 1015 cell layer (L0). This method establishes a direct link for transmitting information between the host brain cortex 1021 and the external ECoG array 1028. The ECoG 1028 measures cortical fields potentials using elec-

trodes **1046** placed on the surface of the cortex **1021**. The threads **1063** connect the ECoG **1028** to the electrodes **1063**.

[0116] In another approach, as shown in FIG. 1C, an ECoG **1028** is implanted by a craniotomy into the skull **1010**. Implanted neuronal cells **1015** are “tethered” to the electrodes **1046** of ECoG **1028** array prior to the implant surgery and placed flat on top of the cortex **1021**. Advantageously, this approach leads to 100% juxtacellular recording yield.

[0117] In still yet another approach, as shown in FIG. 1D, the implanted cells are tethered to a ECoG device, and the cells are cultured and deposited in an implantable hydrogel prior to surgery. Implanted neuronal cells **1015** are “tethered” to the electrodes **1046** of ECoG **1028** array prior to the implant surgery. The cells are packaged into hydrogel **1051** and inserted into the cortex **1021**. The threads **1063** connect the ECoG **1028** to the electrodes **1063**, which are connected to the hydrogel package **1051**. This allows L0 cells to be placed and patterned in the optimal formation (with channels for vascularization and optionally with drugs embedded in the hydrogel that would release over time to help prevent inflammation, graft rejection, and scarring) for long term recording capabilities and guarantees a 100% juxtacellular recording yield.

[0118] In certain aspects, the hydrogel package is a hyaluronic acid-based hydrogel. The hydrogel package can contain a conductor, such as graphene or a graphene-like based material. Other conductors are known in the art. The package can be porous. The porous package can be formed over an electrode array.

[0119] In certain instances, the hydrogel package further comprises a solid substrate onto which the hydrogel package is cross-linked. In some instances, the hydrogel package comprises a cell medium comprising nerve growth factor (NGF) at a concentration from about 5 to about 20 picograms per milliliter.

[0120] In still another embodiment, the present disclosure provides a method of connecting a biological brain-machine interface with a subject, the method comprising:

[0121] depositing neuronal cells onto a cortical surface of a brain of a subject, the cells being selected to emit light or an electrical signal in response to a neural signal;

[0122] allowing the cells to form an additional cortical layer that grows and integrates into the brain; and

[0123] recording light or an electrical signal emitted from the cells in response to a neural signal in the brain.

[0124] In still yet another embodiment, the present disclosure provides a method of stimulating a brain with a biological brain-machine interface, the method comprising:

[0125] depositing neuronal cells onto a cortical surface of a brain of a subject, the cells being selected to convert light or an electrical signal to an electrical signal compatible with neurons in the brain;

[0126] allowing the cells to form an additional cortical layer that grows and integrates into the brain;

[0127] directing light at or an electrical signal to the cells in the additional cortical layer such that the cells convert the light or the electrical signal to a neural signal; and

[0128] measuring a response or a behavior of the subject correlated with the directed light or electrical signal.

#### External Device

[0129] In certain aspects, the electrocorticographic apparatus (ECoG) is a device that uses an electrode array, microarray or thin-film array placed directly on the exposed surface of a subject's brain to record electrical activity from the cerebral cortex. In certain aspects, the external ECoG device is disclosed in WO 2021/011401 to Seo. The application is drawn generally to a brain electrode implant system that includes one or more cylindrical sensors that fit flushly into burr holes in a subject's skull with wires that lead to a subcutaneous relay/router device behind the subject's ear. The relay communicates inductively with a device worn by the subject, which in turn communicates wirelessly or otherwise with a base station.

[0130] Each sensor nestled within its burr hole receives signals from a microfabricated polymer cable embedded with hundreds or thousands of metal electrodes descending into the subject's brain. The electrodes are implanted using a specialized surgical robot that pulls each electrode with a rigid needle into the brain during surgery before pulling out and pulling in another electrode. The received electrical signals, analog voltages and currents, are converted onboard the sensor to digital and then assessed. If an electrical signal denotes a neural spike or other interesting event, then it is multiplexed with other events and fed through a serial cable to the relay. The relay then transmits it off-board to the base station.

[0131] The implants are located in different lobes, or areas of the brain, to capture or stimulate targeted sections. The thin film electrodes merge into ribbon cable **204** at one end, which in turn is preconnected to the implant. Each implant is carefully set on top of the ribbon cable to cover the burr hole.

[0132] Physically, the sensor is a silicone- or other polymer-casted package that is molded into a cylindrical puck with a thin film of electrodes emerging from one end, and the wires to connect to the implanted router from the other. Inside the puck is a hermetic glass or other biocompatible material package containing electronics and thin film attached through vias or otherwise to a custom system on a chip (SoC).

[0133] In the exemplary embodiment, each sensor pill has 1,024 channels. Each array has 64 threads of 16 electrodes each. Every channel supports both stimulation and recording. The sensor's physical package is an 8 mm cylindrical “puck” that fits into an 8 mm drilled burr hole to sit flush with the surface of the skull.

[0134] In the exemplary system, there are no radios and batteries in the implant. If a patient takes off the pod device, then the implant loses power and he or she disconnects his or her implant from the outside. In an alternative embodiment, a small battery can be included in the implant.

[0135] Within each implant is circuitry, including integrated circuit (IC) chips, capacitors, and other components. The ICs receive from, and/or transmit to, the thin film electrodes that are surgically implanted within the subject's cranium. The ICs can include analog-to-digital converters (ADC) and/or digital-to-analog converters (DAC) in order to convert analog signals in the brain to or from digital signals of a computer.

[0136] The IC chips that include the ADCs can also include multiplexers/demultiplexers that multiplex digital signals together to put on the serial cable, or demultiplex serial signals from the serial cable apart for output to the

DACs. The former is for reading out from the brain, while the latter is for stimulating the brain. Sitting in the burr hole, within the biocompatible housing, are a tight pack of electrical components. The components are carefully positioned to interface with the thin film ribbon cable of what may be thousands of individual, electrically isolated electrodes.

[0137] The leads and electrodes are manufactured using microelectromechanical systems (MEMS) technologies. The leads are manufactured monolithically with the hermetic package substrate and connect with electrodes. Each electrode site is oval and has a geometric surface area of ~370  $\mu\text{m}^2$  that is coated with a high surface area material.

[0138] Those of skill in the art will know of other ECoG devices useful in the present disclosure.

#### Methods of Use

[0139] The present disclosure can be practiced in various methods of use and treatment. The present methods comprise a step of administering a cellular composition for engraftment to a subject (e.g., a patient) to generate a L0 layer. Cellular engraftment generally encompasses transplantation of human or animal cells to a subject to generate a L0 layer or used to repair spinal cord injuries or aid patients with neurological disorders such as Alzheimer's disease, Parkinson's disease, paralysis, neurodegenerative conditions or epilepsy.

[0140] The present disclosure can be used in applications where it is useful to grow cells for a period of time for use in later cell engraftment for L0 generation or therapies. This can include for example, growing a patient's own cells for later transplantation, as well as for use in research or therapies. The disclosure includes the use of grafted cells (e.g., neuronal cells) to ameliorate a neurodegenerative condition.

[0141] The present disclosure also provides methods for transplanting cells (e.g., neuronal cells) into a subject using cultured cells (e.g., neuronal cells) for transplantation. In some aspects, the transplanted cells (e.g., neuronal cells) are xenogenic to the non-human animal. In some aspects, the transplanted cells (e.g., neuronal cells) are human cells. Disclosed herein are methods for treating neurodegenerative disease including, but not limited to, Alzheimer's disease, Parkinson's disease, Huntington's disease or paralysis by transplantation of cells (e.g., neural cells).

[0142] The cells of the disclosure include cells that, upon transplantation or engraftment, generate an amount of neurons sufficient to integrate within the neuronal infrastructure of the brain, mammalian cortex, spinal cord, cranial nerve or a combination thereof, to ameliorate a disease state or condition or generate a L0 layer. Disclosed herein are methods including treating neurodegenerative diseases or conditions by transplanting cells (e.g., neuronal cells) isolated from a mammal such as the central nervous system of a mammal and that have been expanded in vitro. For example, transplantation of the neuronal cells can be used to improve ambulatory function in a subject suffering from spasticity, rigidity, seizures, or paralysis by generating a L0 layer.

[0143] A method of use and/or treatment can include supplying to an injured neural area, via transplantation, a suitable number of neuronal cells to attenuate defective neural circuits, including hyperactive neural circuits.

[0144] In one aspect, the disclosed method includes restoring motor function in a motor neuron disease. A suitable

number or a therapeutically effective amount of cells (e.g., neuronal cells) can be provided to at least one area of neurodegeneration, such as a degenerative spinal cord, to restore motor function. The neuronal cells exert their therapeutic effect by replacing degenerated neuronal cells. In some aspects, the neuronal cells exert, their therapeutic effect by expressing and releasing trophic molecules which protect the neurons of the degenerating tissue so that more of them survive for longer period of time. Neuronal cells can be prompted to project into ventral roots and innervate muscle where they engage in extensive reciprocal connections with host motor neurons in subjects with degenerative motor neuron disease. Neuronal cells can be grafted into the lumbar cord where these cells can form synaptic contacts with host neurons and express and release motor neuron growth factors.

[0145] The disclosure includes providing neuronal cells that integrate with the host tissue and provide one or more growth factors to the host neurons thereby protecting them from degenerative influences present in the tissue. The methods include introducing a sufficient number of neuronal cells to an area of a spinal cord such that an effective amount of at least one growth factor is secreted by the neuronal cells.

[0146] The disclosure includes providing a method for using animal models in the preclinical evaluation of stem cells for cell replacement in neurodegenerative conditions.

[0147] The cells can be either undifferentiated, pre-differentiated or fully differentiated in vitro at the time of transplantation. In one aspect, the cells are induced to differentiate into neural lineage. The cells of the disclosure can undergo neuronal differentiation in situ in the presence of pro-inflammatory cytokines and other environmental factors existing in an injured tissue.

[0148] Using the disclosure, neural circuits can be treated by transplanting or introducing the cells into appropriate regions for amelioration of the disease, disorder, or condition. Generally, transplantation occurs into nervous tissue or non-neural tissues that support survival of the grafted cells. Neuronal cell grafts employed in the disclosure survive well in a neurodegenerative environment where the neuronal cells can exert powerful clinical effects in the form of delaying the onset and progression of neurodegenerative conditions or disease.

[0149] In some instances, transplantation can occur into remote areas of the body and the cells can migrate to their intended target. Accordingly, the disclosure can also include partial grafting of human neuronal cells. As used herein, the term "partial grafting" can refer to the implantation of expanded neuronal cells in only a portion of an area or less than an entire area of neurodegeneration. For example, partial grafting of human neuronal cells into the lumbar segments of spinal cord. At least a portion of the effects of neuronal cells on degenerating motor neurons include delivery of neurotrophies and trophic cytokines to degenerating host motor neurons via classical cellular mechanisms.

[0150] As used herein, a neurodegenerative condition can include any disease or disorder or symptoms or causes or effects thereof involving the damage or deterioration of neurons or the nervous system. The conditions which may be treated as disclosed herein may derive from traumatic spinal cord injury, ischemic spinal cord injury, traumatic brain injury, stroke, multiple sclerosis, cerebral palsy, epi-

lepsy, Huntington's disease, amyotrophic lateral sclerosis (ALS), chronic ischemia, hereditary conditions, or any combination thereof.

[0151] As disclosed herein, introducing a L0 layer or a therapeutically effective amount of the neuronal cell population may include transplanting or injecting at least a portion of the therapeutically effective amount into a plurality of areas of the recipient spinal cord. In one aspect, the method comprises treatment of neuropathic pain (e.g., neuropathic chronic pain).

[0152] The cell density for administration can vary from about 1,000 cells per microliter to about 1,000,000, cells per microliter such as 100,000, 200,000, 300,000, 400,000, 500,000, 600,000, 700,000, 800,000 900,000, or 1,000,000 cells/mL depending upon factors such as the site of the injection, the neurodegenerative status of the injection site, the minimum dose necessary for a beneficial effect, and toxicity side-effect considerations. In an aspect, the disclosure include injecting cells at a cell density of about 5,000 to about 50,000 cells per microliter.

[0153] The volume of media in which the expanded cells are suspended for delivery a treatment area can be referred to herein as the injection volume. The injection volume depends upon the injection site and the degenerative state of the tissue. More specifically, the lower limit of the injection volume can be determined by practical liquid handling of viscous suspensions of high cell density as well as the tendency of the cells to cluster. The upper limit of the injection volume can be determined by limits of compression force exerted by the injection volume that are necessary to avoid injuring the host tissue, as well as the practical surgery time.

## EXAMPLES

### Example 1—Preparation of BCI in Mice

[0154] To test the possible usefulness of a BCI based on a biological interface, we attempted to train mice to perform BCI tasks using transplanted neurons. We reasoned that a biological BCI should reside on the cortical surface, allowing straightforward connection to recording devices (FIG. 1E). We therefore developed an experimental preparation to create an artificial cortical L0 above layer 1 (L1) by combining techniques for primary neural cell culture and cranial windows for 2P imaging in mice. To achieve this, mouse primary cortical neurons (E14-17) were isolated and electroporated with plasmid DNA, then deposited onto the cortical surface of adult mice. After waiting for cells to adhere to the cortex, we applied a glass coverslip to allow optical access to L0 to study its development, maturation, and function.

[0155] To determine electroporation efficiency, a subset of neurons were electroporated with DNA encoding a red fluorescent protein under a ubiquitous promoter and then cultured in an incubator instead of being transplanted. By image analysis, we estimate transfection efficiency to be ~11%. Non-electroporated plasmid DNA is digested by DNase before transplantation, eliminating the possibility of off-target expression and ensuring that we are recording only from engrafted cells.

### Example 2—Microscopic Imaging of Neuron Growth and Activity

[0156] We first asked if L0 survives, integrates, and exhibits spontaneous activity. We therefore transplanted neurons

electroporated with pCAG-GCaMP7s-P2A-H2B-mRuby3 to allow for cell counting and visualization of neural activity. We periodically imaged the awake, head-fixed mice on a circular treadmill under a 2P microscope. Strong H2B-mRuby3 signal was visible ~2 days after transplantation, allowing us to identify a thin band of cells on the cortical surface (FIG. 1F). The thickness of L0 doubled over the first two weeks of engraftment before stabilizing and maintaining thickness throughout our experiments (FIG. 1G, day 3: 94±20 µm, day 18: 194±14 µm, p=0.001, Kruskal-Wallis Test). We next looked for evidence of cell death by quantifying the number of red nuclei per field of view over time. We did not observe any evidence of decreasing cell numbers, but instead found a nonsignificant trend for an increased number of labelled neurons over time. This apparent increase in the number of labelled cells could be explained by a constitutively active promoter driving an increase in average red fluorescence values, since weakly expressing neurons may emerge from the noise floor. However, we cannot eliminate the possibility that a small progenitor population was electroporated and divided post-engraftment.

### Example 3—Calcium Imaging

[0157] We also performed functional imaging to characterize changes in spontaneous activity of L0 after engraftment. The first calcium signals we observed were large, infrequent population events that began around one week after engraftment (FIG. 1H). Two weeks after engraftment, population events were more frequent, but the entire layer no longer fired synchronously. Instead activity exhibited more localized spatial clustering. By four weeks after engraftment, spontaneous activity in L0 qualitatively resembled typical cortical activity, with generally asynchronous calcium signals that exhibited no apparent spatial structure (FIG. 1I). To quantify the evolution of spontaneous activity over the development of L0, we identified population events using the rise of the calcium transients on the full-field fluorescence. Population events in the first 10 days after engraftment tended to involve a large fraction of cells (30±31% of all cells active per event, med±s.d.). These events significantly sparsened 10 days later (7±15% of all neurons active per event, med±s.d, p<1×10-15 KS-test, FIG. 1I). Conversely, early in the graft, individual neurons participated in the majority of population events (active in 66±29% of events, med±s.d), but 10 days later they were active during significantly fewer events (27±34% med±s.d., p<1×10-16 KS-test). Quantifying the mean frequency and amplitude of population events revealed a switchero from large, infrequent events to small and rapid events in L0 that occurred 12-14 days after engraftment, matching reports of similar changes in visual cortex around the same time after onset of sensory experience (FIG. 1J). This sparsification of population events in L0 occurred concomitantly with a significant decrease in the mean pairwise correlation of L0 neurons by one month of engraftment (p=0.0013, Kruskal-Wallis with Dunn's post-hoc test, FIG. 1K). Mean pairwise correlation of mature grafts during spontaneous activity was similar to or slightly below correlations found in spontaneous activity in layer 2 (FIG. 1L, p=0.053, two-sided t-test).

### Example 4—BCI Morphology

[0158] To assess the morphology of engrafted L0 neurons during this period, we sparsely labeled neurons with

mRuby3, allowing visualization of neurites during development using 2P imaging (FIGS. 6A-6E). These images revealed that neurons extended processes as soon as three days after engraftment. Sholl analysis on traced neurites revealed that the complexity of dendritic and axonal arbors increased over time and stabilized by 2 weeks, in advance of the maturation of firing patterns (FIGS. 6A-6E). Together, this data shows that L0 survives transplantation onto the cortical surface, extends neuronal arbors, and undergoes developmental changes in spontaneous activity patterns from synchronous waves to decorrelated activity that resembles endogenous cortical activity.

**Example 5—BCI Integration, Function, and Sensitivity**

**[0159]** Having established the viability of the graft, we sought to test the degree to which L0 integrated into the host cortex. Structural 2P imaging revealed neurites descending from the cell body, hinting at functional integration of L0 with the host cortex (FIG. 6E). We reasoned that the best way to tell if the graft integrated enough to allow for a useful BCI was to directly attempt to use it for that purpose. We therefore leveraged previous demonstrations of a rodent BCI task using 2P imaging where the animal is operantly conditioned to modulate neural activity for water rewards, and asked if the mice could use the engrafted cortical layer to complete this task.

**[0160]** To validate the behavior in our hands, we first performed control experiments using wild type mice virally expressing GCaMP6 in layer 2 (depth: 136±26  $\mu$ m, FIG. 7A). As in previous reports, we defined a neural cursor as the difference between the mean activity of an ensemble of ‘go’ neurons (E1) and ‘no-go’ neurons (E2) so that animals could not get rewards by simply increasing the mean activity of all neurons. This cursor is transformed into a tone played back to the mouse to provide information about the cursor value. The mouse must modulate the activity of the cursor to a threshold value within 30 seconds to receive a water reward; this counts as a ‘hit’ trial, whereas failure to gain a reward within 30 seconds is considered a ‘miss’ trial, and triggers a timeout. After receiving a reward, we required that the animal modulate the neural cursor back to the baseline value to initiate another trial, such that the animal must move the cursor up and back down, and cannot gain rewards by maintaining the cursor in a reward zone.

**[0161]** In our hands, mice using L2 neurons to control a neural cursor performed above chance on their fourth day of training, and after a regression on the fifth day performed above chance for the remainder of the training sessions (FIG. 7B,  $p<0.05$  hit-rate versus chance, Wilcoxon signed-rank test with Bonferroni post-hoc correction). As in previous reports, a reward-triggered average of ensemble activity showed that rewards were achieved by a large increase in E1 activity that began one second before reward, coupled with long-term suppression of E2 that occurred gradually over the session and was not time-locked to rewards (FIGS. 7C and 7D).

**[0162]** Having validated the calcium-imaging BCI task in wild-type mice, we asked if engrafted mice could volitionally control the activity of L0 neurons for rewards (FIG. 2A). Engrafted mice performed above chance by day three, and maintained performance for the duration of the experiment (FIG. 2B,  $p<0.05$  hit-rate versus chance, Wilcoxon signed-rank test with Bonferroni post-hoc correction). As with

control mice, a reward-triggered average of calcium waveforms showed that rewards were associated with a large peak in E1 activity and a chronic suppression of E2. Unlike control mice, in L0 mice, both E2 and non-target neurons exhibited a small peak in fluorescence time-locked with the reward (FIGS. 2C and 2D). This effect may result from contamination of calcium sources with fluorescence from axons and dendrites, which were much more prominent in L0 than L2. This is likely due to the sparse transfection of L0 and the increased signal-to-noise due to lack of scattering and improved GCaMP variant (FIGS. 2C and 2D).

**[0163]** In sessions where animals performed above criterion, they were able to rapidly achieve rewards at a rate well above chance early in the session and maintained high reward rates before a decrease after around 25 minutes, perhaps due to encroaching satiety (FIG. 2E). In contrast, for sessions where animals failed to hit criterion, average reward rates showed a modest increase and were maintained slightly above chance for the duration of the session. This suggests that overall success depended upon the animal’s ability to rapidly learn the mapping between neural activity and cursor value early in a session (FIG. 2E). Similar results were observed with control mice (FIG. 7E), suggesting that our task design, rather than the use of L0, encouraged dependence on rapid formation of associations. We next asked if the change in fluorescence of the target ensembles over the course of a session reflected the mouse’s behavior. Non-target neurons on average did not change brightness, whereas E1 neurons began increasing early, and were significantly above the E2 neurons for the last 70% of the session ( $p<0.05$  repeated measures ANOVA with Tukey’s test). This rise in E1 fluorescence preceded the persistent suppression of E2 neurons, which began 40% through the session (FIG. 2F). These changes were only apparent in trials where the animal learned; in sessions where the animal failed to achieve criterion, there was no significant difference between ensemble fluorescence (FIG. 2F).

**[0164]** We performed two control experiments to ensure that the mice were using auditory feedback to solve the task. We first asked if the mere onset of auditory stimuli, which would also signal the availability of rewards to trained mice, could by itself trigger a brain-state change that altered neural activity such that the mouse gained a large number of rewards without really learning the mapping from neural activity to cursor. To test this, after the final training session, we performed an auditory decoupling experiment. Mice still controlled a neural cursor that would trigger a reward at a given threshold, but the tone was played back from a previous session, and therefore contained no information about the cursor’s state. Under these conditions, mean population performance degraded to chance levels for both L0 and L2 mice (FIG. 2G, FIG. 7F, task:  $p<0.002$ , tone decoupling:  $p=0.7$ , Wilcoxon signed-rank, hit-rate versus chance). Many mice performed well below chance, perhaps giving up in frustration when the tone previously associated with reward delivery failed to yield water. Interestingly, two mice were able to achieve high levels of performance without auditory information. While we observed these sessions with an infrared camera, we could not associate any overt motor actions with performance in these or any other mice. Although we cannot rule out that mice solved this task by initiating a motor program, if they did, this would still represent a valid solution to the task, and would demonstrate that L0 neurons have access to motor signals.

**[0165]** We next tested if L0 neurons were sensitive to the contingency of the reward by transiently reversing reward contingency mid-session. We trained mice for 40 trials using the standard tone-mapping that they had previously learned to allow them to learn the brain-tone mapping, which we changed daily. After 40 trials, we reversed the mapping such that rewards were given at ‘negative’ threshold, requiring the mouse to modulate E2 over E1 instead of vice versa. This also required the mouse to associate the lowest, rather than the highest, tone with rewards. Task performance dropped precipitously for 40 trials when this change was implemented. We then restored the original mapping for another 40 trials and observed recovery of behavioral performance (FIG. 2H,  $p=0.023$ , Kruskal-Wallis with Dunn’s post-hoc test). These data indicate that modulation of L0 neurons is sensitive to reward contingency. Together these results demonstrate that mice can volitionally control the activity of L0 neurons to perform a simple BCI task.

#### Example 5—Histological Analysis of BCI

**[0166]** Next, we performed a histological evaluation of engrafted animals to assess how L0 connects with the brain. We found that L0 consists of neurons located in a 50-500  $\mu$ m band of cells located above L1 (FIGS. 3 and 5A-5C, FIGS. 8A, 8B, and 9A-9C). To see where L0 neurons project, we imaged brain sections from perfused mice with confocal fluorescence microscopy or light microscopy. These images show that L0 neurons extend dense processes both laterally within L0 and downward across the L0-L1 border, into the brain (FIGS. 3 and 5A-5C, FIGS. 8A, 8B, and 9A-9C). Thicker process resembling dendrites extended from L0 into L1 and the top of L2 (FIGS. 4A-4C, FIGS. 8A and 8B), but axons originating from L0 were not restricted to the superficial layers of the cortex. Instead, axons infiltrated the entire cortical volume beneath the L0 graft (FIG. 3, FIGS. 8A, 8B, and 9A-9C). The density of processes decreased laterally away from the graft, and in some instances could be observed projecting to subcortical structures (FIG. 3).

**[0167]** High resolution confocal imaging with sparsely labeled L0 neurons confirmed that dendrites originating in L0 and extending into L1 featured mature spines (FIGS. 4A-4C). Optical sectioning of tissue stained with synaptic markers showed that the postsynaptic marker SynGAP1 was present in spines from L0 dendrites, and was closely opposed to the presynaptic marker synaptophysin in L1, showing that the molecular machinery of excitatory synaptic input is present in the superficial layers (FIGS. 4A-4C). This suggests that the host brain forms excitatory chemical synapses with the graft, providing a possible mechanism for the graft’s ability to modulate activity to perform a BCI task. Axons from L0 feature numerous putative boutons (FIGS. 3 and 4A-4C, FIGS. 8A, 8B, and 9A-9C), suggesting that L0 can release neurotransmitters onto host neurons. Indeed, staining with synaptic markers showed colocalization of synaptophysin with L0 axons deep in the cortex in close proximity to SynGAP1 puncta (FIGS. 4A-4C). Staining with GAD65 puncta indicated that L0 neurons receive apparent GABAergic input on their soma and proximal dendrites, although we could not determine if this input originates from the cortex or from inhibitory neurons present within the graft (FIGS. 4A-4C). Together, this data showed extensive integration between the graft and the cortex.

#### Example 6—Glial Response to BCI

**[0168]** We next evaluated the glial response to the graft. Since the graft and host cells shared a uniform genetic background, we did not anticipate a generalized immune response. Staining for astrocytes and microglia with GFAP and Iba1, respectively, revealed that both were present throughout L0 (FIGS. 5A-5C). Glia did not exhibit ‘activated’ or phagocytotic morphologies on the L0-L1 border, or deeper in the brain. This indicates that implantation of L0 did not cause an immune rejection or extensive glial scarring (FIGS. 5A-5C). Although we observed both astrocytes and microglia in L0, we did not observe colocalization of these markers with electroporated graft cells (FIGS. 5A-5C), suggesting that these cells originated in the brain. The elevated GFAP expression and lack of ‘activated’ morphology suggests these cells may be in a proliferative state, as would be expected if they were infiltrating L0 to provide metabolic and structural support. Indeed GFAP positive cells were predominantly oriented parallel to the cortical surface, apparently creating a seal between the glass cranial window and the graft. Astrocytes in L0 also appeared to engulf blood vessels that appeared to vascularize L0 (FIGS. 5A-5C). This suggests that glia in the graft may be actively remodelling the tissue, but are not neurotoxic. Together, this data shows that grafting an artificial cortical layer above L1 can be achieved without a foreign body response or immune reaction and results in extensive infiltration of the brain by axons and dendrites that form and receive synaptic connections allowing bidirectional interfacing with the brain.

#### Example 7—Discussion

**[0169]** In this study, we demonstrated an approach to BCI using an artificial cortical L0 formed from transplanted neurons that functions as an interface between recording devices and the brain. We show that this layer survives, develops, and integrates with the brain. We used L0 for BCI by requiring the mouse to volitionally modulate L0 activity to obtain rewards. This implies that L0 is integrated with the brain to a degree sufficient for the animal to control, or at least modulate, its activity patterns. Histology supports this idea, revealing that L0 extends spiny dendrites that possess synaptic markers into the superficial layers of the cortex. L1 is a hub of long-range and higher order inputs, potentially allowing L0 to tap into multimodal contextual information. Dense axonal arborizations from L0 in the cortex implies that ongoing L0 activity is monitored by the cortex, providing a mechanism whereby the brain could sense L0’s activity state, although in our task this feedback was provided by auditory information. The dense axonal fibers from L0 imply that electrical or optogenetic stimulation of L0—potentially with single cell resolution—could be used to write information to the brain. By grafting neurons to form L0, recordings from the brain at single neuron resolution are obtained without genetic modification of the host organism and with no traumatic penetration of the brain’s parenchyma. Instead, the brain is penetrated by naturally in-growing neurites, and bidirectional communication is achieved via chemical synapses, blurring the boundary between implant and host.

**[0170]** The fundamental challenge for any BCI is to collect signals distributed throughout the three dimensional volume of the brain and route it to silicon-based electronics, and conversely to route electronic input signals to appropri-

ate sites in the brain. This must be accomplished with high resolution and low damage to the brain, two requirements which are fundamentally at odds. Functional imaging techniques break this relationship at the expense of viral infection of the brain and over-expression of fluorescent calcium reporters. L0 decouples the relationship between channel count and cell damage by using neurons to non-destructively integrate with the brain and project cortical signals onto a flat structure on top of the cortex that can be safely accessed. By using electroporation *ex vivo*, our approach leveraged modern activity sensors while avoiding modifying the host organism's genome and the use of viruses. This approach does not elicit a foreign body response; indeed, astrocytes and microglia from the brain appear to colonize the graft to provide support or surveillance. In contrast, injecting neurons or destructively penetrating the brain with a living graft or organoid forfeits many of the advantages of a cell-based probe. In this study, we recorded L0 activity using 2P calcium imaging because of the ease with which this method facilitated studying the growth, development, and integration of the graft. Because of the superficial location of the graft, clear signals could also be observed using 1-photon miniature head-mounted microscope (Sup Video 4), providing a path to translation of an optical interface that does not rely on expensive and cumbersome multiphoton optics. However, there is no requirement for future versions of this interface to be optical in nature: future iterations of a L0 implant could use electrical instead of optical recording by engineering the tissue-electronics interface *in vitro* before engraftment.

[0171] Using an engineered bioelectronic bridge layer between electronics and biology has the potential to address key challenges for implanted BCIs. Penetration of the brain by neurites avoids cell death, damage, disruption of vasculature and gliosis. Since neurons intrinsically share the material properties of the brain, the biological 'leads' are unaffected by micromotions and are in no danger of experiencing encapsulation failure, trace breakage, or leaching materials over time. By tethering transplanted neurons to electrode pads, future versions of a L0 interface could record high-amplitude spikes on all channels. This would substantially decrease the need for signal amplification, thereby decreasing the heat generated per channel, allowing implants with significantly increased channel count compared to existing fully implanted devices.

[0172] Biological electrodes could also allow optical or electrical stimulation that is more precise and multimodal than conventional ICMS. Since neurons are accessible at the top of the brain, they could be addressed for stimulation individually; this could be accomplished either by direct current stimulation using very low powers due to proximity between the living probe and electrode or via optogenetics using a microLED array. With stimulation featuring both single-cell resolution and functioning via chemical synapses, input from the implant could in theory be indistinguishable from input from host neurons. Furthermore, by engineering the neurotransmitter phenotype of engrafted cells, stimulation of L0 could potentially manifest as inhibition or neuromodulation instead of just excitation. This could open the door to novel applications of stimulation from a living graft.

#### Example 8—Methods

##### Cell Engraftment

[0173] Pregnant C57/Bl6 mice were CO<sub>2</sub> euthanized at approximately day 15 of embryonic development (E14-17). The embryos were removed from the uterus and placed in Hank's Balanced Salt Solution (HBSS) and transferred to a laminar flow hood on ice. Embryos were removed from the uterus and placed in ice-cold dissection medium (DM) (HBSS+10 mM MgCl<sub>2</sub>\*6 H<sub>2</sub>O, 10 mM HEPES, 1.5 mM kynurenic acid, pH 7.2). The embryos were decapitated, the brains isolated, and the meninges removed from the cortex using sharp forceps under sterile conditions. Cortices were separated from the hippocampal formation and midbrain and stored in ice-cold DM until the dissection of all embryos was complete.

[0174] Isolated cortices were placed in a 1.5 mL tube and allowed to sediment. The supernatant was removed and 1-2 mL of pre-warmed Papain-solution (1:50 Papain, Sigma 76216 and 2.5 mM L-Cysteine in DM). The cortices were placed in a standard cell culture incubator for 6-15 minutes. After the tissue began to clump together, the tube was returned to the flow-hood. The Papain was carefully removed so as not to disturb the tissue, and the clumped tissue was washed three times with 1 mL of warm Light Trypsin Inhibitor (1 mg/mL Trypsin inhibitor Sigma T9003 and 1 mg/mL Bovine Serum Albumin, Sigma 05470 in DM), followed by three washes with 1 mL of Heavy Inhibitor (10 mg/mL Trypsin inhibitor Sigma T9003 and 10 mg/mL Bovine Serum Albumin, Sigma 05470 in DM). The tissue is then washed once with 1 mL of sterile PBS, and then removed. 0.5-1 mL of Resuspension Buffer R (Invitrogen™ Neon™ Transfection System, Thermo Fisher Scientific MPK10096) was then added to the preparation at room temperature, and the tissue was triturated 20-30 times to form a single-cell suspension. The concentration of this cell suspension was determined using a BioRad TC20 automated cell counter. The cell suspension was diluted to 1x10<sup>7</sup> cells/mL in Resuspension Buffer R.

[0175] To electroporate the cell suspension, 3 mL of Electrolytic buffer "E" was added to the electroporation chamber containing the cell suspension. Plasmid DNA (pCAG-H2B-mRuby3-P2A-GCaMP7s, pCAG-ChRimson-tdTomato, pCAG-ChR2-tdTomato, or pCAG-mRuby3) was added to cell suspension at a final concentration of 0.01 µg/µL. Cells were electroporated using the Invitrogen Neon Transfection System. Using the electroporation syringe and tips provided by the manufacturer, 100 µL of cell suspension at a time was electroporated using the following conditions: 1500 V, 20 ms, 1 pulse. The cells were then pelleted (400 RCF, 5 min, 6° C.) using a microcentrifuge and the supernatant was discarded. A mixture of L-15 (L-15 Medium, Sigma L5520) with 10% DNase I (RNase-free, New England BioLabs Inc. M0303L) was then added to the electroporated cells and the pellet of cells was gently resuspended with a pipette to a concentration of 300K cells per microliter. The cells were then kept on ice until transplantation (0-3 hours).

[0176] While cells were being electroporated, wild-type adult C57/Bl6 mice (Jackson Labs or Charles River Laboratory) were anesthetized under isoflurane on a heated pad, head fixed in a stereotactic apparatus (Kopf), and administered buprenorphine (0.05 mg/kg) and dexamethasone (2 mg/kg). Hair was removed and the surgical site was steril-

ized. The scalp was removed, the fascia retracted, and the skull lightly etched. The skull was cleaned and sealed with a thin layer of vetbond (3M) and a 3 mm circular craniotomy was drilled over the primary somatosensory cortex using a dental drill, and the dura was removed. Bleeding was stopped using gelfoam (Pfizer) and room-temperature sterile artificial cerebrospinal fluid (aCSF). A thin well was created around the craniotomy using UV-cure acrylic (Flow-It Accelerated Light Cure, Pentron N11WA). 10  $\mu$ L of the ice-cold cell suspension was applied to the craniotomy while the mouse was maintained under anesthesia. The cells were allowed to settle on the cortical surface while the supernatant evaporated (~15-30 minutes per application, 2-4 applications of 10  $\mu$ L at least 10 minutes after the final cell application, the craniotomy was washed with sterile aCSF, and the craniotomy covered with a sterile glass plug, a 5 mm coverslip adhered to two 3 mm coverslips (Small Diameter Coverslips #1 thickness, Harvard Apparatus 1217H19/1217N66) with optical adhesive (Norland 71). The glass coverslip was secured to the well using metabond (C&B Metabond® Quick Adhesive Cement System, Parkell S380). The rest of the exposed skull was then covered by metabond, and a metal headbar was adhered to the skull. The animal was allowed to recover in a heated recovery cage before returning to their home cage.

[0177] For animals engrafted over primary motor cortex for use with a miniscope, this approach was slightly altered. For these surgeries, the entire skull, except for the region to be drilled away, was covered with a thin layer metabond before drilling. The craniotomy was exposed, and the height differential between the brain and the metabond was sufficient to form a well that could hold 2-5  $\mu$ L of the cell suspension. A single glass coverslip covered the craniotomy and was sealed with additional metabond, and no headbar was attached. A UCLA V4 miniscope baseplate was attached to the cranial window using dental acrylic under anesthesia more than a week after engraftment.

#### Stereotactic Injection

[0178] Wild-type C57/Bl6 mice were anesthetized under isoflurane on a heated pad, head fixed in a stereotactic apparatus (Kopf), and administered buprenorphine (0.05 mg/kg) and dexamethasone (2 mg/kg). After sterilizing the incision site, the skin was opened, and a small burr hole was drilled over S1 using a 0.24 mm drill bit (Busch) (3.5 mm lateral, 1.4 mm posterior to bregma). The glass micropipette was lowered into the burr hole, and we waited five minutes before beginning the injection. 300-400 nL of AAV9 pSYN-GCaMP6s (Vigene) virus was injected using a micro syringe pump (Micro4) and a wiretrol II glass pipette (Drummond) at a rate of 25-50 nL/second at a depth of 150-300  $\mu$ m below the pia surface. After the injection was complete, we waited five minutes before retracting the needle and closing the scalp using sutures. Mice were used 2-6 weeks post injection.

#### Cranial Window and Headbar

[0179] Mice that were previously injected with virus (1-3 weeks post injection) were anesthetized under isoflurane and administered buprenorphine (0.05 mg/kg) and dexamethasone (2 mg/kg). Hair was removed and the surgical site was sterilized. The scalp was removed, the fascia retracted, and the skull lightly etched. The skull was cleaned and sealed

with a thin layer of vetbond (3M) and a 3 mm circular craniotomy was drilled over primary somatosensory cortex using a dental drill, and any bleeding was stopped using gelfoam (Pfizer) and sterile artificial cerebrospinal fluid (aCSF). The craniotomy was covered with a sterile glass plug, a 5 mm coverslip adhered to two 3 mm coverslips with optical adhesive (Norland 71). The glass coverslip was secured to the well using metabond. The rest of the exposed skull was then covered by metabond, and a metal headbar was adhered to the skull. The animal was allowed to recover in a heated recovery cage before returning to their home cage.

#### Two-Photon Imaging

[0180] For calcium imaging, mice were head-fixed on a freely spinning running wheel under a Nikon water immersion objective (16 $\times$ , 0.8 NA Nikon) and imaged with a Sutter moveable objective (MOM) two-photon resonant scanning microscope within a darkened box. The imaging laser source was a Mai Tai Ti: Sapphire laser (Spectra-Physics) mode locked at 920 nm for calcium imaging or at 1000 nm for structural imaging. Signal was collected with a Hamamatsu photomultiplier tube (H10770PA-40). The imaging system was controlled by Scanimage 2018 (Vidrio) running on Matlab (v2019b, Mathworks). Functional images were acquired at 920 nm with ~50 mW average power. For developmental structural analysis, volumes were acquired at 1250 $\times$ 1250  $\mu$ m field of view covering 300  $\mu$ m in Z with 2  $\mu$ m steps. For imaging of spontaneous L0 events, a single 1250 $\times$ 1250  $\mu$ m field of view was imaged at 30 Hz. For online BMI, a single plane 430 $\times$ 430  $\mu$ m was imaged at 30 Hz with online 3D motion correction enabled (Scanimage 2018, vidrio). For neuronal morphology, images were acquired from a 215 $\times$ 215  $\mu$ m FOV.

#### Analysis of Graft Development

[0181] For analysis of graft thickness, z-stacks were acquired from a 1250 $\times$ 1250  $\mu$ m field of view with 300  $\mu$ m thickness and 2  $\mu$ m spacing (920 nm). Cell nuclei (H2B-mRuby3) were segmented using Cellpose and nuclei assigned to a given z-level based on the location of their centroids. The thickness of L0 was calculated by identifying the range in z that contained 90% of the segmented cell nuclei.

[0182] To characterize spontaneous activity during graft development, 5-10 minutes of spontaneous activity was recorded (1250 $\times$ 1250  $\mu$ m FOV, 30 Hz, 920 nm, 50 mW average power). Calcium imaging analysis packages typically identify calcium sources by finding spatially isolated groups of locally co-varying pixels. However, the massive population events we observed early in graft development (Sup Movie 1) and the numerous silent neurons we observed later in development were significantly different from the typical use case of these packages, and produced poor results in our hands. Instead, we used Suite2P's registration function to motion correct movies using the red nuclear signal as a reference, and then used Cellpose to segment nuclei, choosing a model that dilated the nuclear mask to capture surrounding cytoplasm, only several pixels on the low zoom were used. We did not correct for neuropil contamination, since the sparse labelling of L0 achieved using electroporation resulted in clear separation between neurons. This

strategy allowed us to sample all transfected L0 cells, regardless of whether they exhibited any spontaneous activity.

[0183] We extracted average fluorescence for each mask and for the full frame. dF/F was calculated using  $F_0=30$ th percentile of the recorded fluorescence values. To identify population events, we convolved the full-field dF/F signal with a linear function to identify event rise times. Population events were defined as frames where the signal was 3.5 standard deviations above baseline signal. Neurons were considered to participate in a given population event if their convolved dF/F signal was above threshold during frames assigned to population events. Pairwise correlation was calculated using the dF/F signal from the full duration of the recording. For comparison of L0 and L2 spontaneous pairwise correlation, the L2 correlations were computed using online data from the baseline period of the first day of BMI training, before the animals had been exposed to the task.

[0184] For analysis of dendritic complexity, sparse labeling was achieved by mixing a population of cells electroporated with pCAG-mRuby3 1:50 with a population of non-electroporated cells, thereby maintaining the density of cells in the graft while reducing the number of labelled cells. Z-stacks of 300  $\mu\text{m}$  with 2  $\mu\text{m}$  steps were obtained at several timepoints after development. Sholl analysis was performed on traced dendritic arbors from maximal intensity projections using ImageJ and depth-coded Z-stacks were obtained using the Z-stack Depth Color Code package for ImageJ.

#### Optical Brain-Computer Interface Task

[0185] Mice were placed on a high-fat diet (PicoLab Mouse Diet 21) 5-7 days before water restriction. Upon beginning water restriction, mice were fed water from a syringe for two days, and for the next two days they received their water for free in the 2P experimental rig. Mice performed the BCI task for 8 sessions, and then performed two control experiments, contingency reversal and tone decoupling, described below.

[0186] The BCI task required the mouse to volitionally modulate the calcium dynamics of target neurons to achieve a reward, and was conducted largely as described. To perform BMI experiments, mice were placed on the experimental apparatus, and an imaging field was chosen with bright, active neurons. We did not attempt to find the same region or same neurons from day to day. To select ensembles, we imaged a 430 by 430  $\mu\text{m}$  field of view for several seconds, and calcium sources were segmented using custom Matlab software using the GCaMP6s signal from control mice or the H2B-mRuby3 (nuclear) signal from engrafted mice. We used laser power  $\sim$ 50 mW, and depths of  $144\pm37$   $\mu\text{m}$  for control mice and  $136\pm26$   $\mu\text{m}$  for engrafted mice (these depths are relative to the first observed signal, and do not necessarily correspond to cortical depth). We then acquired a reference z-stack to allow online 3D motion correction to compensate for any slow drift over the course of the experiment (Scanimage, Vidrio). To establish baseline activity, we imaged the field of view for 10-20 minutes while tracking the activity of all segmented cells. During this period the experimenter selected appropriate calcium sources for BCI. Appropriate calcium sources met the following criteria: 1) they were not over-filled cells, which might indicate poor cell health, 2) they were well-isolated from other nearby neurons, ensuring that the signal was not contaminated by a nearby cell, 3) they exhibited well-

defined spontaneous calcium transients and did not exhibit plateau, or step-function behavior, 4) their signals were unaffected by small motions associated with movement, and 5) they had a sufficiently bright baseline intensity so that photobleaching would not be a concern. The raw fluorescent values from calcium sources were calculated on-line and were smoothed over 200 ms (rolling average of 6 frames at 30 Hz). No auditory stimuli was played during the baseline period.

[0187] At the end of the baseline period, we selected four neurons to compose the output population. The output of the BCI task was a cursor value that was defined as the difference between the average z-scored fluorescence values of the activation ensemble (E1) minus the average z-scored fluorescence values of the control ensemble (E2).

$$\text{Cursor}(t)=\sum F_{e1}(t)/n_{e1}-\sum F_{e2}(t)/n_{e2}$$

[0188] To select neurons to compose these ensembles, at the conclusion of the baseline period, we randomly assigned valid neurons to these populations, and put the neural activity recorded during the baseline period through a virtual behavior session using the trial structure defined below. We chose thresholds for the cursor value that would have resulted in a hit-rate between 15-25% during the baseline period. During the task, the cursor value was computed on-line from neural activity using Scanimage's integration function, and auditory feedback indicating the cursor value was delivered to the mouse with an ultrasonic speaker (Tucker-Davis Technologies, EC1). The online cursor value was linearly mapped to auditory feedback so that 24 kHz indicated the threshold cursor value to trigger a reward, whereas 1 kHz indicated 'negative' threshold. To measure the performance of mice on this task, we imposed a trial structure as follows. Trial start was indicated by beginning auditory playback of the neural cursor. Trials were 30 seconds long; failure to move neural activity past the target threshold constituted a 'miss' trial, and movement of the neural cursor past the threshold in less than 30 seconds after trial start defined a 'hit' trial. After a 'miss' trial, auditory feedback stopped for several seconds during a variable inter-trial interval, and the start of the next trial was cued by resumption of auditory feedback. For a 'hit' trial, moving neural activity to the target zone triggered the immediate delivery of a water reward. In order to conclude a 'hit' trial, we required the neural cursor to return to below the middle of the cursor range. This ensured that mice could not solve this task by entering a state where activity was constantly maintained above threshold; instead, they had to actively modulate the neural cursor from rewarded value back to a neutral value to start another trial. After successfully moving the cursor from a rewarded to a neutral value after a hit trial, auditory feedback stopped during a randomized inter-trial-interval before the next trial began. Training sessions lasted  $108\pm28$  minutes for engrafted mice and  $109\pm28$  minutes for controls (engrafted:  $86\pm15$  trials, controls  $97\pm21$  trials).

[0189] After mice performed 8 BCI sessions, we performed two control experiments. The first, contingency-reversal (CR), mice performed a standard BCI session for the first 40 trials. We then altered how the cursor was computed on-line so that the cursor was given by E2-E1 instead of E1-E2. All else remained constant, so that the effect was that the mapping of neural activity to gain a reward was reversed. After 40 more trials we restored the

map to the original values that the mouse learned in-session, and allowed the mouse to perform 40 more trials.

[0190] On a separate day we tested whether the simple presence of auditory stimuli itself was sufficient to modulate neural activity in a manner consistent with solving this task. We therefore set up a normal BCI experiment, but instead of playing auditory feedback that reflected the value of the neural cursor, we replayed the cursor values from a previous experiment. In this way the animal still had the ability to get water rewards by modulating neural activity, but the feedback was unrelated to current brain state.

#### Histology

##### [0191] Tissue Processing

[0192] Mice were deeply anesthetized and transcardially perfused with heparinized saline (25 ku/mL) followed by 10% Neutral Buffered Formalin (NBF, VWR); brains were extracted and postfixed in NBF for 24 hours, then placed in 30% sucrose for 24-48 hr at 4° C., frozen and sectioned using a Leica CM2050S Cryostat into 50 µm thick coronal sections. Sections were collected into 48-well dishes filled with a cryoprotective solution (30% glycerol, 30% ethylene glycol and 40% PBS) and kept at -20° C.

[0193] Free-floating sections were rinsed 3x in PBS and incubated in a blocking solution containing 10% Normal Donkey Serum (NDS, Sigma, D9663), 0.3% TritonX-100 (Sigma, T8787), 0.1M glycine (Sigma, 410225) and a drop of iT-FX Signal Enhancer (Invitrogen, 136933) for 1 hr at room temperature. Then, sections were incubated in a mixture of primary antibodies (Table) diluted in PBS containing 1% NDS for 24-48 hours on a rocker platform at 4° C. Sections were then washed 3x in PBS containing 0.05% TritonX-100 (PBS-T), followed by incubation with fluorophore-conjugated secondary antibodies (Table 2) in PBS with 1% NDS 1-2 hours at room temperature, and if applicable, sections were counterstained with DAPI. Finally, sections were washed 3x with PBS-T, then rinsed in PBS and mounted on microscope slides using ProLong™ Gold antifade mounting media (Invitrogen).

[0194] Alternatively, sections were processed for GFP immunoperoxidase in which sections were first pretreated with 3% hydrogen peroxide to inactivate endogenous peroxidase, rinsed in PBS and then processed as described above. Following incubation with anti-GFP primary antibody, sections were rinsed in PBS and incubated in biotinylated secondary antibodies (Jackson Immunoresearch, 711-065-152) diluted in PBS-T. Sections were then incubated in ExtrAvidin (1:2,000, Sigma) and followed by Diaminobenzidine DAB (Sigma) enzymatic detection. Sections were rinsed in PBS, mounted on gelatinated slides, air dried and coverslipped with Neo-Mount mounting media (Sigma, 109016) counterstained with 0.1% Cresyl Violet (Sigma C5042-10G OR FD NeuroTechnologies, PS102-2).

##### [0195] Imaging

[0196] Fluorescent images were obtained using the ZEISS LSM 900/980 confocal microscope with the Airyscan 2.0 detector, utilising 5x/0.25 air, 10x/0.45 air, 20x/0.8 air, and 63x/1.4 oil immersion objectives (Carl Zeiss Microscopy, Jena, Germany). Fluorophores were excited using laser lines 405, 488, 561 and 639 nm, with corresponding emission bandpass filters of 420-480 nm, 495-550 nm, 573-615 nm and 607-750 nm. Widefield images were collected on an Axiocam 705. Large scale images (10x or 20x) were taken using z-stacks together with a tilescan overlap of 10%, with

pixel size of 0.487 µm (x)×0.487 µm (y)×2 µm (z). Super resolution images (63x) were taken using z-stacks and/or tilescans with 0-10% overlap with pixel sizes of 35 nm (x)×35 nm (y)×0.13-0.5 µm (z). Airyscan processing was done in ZEN Blue 3.3 software using the auto-filter setting with standard strength. Stitching of tilescans and max intensity projection processing of z-stacks was done in ZEN Blue.

TABLE 1

Target	Species	Dilution	Product Number
GFP	Ch	1:1000	Invitrogen, A10262
GFP	Rb	1:10,000	Abcam, ab290
SynGAP1	Rb	1:1000	Abcam, 77235
Synaptophysin	Mo	1:1000	CST, 7H12
NeuN	Rb	1:1000	Abcam, 177487
IBA1	Gt	1:1000	Abcam, 5076
GFAP	Ch	1:2000	Abcam, 4674
GAD65	Mo	1:500	Synaptic Systems, 198111

TABLE 2

Target	Fluorophore	Dilution	Product Number
Donkey anti Ch	488	1:1000	Biotium, 20166
Donkey anti Ch	633	1:500	Biotium, 20168
Donkey anti Rb	488	1:500-1000	Invitrogen, A21206
Donkey anti Rb	555	1:500-1000	Abcam, 150062
Donkey anti Gt	555	1:500	Abcam, 150130
Donkey anti Gt	405	1:500	Abcam, 175664
Donkey anti Gt	488	1:500	Abcam, 150129
Donkey anti Mo	647	1:500	Abcam, 150107
Donkey anti Rb	Biotin	1:1000	Jackson Labs, 711-065-152

#### Stimulation

[0197] The BCI experiment showed that L0 can be used to read out information from the brain. We next asked if stimulating L0 can input information into the brain. To test this, we leveraged an optical microstimulation task wherein mice are trained to report optogenetic activation of a population of neurons. In this task, mice with a cranial window and a ferrule for an optical fiber are placed into a custom behavior box with three ports. Trials are initiated by a nose-poke to the middle port, which triggers a masking LED located in the middle port on every trial. Mice then have 10 seconds to select left or right by poking their nose in the respective port. On some trials, optogenetic stimulation is provided via a fiber-coupled LED (470 nm, 10x pulses at 20 Hz). On trials where stimulation is provided, animals are rewarded for a left selection, and they are rewarded on the right port on trials with no stimulation. There is no punishment for an incorrect selection.

[0198] We first validated this task by training positive control mice injected in S1 with AAV-CAG-ChR2-tdTomato and negative control mice with no opsins. We trained mice for three weeks or until they exceeded criterion (D'=1). Since these mice were implanted with optic fiber ferrules, we could not screen them for expression before behavior, so after their behavioral experiments were completed we perfused, sectioned, and imaged their brains. Images were blinded and scored for expression, and mice were marked for inclusion in the dataset based solely on their expression levels, without reference to their behavior. Positive control mice all learned the task in 10.83±6.1 days (n=6). Negative

control mice failed to learn the task after three weeks of training (0 of 5 mice met criteria after 3 weeks). We then trained mice engrafted with layer zero neurons electroporated with pCAG-ChR2-tdTomato three to five weeks after engraftment. Similarly to the positive controls, we screened the mice post-hoc blind to behavioral performance and included mice that had a healthy L0 graft without knowledge of behavioral outcome. Mice implanted with L0 were able to hit criterion  $21\pm4$  days ( $n=3$  of 7 total) after beginning training. Given that 4 of the implanted mice did not hit criterion in time, we believe this outcome is due to the diminished transfection efficiency of electroporation of our transplanted cells. Stimulation may require a greater transfection efficiency of transplanted L0 cells in order to input salient information more reliably. Nevertheless, this data shows that stimulation of L0 can be used to transmit information to host brains on which it is engrafted, demonstrating that layer zero can be used as a bidirectional interface layer with the brain.

#### Optical Microstimulation Detection Task

[0199] Mice that had been engrafted with electroporated L0 neurons expressing pCAG-ChR2-tdTomato for 3-5 weeks were enrolled in behavior. Positive control mice expressing viral AAV9-CAG2-hChR2(H134R)-TdTomato (Vector BioLabs VB2896) and negative controls that underwent craniotomies, durotomy, and windowing (no viral injection) were entered into the task 3-5 weeks post-surgery. Mice were placed on a high-fat diet (PicoLab Mouse Diet 21) 5-7 days before water restriction. Upon beginning water restriction, mice were fed water from a syringe for two days, after which they began the first stage of training for the stimulation task which included habituation to the operant box.

[0200] The operant box featured three nose-poke ports each with an IR beam sensor. The center port contained a masking LED (470 nm), and the left and right ports contained lick spouts. A hole in the top of the box allowed entry of a rotary joint patch cable with 400  $\mu$ m multimode fiber and 1.25 mm ferrules with heat-shrink tubing (ThorLabs RJPSL4). Water was delivered using a solenoid valve triggered by custom behavior software running on a Teensy 4.0 board.

[0201] Training was split into 3 phases: habituation, shaping, and stimulation. During habituation, water-restricted mice were exposed to the enclosure and received a water reward at either of the two lateral ports, with a 10 second inter-trial-interval and 60 second timeout per 'trial'. Once the mice got water rewards on >65% of the total trial count for 2 consecutive days, they were moved on to shaping, where rewards were available on the left and right ports for 10 seconds only after triggering the center port. Mice that achieved >65% success rate for 2 consecutive days were moved on to the stimulation detection task.

[0202] For the detection task, trials were initiated by poking the center port. On every trial, masking LEDs (470 nm) were active for the duration of every trial, and optical stimulation was delivered to the cranial window using a fiber-coupled LED directly touching the glass window (590 nm, Thorlabs M590F3) on GO trials. The response period extended 500 ms after the stimulation presentation was over, followed by different tones to indicate success or failure, followed by a variable inter-trial interval. Licking during a GO trial resulted in an immediate water reward, and the trial

was classified as a hit. Failing to lick during a GO trial (miss' trial) triggered a 4 second timeout. Licking during a catch trial ('false alarm' or FA) resulted in an airpuff to the face, whereas not licking during a catch trial ('correct reject' or CR) was a correct trial, but unrewarded.

[0203] Mice gradually acclimated to the main task, starting with 'autoreward' where water was paired with stimulation for free. Mice were kept on autoreward until licking for 50% of rewards, usually just one session. Mice were then advanced to a session with only go-trials, where they had to lick during the response period to receive a water reward. After achieving performance of 50%, mice were advanced to the main task until they achieved sessions above criterion ( $D'>1$ ). Controls could advance to the main task by associating masking light with reward.

#### Example 8—Replacing Embryonic Mouse Neurons with Human Stem Cell Derived Neurons

[0204] Two cohorts of mice were used: one cohort was daily IP injected with 35 mg/kg cyclosporine, 4-5 days before implantation and every day until euthanasia, to immunocompromise the mice, and the other cohort had naïve mice. Identical to mouse-mouse surgeries were performed, albeit done in a biological safety cabinet to maximize sterility. Plasmids used during surgery include: pCAG-H2B-mRuby3-P2A-GCaMP7s; pCAG-ChR2(H134R)-tdTomato; Cag-mRuby3; and pCAG-ChrimsonR-tdTomato. Human neurons were obtained using a modified version of the protocol described in Nehme et al., *Cell Rep*, 23(8): 2509-2523, 2018. The stem cells that were used (iP11N from ALSTEM) have been genetically modified to harbor a doxycycline inducible NGN2 cassette at the AAVS1 locus for rapid neuralization of stem cells. Nehme et al. used a lentiviral approach to insert the NGN2 cassette into the cells. Due to these differences, puromycin was not used for selection. EdU, an anti-mitotic, was used instead. The cells were also passaged on Day 3 and Day 5 due to excessive progenitor proliferation. FIG. 10A-10G show stem cell to human neuron differentiation from Day 1 to Day 7.

[0205] Following surgery, mice were subjected to the same behavioral testing (where applicable) as the mouse-mouse pour overs. After time, the mice were transcardially perfused with formalin, and their brains excised and processed for immunohistochemistry. The results of neuron differentiation include a massive immune response by the infiltration and activation of astrocytes (gfap); and microglia (ib4) around implant site. The results demonstrate that immune-compromization is necessary for grafting human cells into/onto the mouse cortex.

#### Example 9—Cell-Tethering

[0206] This example illustrates the development of an in vitro model to test the efficacy of standard coating on neural health. FIG. 11 shows neuronal growth on an indium tin oxide (ITO) substrate in the presence of poly-D-lysine and laminin. Neurospheres are cell aggregates (neural network) that consist of neural progenitor cells (NPCs) and are cultivated in the presence of growth factors. In the absence of growth factors and when seeded on 2D poly-D-lysine/laminin (PDL/LAM)-coated surfaces, NPC neurospheres migrate and differentiate into neurons, astrocytes, and oligodendrocytes, thereby generating complex networks. Hydrogel readily adheres to (PDL/LAM)-coated surfaces.

[0207] Modifications and variations of the present invention will be obvious to those skilled in the art from the foregoing detailed description and are intended to fall within

the scope of the following claims. The teachings of all references cited herein are specifically incorporated by reference.

## Informal Sequence Listing

- continued

## Informal Sequence Listing

ACGACGGCAACTACAAGACCCGGCGGAGGTGAAGTTCGAGGGCGACACCCGGTG  
 AACCGCATCGAGCTTAAGGGCATCGACTTAAGGAGGACGCCAACATCTGGGCA  
 CAAGCTGGAGTACAACCTCTGACCAACTGACTGAAGAGCAGATCGCAGAAATTAA  
 AAGAGCTTTCTCCCTATTGACAAGGGAGGGGATGGGACAATAACAAACCAAGGGAG  
 CTGGGGAGGGTGTGCGGTCTCTGGGGCAGAACCCCCACAGAAGCAGAGCTGCGAGGA  
 CATGATCAATGAAGTAGATGCCGACGGTGACGCCAACATCGACTTCCCTGAGTTCT  
 GACAATGATGGCAAGAAAATGAAATACAGGGACACGGAAAGAAGAAAATTAGAGAA  
 GCGTTCTGTGTTGATAAGGATGGCAATGCTACATCACTGAGCAGAGCTTGC  
 CACCTGATGACAACACCTGGAGAGAAGTTAACAGATGAAGAGGTTGATGAAATGAT  
 CAGGGAAAGCAGACATCGATGGGATGGTCAGTAAACTACGAAGAGGTTGATACAAA  
 TGATGACAGCGAAGTGTAGTAAGTATCAAGGTTACAAGACAGGTTAACAGGAGACCAA  
 TAGAAAATCTGGGTTGCGAGACAGAAGACTCTTGCGTTCTGATAGGCACCTTATT  
 GGTCTTACTGACATCCACTTGCCTTCTCCACAGGTGTCGACAATCAACCTCTGG  
 ATTACAAAATTGTAAGAGATTGACTGGTATTCTTAACATAAGTGTGCTCTTTACGCT  
 ATGTGGATACGCTGTTTAATGCTTGTATCATGCTATTGCTTCCCGTATGGCTTC  
 ATTTCCTCTCTTGATAAAATCTGGTTGCTCTTTATGAGGGAGTTGGCCCG  
 TTGTCAGGCAACGTGGCTGGGTGACTGTGTTGCGACTGACGCAACCCCCACTGGT  
 GGGGCAATTGCCCCACCTGTCACTCTTCCGGACTTGCCTTCCCCCTCCCTAT  
 TGCCACGGCGGAACATCGCCGCCTGCGCTGCCGCTGCTGGACAGGGGCTCGGCT  
 GTTGGGCACTGACAATTCCTGGTGTGCTGGGAGGCTGACGCTCTTCCATGGCT  
 GCTCGCCCTGTGTGCGCTGGGAGGCTGACGCTCTTCTGCTACGTCCTTC  
 GCCCTCAATCAGCGGACCTTCTTCCCGCGCCCTGCTGCCGCTCTGCCCTCTTC  
 CGCGCTTCGCCTCGCCCTCGAGCAGTCGGATCTCCCTTGGGCCCTCCCCGCC  
 TGAATTGCGAGTCGCTACGATCAGCCTCGACTGTGCTTCTAGTTGCGACGCATCT  
 GTTGTGTTGGCCCTTGGCTTCTGACCTGGAAAGGTTGCGCACTCCACGTGCTCC  
 TTCCCTAATAAAATGAGGAAATTGACATCGCATGTCGAGTAGGTGTCATTCTATT  
 GGGGGGTGGGGTGGGGCAGGACAGCAAGGGGGAGGATTGGGAAAGACAATAGCCA  
 GCTTTTGTCTCTTTAGTGAGGGTTAATTGCGCGTTGGCGTAATCATGGTCATAGCT  
 GTTCTCTGTGTTGTAATTCTACTCCTCAGGGTCTGGCTCATAGTGGCTATCA  
 GAAGGTGTTGGCTGGGCAATGCCCTGCGTCACAAATACCAACTGAGATCTTT  
 TCCCTGCCCCAAATTATGGGACATCATGAAGCCCTTGAGCATCTGACTCTGG  
 CTAATAAAGGAAATTTTTCTATTGCAATAGTGTGTTGGAAATTTTTGTGCTCTCA  
 CTCGGAAGGACATATGGGAGGGCAATCATTTAAACATCAGAATGAGTATTGTT  
 TTAGAGTTGGCAACATATGCCCATATGCTGGCTGCCATGAACAAAGGTTGCGTATA  
 AAAGAGGTCACTAGTATATGAAACAGCCCCCTGCTGTCCTTCTTCTTCTAGAAA  
 AGCCCTGACTTGAGGTAGATTTTTTTATTTGTTGTTATTGTTCTTAA  
 CATCCCTAAATTCTTCTTACATGTTACTAGGCCAGATTTTCTCTCTGACTA  
 CTCCCACTGCTCATGCTCCCTCTCTTATGGAGATCCCTCGACCTGCAAGCCAAAGC  
 TTGGCGTAACTCATGGTCACTGCTGTTCTGTGAAATTGTTATCGCTCACAATT  
 CACACACATAGGAGGCCGAACGATAAAGTAAAGCTGCTGGGTGCGCTAATGAGT  
 AGCTAACTCATAATTGCTGCGCTACTGCCCCCTTCAGCTGGGAACACTG  
 TCGTGCAGCGGATCCGCATCTCAATTAGTCAGCAACCATAGTCCGCCCTAACTC  
 CGCCCATCCGCCCTAACTCGCCAGTTCCGCCCCATTCTGCCCTGCGTACT  
 AATTTTTTTATTATGAGGAGGCCGAGGCCCTGGCTCTGAGCTATTCCAGAA  
 GTAGTGGAGGAGCTTTTGGAGGGCTAGGCTTTGCAAAAAGGTAACCTGTTTATT  
 GAGCTTATAATGGTACAATAAGCAATAGCATCACAAATTCAAAATAAAGC  
 ATTTTTTCTACTGCATTCTAGTGTGTTGCTCAAACATCATCATGATCTTATCATG  
 TCTGGATCCGCTGCATTATGAATCGGCCAACCGCGGGGGAGGGCGTTGCGTAT  
 TGGCGCTCTCGCGCTCTCGCTACTGACTCGCTGCGCTCGGTGCGCTCGGG  
 CGAGCGGTATCAGCTCACTAAAGCGGTAAATACGGTTATCCACAGAATCAGGGG  
 TAACCGAGGAAAAGACATGTGAGCAAAGGCCAGAAAAGGCCAGGAACCGTAA  
 AAGGCCGCGTGTGGCTTCCATAGGCTCCGCCCCCTGACGAGCATCACAAA  
 ATTCGAGCTCAAGTCAGAGGGCAAAACCGACAGGACTATAAAAGATAACCGAGC  
 GTTCCCTGGAGACTCTCTGGCGCTCTCTGTTCCGACCCCTGCCGTTACCGGA  
 TACCTGTCCGCTTCTCCCTCGGGAGCGTGGCGCTTCTCATAGCTCACGCTGTA  
 GGTATCTCAGTTGGTGTAGGTGTCGCTCAAGCTGGCTGTGTCAGAACCCCC  
 CGCTTCAAGCCCCCTGCCCTGGCTTAACGTTAGTGTGCTGTTACCGGG  
 TAAGACAGCACTTATCGCCACTGGCAGCAGCAGCTGGTAACAGGATTAGCAGAGCG  
 AGGTATGTTAGGGGTGCTACAGAGTTCTGAGGTGTTGGCTTAACAGCTACACT  
 AGAAGAACAGTATTGTTGATCTGCGCTCTGCTGAAGCCAGTTACCTCGGAAAAGA  
 GTTGGTAGCTCTGATCCGGAAACAAACCCCGCTGGTAGCGGTGTTTTTTGTT  
 GCAAGCAGCAGGATTCAGCGCAAGAAAAGGATCTCAAGAACGATCTTGTGCTT  
 TCTACGGGGTCTGACGCTCAGGAAACACTCAGCTTAAGGGATTGGTGTG  
 AGATTATCAAAGGATCTCACCTAGATCTTTAAATTAAAGTGAAGTTTAA  
 TCAATCTAAAGTATATGAGTAAACTGGTCTGACAGTTACCAATGCTTAATCAGT  
 GAGGCACCTATCTCAGGATCTGTTATTCGTTCATCCATAGTGTGCTGACTCCCC  
 TCGTGTAGATAACTACGATACGGGAGGGCTTACCGTACGCTGGCCCCAGTGTGCAATGA  
 TACCGCGAGACCCACGCTCACCGGCTCCAGATTATCAGCAATAACCCAGCCAGCC  
 GGAAGGGCCGAGCGCAGAAGTGGTCTGCACTTATCGGCCCTGCGTCACTGCTATT  
 AATTGTTGCGGGAGCTAGAGTAAGTAGTGTGCGCTTAATAGTTGCGCAACGTT  
 GTTGTGCTACAGGATCTGTTGTCAGCTGCTGTTGGTATGGCTTCACT  
 GCTCCGGTTCCCAACGTAAGGCGAGTTACATGATCCCCCATGTTGCAAGGAAAG  
 CGGTTAGCTCTCGGTCTCCGATCGTGTGCAAGAGTAAGTGGCCGAGTGTAT  
 CACTCATGGTTATGGCAGCACTGCAATAATTCTTACTGTCATGCCATCGTAAGG

- continued

## Informal Sequence Listing

- continued

---

Informal Sequence Listing

---

ggcacccggcagcacccggcagcggcagctccggcaccgcctcccgaggacaaca  
acatggccgtcatcaaaagagtcatgcgcctcaagggtgcgcatggagggtccatgaacgg  
ccacagttcgagatcgagggcgagggcgaggggcccccatacgaggccaccagac  
cgccaaagctgaagggtgacccaaaggccggcccccgtggacatctg  
tccccccaggatgtacgggttcaagggtcaagttggagcgtatgtgaacttcga  
gattacaagaagcttccttcccgagggttcaagttggagcgtatgtgaacttcga  
ggacggcggtctggtgcacgtgaccaggactctccctgcaggacggcagctg  
atctacaaggatggaaatgcgcggcacaacttccccccgacggccccgtaaatg  
cagaagaagacatgggtggggccacccggccgtgtaccccgca  
cggtgtctgaaggcgagatccacccaggccctgaagctaaaggacggccgc  
caactctggtgagttcaagacatctacatggcaagaagccgtcaactgc  
ccggctactactacgtggacaccaaggctggacatcacctccacaaacgggact  
acaccatcggtggacatgtacggcgtccggggccggccaccacccgttc  
ctgtacggcatgtacggatgtacaagtaaCTAAGTATCAAGGTTACAAG  
ACAGGTTAAGGAGACCAATAGAAAATGGGCTGTCGAGACAGAGAAAGACTCTTGC  
GTTCTGATAGGCCACCTATTGGCTTACTGACATCTCCTTCTCCACAGG  
TGTCGACAATCACCTCTGGATACAAAATTGTGAAAGATTGACTGGTATTCTTAA  
CTATGTTGCTCTTACGCTATGTTGATACGCTTAAATGCTTGTATCATGCT  
ATTGCTTCCCGTATGGCTTCTTCTCCTGTATAAATCCTGGTTGCTGCTCT  
TTATGAGGAGTGTGCCCCGTGTCAGGAACTGTGGCGTGGTGTGCACTGTGTTG  
TGACGCAACCCCCACTGGTGGCCATTGCCACCCACTGTGAGCTCCTTCCGGGAC  
TTTCGCTTCCCCCTCTGGCACGGGAACTCATGCCGCTGCGCTTGGCC  
TGCTGGACAGGGGCTGGCTGTGGGACTGACAATTCGTGGTGTGCGGGAAAG  
CTGACGCTCTTCCCATGGCTCTCGCCTGTGTCGACCTGGAATTCTGCGGGAGCT  
CCTTCTGCTACGGCTTCCGGGCTCAATCCAGGGACCTTCCTTCCCGGGCTGCT  
GCCGGCTCTGGCCCTTCCGGCTTCCGGCTCAGACGAGTCGAGATCTCC  
CTTGGGCGCCCTCCCGGCTGGAATTGAGCTCGGTACGATCAGCCTGACTGTGC  
CTTCTAGTTGAGGACATCTGTGTTGCCCCCTCCCGTGCCTTCTTGACCCCTGGA  
AGGTGAGGACTCCACTTCTCTTCTCTTCTCTTCTCTTCTCTTCTCTGGA  
GAGTAGGTGCTATTCTATTCTGGGGGGTGGGGCAGGACAGCAAGGGGAGG  
ATTGGGAAGACATAGCCCAGCTTGTCTTCTAGTGAGGGTTATTGCGCGTT  
GCCGTAATCATGTCATAGCTTCTGTGAAATTGTTATCGCTAATTCACTCC  
TCAGGTGAGGCTGCTTCAAGGTTGGCTTCAATGAGGCTGGCTGGCAATGCGCTG  
CAAATACCAACTGAGATTTTCCCTCTGCAAAATTATGGGACATCATGAAGCC  
CCTTGAGCATCTGACTCTGGCTAATAAGGAAATTATTTCTATTGCAATAGTGT  
TGAATTGTTTCTGCTCTCACTCGGAAGGACATATGGGAGGCAATATTAAAA  
CATCAGAATGAGTATTGGTTAGGTTGGCAACATATGCCCATATGCTGGCTG  
ATGAACAAAGGTTGGCTATAAGAGGTCTAGTATATGAAACAGCCCCCTGCTG  
CCATTCTTATCCATAGAAAGCCTTGACTTGAGGTTAGATTTTTATATTGTT  
TTGTGTTATTCTTCTTAACTCCCTAAATTCTTCTTACATGTTTACTAGCCAGA  
TTTTCTCTCTCTGACTACTCCAGTCAGCTGCTCTCTCTTATGGAGATC  
CCTCGACCTCGGCCAACGCTGGCTTAATCATGGTCATAGCTGTTCTGTG  
ATTGTTATCCGCTACAATTCCACAAACATACGAGCCGAAGCATAAAGTGTAAA  
GCCGGGGGTGCCCTAATGAGTGAAGCTAACCTCACATTAATTGCGTTGCGCT  
GCTTCCAGTGGGAAACCTGCTGTCGAGGCGATCGCATTCAATTAGTCAGCAA  
CATAGTCCGCCCTAATCCGCCCATCCGCCCTAACTCCGCCAGTCCGCC  
ATTCTCCGCCCATGGCTGACTATTCTTATTGAGGAGGCTTTTGAGGCTTAGG  
GCCCTCTGAGCTATTCCAGAAGTAGTGAGGAGGCTTTTGAGGCTTAGG  
CAAAAAGGCTAACGTTATAAGGTTAGGTTACAAATAAGGAAATAGCATC  
ACAATTTCAAAATAAGGATTTTCTACTGCAATTCTAGTTGTTGTTG  
TCATCAATGTTCTTACATGCTGCTGATCCGCTGATTAAATGAAATGGC  
GGGGAGGGGGTTGCTATTGGCGCTTCCGCTTCCGCTACTGACTCGCT  
GCCGCTGCTGCTGGCTGCGCGAGGGTATCAGCTCAGCTCAAAGGCGTAATAC  
GGTTATCCACAGAATCAGGGGATAACGCGAGGAAGAACATGTGAGCAAAGG  
GCCAAAAGGCCAGAACGTTAAAAGGCCGCTGCTGGCTTTCCATAGGCTCC  
GCCCCCTGAGGAGCATCACAAATGACGCTCAAGTCAGAGGTGGC  
ACAGGTAACAGGATACCGAGCGTTCCCGCTTGGAGGCTCCCTGTGCGCT  
GTTCCGACCTCTGGCTTACCGGATACCTGTCGCGCTTCTCCCTGGGAAGCG  
GCCCTTCTCATAGCTCACGCTGTAGGTATCTCAGTTGCGTGTAGGCT  
AGCTGGGCTGTGCAAGAACCCCCGGTCAAGGGCAGCGCTGCGCTTATCGG  
ACTATGCTCTGAGTCAAACCCGGTAAGACAGACTATGCCACTGGCAGCAG  
CTGGTAACAGGCTACAGGAGGCTATGAGGAGGCTACAGAGTTCTTGAAG  
TGGTGGCTTAACCTCGGAAAAGAGTTGGTAGCTTGTGTTGCAAGCAG  
CGCTGGTAGCGGGGTTTTTGTGCAAGCAGCAGATTACGGCAGAAAAAGG  
ATCTCAAGAAGATCCTTGTATTTCTACGGGCTGTGACGCTCAAGTGG  
CTCACGTTAACGGGATTGGTCAAGGATTCAAAAGGATCTTCACCTAGATC  
TTAATTAAGGATTAATCTAAAGTATATGAGTAAACTGGT  
TGACAGTTACCAATGCTTAATCAGTGGAGGACTATCTCAGCAGTCG  
TCATCCATAGTTGCTGACTCCCGCTGTAGATAACTACGATACGGGAGGG  
CCATCTGGCCCCAGTGTCAATGATACCGGAGACCCACGCTCACGGCT  
TTATCAGCAATAACCCAGCCAGCGGAAGGGCGAGCGCAGAGTGGTCT  
TTATCCGCTCATCCAGTATTAAATTGTTGCGGGAAAGCTAGAGTAAGTAG  
GCCAGTTAACGGGATTGGTCAAGGATTCAAAAGGATCTTCACCTAGATC

- continued

## Informal Sequence Listing

CTCGTCGTTGGTATGGCTTCACTCAGCTCCGGTCCCCAACGATCAAGGGAGTTAC  
ATGATCCCCCATGTTGCAAAAAGCCTGGTTAGCTCTTCTCGGTCTCCGATCGTTGT  
CAGAAGTAAAGTGGCCGCGAGTGTATCACTCATGGTTATGGCAGACTGCTATACTTC  
TCTTACTGTCTGCATCCGCAAGATGGTTTCTGTGACTGGTAGACTCAACCAAC  
TCATTCTGAGAATAGTGTATGGCCGACCGAGTTGCTCTTGGCCGGCTCAATACGG  
GATAATACCGCCCATCGAGAACTTAAAGTGTCTCATCGGAAACGTCT  
GGGGGGGAAACTCTCAAGGATCTTACCGCTGTGGAGATCCAGTCTGATTAACCC  
ACTCTGTCACCCAACTGTATCTCAGCATCTTACTTACCTCACCAGGGTTCTGGTGA  
CAAAACAGGAAGGCAAAATGGCGAAAAAGGGATAAGGGCAGACCGGAATG  
TTGAATACTCATCTTCTCTTCAATTATTTGAAGCATTATCAGGGTTATTG  
CTCTAGGGCGATACTATTTGAATGTATTAGAAAAAATACAAATAGGGTTCCG  
CCCACTTCCCGGAAAGTGGCACTGGTC

SEQ ID NO: 3 pDNA: pCAG-ChRimson-tdTomato

Purpose: Delivers genes that express the opsin variant 'ChrimsonR' (allowing cells to be optically stimulated/activated with a specific wavelength), and td-Tomato marker (transfected neurons will emit a 'red' fluorescence)

Sequence:

SEQ ID NO: 4 pDNA: pCAG-mRuby3

Purpose: Delivers genes that express the mRuby3 marker (transfected neurons will emit a 'red' fluorescence)

Sequence:

GACATTGATTATGGACTAGTTATAATAGTAATCAATTACGGGGTCAATTAGTTCAT  
GCCCATATGGAGTCCCGCGTACATAACCTAACGGATAATGGCCCGCTGGCTGAG  
CGCCCAACGACCCCCCGGCAATTGACGTCAATAATGACGTATGGTCCCCATTAGAAC  
CAATAGGACTCTTCATTGACGTCAATGGGTGGAGATTACGGTAAACGCCCCAC

- continued

## Informal Sequence Listing

- continued

---

Informal Sequence Listing

---

AGGCTTTTGGAGGCCAGGTTGCACAAAGCTAACCTGTTATTGCAGCTATA  
 ATGGTTACAATAAGCAATAGCATCACAAATTCAACAAATAAGCATTTTTCAC  
 TGCAATTCTAGTTGTTGTCACAAACTCATCAATGTATCTTATCATGTCGGATCCG  
 CTGCATTAATGATCGGCAACGGCGGGAGAGCGGGTTTGCCTATTGGCGCTCT  
 TCCGCTTCTCGCTCACTGACTCGCCTGGCTCGTTCGGCTGCAGCGGTA  
 TCAGCTACTCAAAGCGGTAATACCGTTATCAGAAGTACGGGATAACGCAGG  
 AAAGAACATGTGAGCAAAGGCCAGCAAAGGCCAGGAACCGTAAAAGGCCG  
 TTGCTCGCGTCTCCATAGGCTCCGCCCTGAGGACATCACAAAAATCGAGC  
 TCAAGTCAGAGCTGGCGAACCCGACAGGACTAAAGATAACAGCGTTTCCCC  
 TGGAAAGCTCCCTCGCGCTCCCTGTCAGGCTTGCGCTACGGATAACCTGTC  
 GCCTTCTCCCTCGGGAAAGCTGGCGTTCTCATAGCTCACGCTGTAGGATCTCA  
 GTGCGTGTAGCTCGTCTCAAGCTGGCTGAGGACAGGCTTACGGGATAACCG  
 CGGACCCGCTGCCTTATCGGTAACTATCGCTTGAGTCCACCCGGTAAGACAG  
 ACTTATGCCACTGGCAGCAGCACTGGTAACAGGATTAGCAGAGCGAGGATATG  
 GCGGGTCTACAGAGTCTTGAAGTGGCTTAACGGCTACACTAGAAAGAAC  
 AGTATTGGTACTCGGCTCTGCTGAAGCCAGTTACCTTCGAAAAAGAGTTGGTAG  
 CTCTTGATCCGCAAACAAACCCGGCTGGTACGGCTGGTTTTGTTGCAAGCA  
 GCAGATTACGCCAGAAAAAGGATCTCAAGAAGATCTTGTATTTTCTACGG  
 GTCTGACGCTCAGTGGAACGAAAATCACGTTAAGGATTTGGTATGAGATTATC  
 AAAAGGATCTCACCTAGATCTTTAAATTTAAAGGTTAAATCAATCTA  
 AAGTATATGAGTAAACTGGTACGAGTACCAATGCTTAATCAGTGAGGCACC  
 TATCTAGCGATCTGCTATTTCGTTCATCCATAGTTGCTGACTCCCGTCTGTAG  
 ATAATCAGATAACGGGGCTTACCATCTGGCCCGAGTGTGCAATGATAACCG  
 AGACCCAGCTCACCGCTCCAGATTATCAGCAATAACCCAGGCCAGGG  
 CGCAGGGCAGAGCTGGCTCTCACGACTTATCCAGTCTTAAATTGTT  
 GCGGGGAAGCTAGAGTAAGTAGTTGCGCAGTTAATAGTTGCGAACGTTGTG  
 TTGCTACAGGCATCGGGTGTACGCTCGTCTGGTATGGCTTATTAGCTCG  
 TTCCAAACGATAAGGGAGTTACATGATCCCCCATGGTGTGCAAAAAGGGTTAG  
 CTCTTGGTCTCGGTCAGTGTGAGAAGTAGTTGGCCAGTGTATCACTCATG  
 GTATGGCAGCAGTGTATACTGTCATGCCATCGTAAGATGTTTCTG  
 TGACTGGTGAGTACTCAACCAAGTCATTCTGAGAATAGTGTATGCGGCGACCAG  
 GCTCTGGCCCGCTCAATACGGGATAATACGGGCCACATAGCAAGAACTTTAAA  
 GTGCTCATATTGGAAACGGTCTTCGGGGCGAAAAGCTCAAGGATCTACCGCTG  
 TTGAGATCCAGTGTGATTAACCCACTCGTGCACCCAACTGATCTTCAGCATTTA  
 CTTTACCAAGCGTTCTGGGTGAGAAAAACAGGAAGGCAAAATGCCGAAAAAG  
 GGAATAAGGGCAGACGGAAATGTTGAATACTCATACTCTCCCTTTCAATATTAT  
 TGAGCATTTATCAGGGTTATGTCATGAGCGGATACATATTGAATGTATTAG  
 AAAAATAACAAATAGGGTTCGCGCACATTCCCGAAGGTGCCACCTGGTC

---

1. A brain-computer interface (BCI) engrafted on a brain of a mammal, the BCI comprising:
  - a cortical graft layer comprising a plurality of neuronal cells transplanted on the brain's cerebral cortex, wherein the plurality of cells engraft on the brain and respond to an external stimulus with a detectable signal.
2. The brain-computer interface of claim 1, wherein the plurality of neuronal cells are transfected.
3. The brain-computer interface of claim 2, wherein transfection is ex vivo with a plasmid by electroporation.
4. The brain-computer interface of claim 2, wherein transfection is via virus-mediated transfection.
5. The brain-computer interface of claim 1, wherein the plurality of neuronal cells are tissue cultured mammalian stem cells.
6. The brain-computer interface of claim 5, wherein the plurality of neuronal cells are chemically tethered to an electrode.
7. The brain-computer interface of claim 3, wherein the plasmid contains a GCaMP nucleic acid sequence.
8. The brain-computer interface of claim 1, wherein the cortical graft layer extends axons and dendrites into the cerebral cortex or striatum.
9. The brain-computer interface of claim 1, wherein the cortical graft layer forms synaptic connections to enable bidirectional communication.

10. The brain-computer interface of claim 1, wherein the cortical graft layer is engrafted over a lobe of the cerebral cortex selected from the group consisting of the frontal lobe, the parietal lobe, the temporal lobe, the occipital lobe and a combination thereof.

11. The brain-computer interface of claim 1, wherein the cortical graft layer is about 50 microns to about 1 mm in thickness.

12. The brain-computer interface of claim 1, wherein the external stimulus is outside the cell, but within the mammalian brain.

13. The brain-computer interface of claim 1, wherein the external stimulus is outside the mammalian brain and is a member selected from the group consisting of a light signal, an audio signal, and an electrical signal.

14. The brain-computer interface of claim 13, wherein the light signal has a wavelength of about 300 nm to about 1.5 microns.

15. The brain-computer interface of claim 1, wherein the detectable signal represents neuronal activity.

16. The brain-computer interface of claim 1, wherein the detectable signal connects to an external device selected from the group consisting of a recording device and a device having a CPU.

17. The brain-computer interface of claim 1, wherein the mammal is a human.

18. The brain-computer interface of claim 17, wherein the human has an impairment selected from the group consisting

of a motor skill, a sight function, an auditory function, a taste function and an olfactory function.

**19.** A method for bi-directional communication between a brain-computer interface (BCI) engrafted on a brain of a mammal and a computer, the method comprising:

providing a cortical graft layer comprising a plurality of neuronal cells transplanted on the brain's cerebral cortex of the mammal; and  
providing an external stimulus to the mammal wherein the plurality of cells engrafted on the brain respond to an external stimulus with a detectable neural signal.

**20-28.** (canceled)

**29.** A method of connecting a biological brain-machine interface with a subject, the method comprising:

depositing neuronal cells onto a cortical surface of a brain of a subject, the cells being selected to emit light or an electrical signal in response to a neural signal;  
allowing the cells to form an additional cortical layer that grows and integrates into the brain; and

recording light or an electrical signal emitted from the cells in response to a neural signal in the brain.

**30-31.** (canceled)

**32.** A method of stimulating a brain with a biological brain-machine interface, the method comprising:

depositing neuronal cells onto a cortical surface of a brain of a subject, the cells being selected to convert light or an electrical signal to an electrical signal compatible with neurons in the brain;

allowing the cells to form an additional cortical layer that grows and integrates into the brain;

directing light at or an electrical signal to the cells in the additional cortical layer such that the cells convert the light or the electrical signal to a neural signal; and

measuring a response or a behavior of the subject correlated with the directed light or electrical signal.

**33-34.** (canceled)

\* \* \* \* \*